The Effect of Fibres on the Compressive Ductility of Lightweight Aggregate Concrete

Johann Helgi Oskarsson

Department of Structural Engineering
Faculty of Engineering Science and Technology
NTNU- Norwegian University of Science and Technology

ACCESSIBILITY:

Open

MASTER THESIS 2013

SUBJECT AREA:	DATE:	NO. OF PAGES:
Concrete Technology.	June 10th 2013	70 + 60 (Appendix)

TITLE:

The Effect of Fibres on the Compressive Ductility of Lightweight Aggregate Concrete

Effekten av fiber på trykkduktiliteten av lettbetong

BY:

Jóhann Helgi Óskarsson

SUMMARY:

The purpose of this thesis was testing the effect of different type of fibre reinforcements to the compressive ductility of lightweight aggregate concrete (LWAC). Concrete with density of about 1800 kg/m^3 and compressive strength of about 40 MPa was used. The fibres used were two types of steel fibres with lengths of 35 and 60 mm and then basalt fibres with length of 45 mm.

Eight full scale over-reinforced LWAC beams with length of 4,2m and cross-section of 0,2x0,3m were constructed with identical structural steel reinforcement but with different type of fibres added. The beams were then tested in a four point bending until failure. The deflection and top and bottom concrete strains were measured with inductive sensors and recorded in a test-log.

Test results of these beams were compared to calculations with input values from testing of the compressive strength and oven-dry density from testing of concrete cylinders. Comparison of test results and calculations showed a generally good compliance.

The fibres had positive effect on the ductility in compression. Even though they didn't increase the load bearing capacity post-failure, they decreased the deflection rate considerably. This test indicated clear difference in effect of the steel fibres versus the basalt fibres to the compressive ductility.

RESPONSIBLE TEACHER: Associate Professor Jan Arve Øverli

SUPERVISOR: Associate Professor Jan Arve Øverli

CARRIED OUT AT: Department of Structural Engineering, NTNU
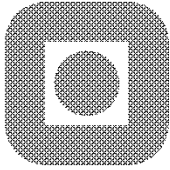
NORGES TEKNISK NATURVITENSKAPELIGE
UNIVERSITET, NTNU
Institutt for konstruksjonsteknikk

Masteroppgave i konstruksjonsteknikk 2013
for
Johann Helgi Oskarsson

Effekten av fiber på trykkduktiliteten av lettbetong

The Effect of Fibres on the Compressive Ductility of Lightweight Aggregate Concrete

OPPGAVE

På grunn av lettbetong sin lave densitet vil den i en del tilfeller være gunstig å bruke i konstruksjoner. I forhold til en normal betong har lettbetong en mye sprøere bruddoppførsel på trykk. Dette gjør at lettbetong ikke kan brukes i en del sammenhenger hvor det er krav til duktil oppførsel, for eksempel i områder med jordskjelvbelastning hvor dissipasjon av energi er sentralt. I regi av instituttets deltakelse i COIN (Senter for forskningsbasert innovasjon innen betong) gjennomføres det forskning innen dette fagområdet. Oppgaven går ut på prøving av bjelker av lettbetong laboratoriet for å studere duktiliteten og effekten av ulike tiltak for å øke duktiliteten

8 lettbetongbjelker med densitet 1800 kg/m^3 skal produseres og lastes til brudd. Siden oppgaven fokuserer på duktilitet i trykksonen av lettbetong, overarmeres bjelkene. Bjelkenes dimensjoner og armering er helt like. Fire varianter av bjelkene lages; 1) uten fiber; 2) Stålfiber med lengde 60mm; 3) Stålfiber med lengde 35mm; 4) Basalt fiber. Av hensyn til reproduserbarhet er to og to av bjelkene helt identiske.

Oppgaven kan deles opp som følger:
- Litteraturstudium om lettbetong og fiberarmert betong
- Dimensjonering av bjelker for prøving
- Produksjon av 8 bjelker som inkluderer forskaling, armering, instrumentering og støping
- Prøving av bjelker til brudd
- Rapportering av prøvingsresultater
- Vurdere effekten av ulike typer fiberarmering på duktiliteten
- Detaljerte beregninger av bjelkene basert på materialdata fra forsøkene

Oppgaven skal være gjennomført innen den 10. juni 2013.

Trondheim den 31.01.2013

Jan Arve Øverli
Førsteamanuensis / Faglærer

Preface

This Master thesis is the final chapter of my two year M.Sc. studies at NTNU, Norges Teknisk-Naturvitenskapelige Universitet, spring 2013 and accounts for 20 weeks work and equivalent to 30 ECTS credits. It is written for the Department of Structural Engineering at the Faculty of Engineering Science and Technology with Jan Arve Øverli Ass. Prof. as a supervisor.

I chose this project about the effect of fibres on the compressive ductility of lightweight aggregate concrete because of my interest in fibre reinforcement and my belief that use of fibres will become much more common in the future.

COIN (Concrete Innovation centre) has been researching ductility in lightweight concrete since the beginning in 2007. This project is done as a part of their research on the subject.

I would like to thank all the employees of NTNU's and SINTEF's laboratory, especially Steinar Seehuus and Gøran Loraas, for their guidance and assistance in the practical part of the thesis. I would also like to thank my fellow students in this project Stian Hoff, Torgeir Steen and Angel Arcadi Sorni Moreno for good cooperation in the laboratory and Tore Myrland Jensen from SINTEF for his input in the project. Finally I would like to thank my supervisor Jan Arve Øverli for his guidance and good advices during this project.

Trondheim, June 2013

Jóhann Helgi Óskarsson

Abstract

The purpose of this thesis was testing the effect of different type of fibre reinforcements to the compressive ductility of lightweight aggregate concrete (LWAC). Production of the LWAC was done by substituting Leca pellets (lightweight aggregate) for the aggregates used in normal concrete. This resulted in a concrete with density of about 1800 kg/m^3 and compressive strength of about 40 MPa. The fibres used were two types of steel fibres with lengths of 35 and 60 mm and then basalt fibres with length of 45 mm.

To improve LWAC's ductility is a very relevant task to make it a more attractive alternative to normal weight concrete and usable in constructions located on seismic active areas since they must be flexible enough to withstand the dynamic forces.

Eight full scale over-reinforced LWAC beams with length of 4,2m and cross-section of 0,2x0,3m were constructed with identical structural steel reinforcement but with different type of fibres added. The beams were then tested in a four point bending until failure. The deflection and top and bottom concrete strains at mid-span of the beam were measured with inductive sensors and recorded in a test-log.

Test results of these beams were compared to calculations with input values from testing of the compressive strength and oven-dry density from testing of concrete cylinders. Comparison of test results and calculations showed a generally good compliance.

The fibres had positive effect on the ductility in compression. Even though they didn't increase the load bearing capacity post-failure, they decreased the deflection rate considerably. This test indicated clear difference in effect of the steel fibres versus the basalt fibres to the compressive ductility. The steel fibres seemed to have almost immediate effect post the failure point. While the basalt fibres took longer time to affect the load bearing capacity of the beams post-failure due to lower E-modulus of the basalt fibres.

This project also emphasized how important it is to be thorough when casting fibre reinforced concrete to achieve good fibre orientation and distribution.

Sammendrag

Målet med oppgaven var å undersøke effekten av forskjellige typer av fiberarmering på trykkduktiliteten av lettbetong. Produksjon av lettbetongen som var brukt i dette prosjektet ble gjort ved å erstatte tilslagene brukt i vanlig betong med Leca lettklinker. Dette resulterte i en betong med densitet på omtrent 1800 kg/m^3 og trykkfasthet på ca 40 MPa. Fibrene som var brukt var to typer stål fibre med lengder på 35 og 60 mm og basalt fiber med lengde på 45 mm.

Å forbedre duktiliteten til lettbetong er svært relevant oppgave for å gjøre det il et mer attraktivt alternativ til normal betong og anvendelig i konstruksjoner på seismisk aktive områder fordi de må være fleksible nok til å tåle de dynamiske krefter.

Åtte fullskala overarmerte lettbetongbjelker av lengde 4,2m og tverrsnitt 0,2x0,3m ble laget med identisk tradisjonell stangarmering men med forskjellige tilsatte fibre. Bjelkene ble deretter testet i en firepunkts belastning inntil brudd. Nedbøyning og betongtøyning i øvre og nedre kant midt på bjelken ble målt med induktive givere og registrert i en test-logg.

Resultatene fra bjelkeprøvingen ble sammenlignet med beregninger med input verdier fra prøving av trykkfasthet og ovnstørr densitet fra testing av betong sylindre. Testresultater og beregninger stemmte generelt.

Fibrene hadde positiv effekt på trykkduktiliteten. Selv om de ikke økte bæreevnen etter brudd, da reduserte de likevel nedbøyningshastigheten betraktelig. Denne testen indikerte tydelig forskjell i virkning av stålfibre versus basalt fibrene på trykkduktilitet. Stålfibrene hadde nesten umiddelbar effekt etter brudd. Mens basalt fiber tok lenger tid å påvirke bjelkenes bæreevne på grunn av lavere E-modul på basalt fibrene.

Denne oppgaven viser også hvor viktig det er å være grundig ved støping av fiberarmert betong for å oppnå god orientering og fordeling av fibrene.

x

Contents

List of Figures

List of Tables

Symbols

Latin upper case letters

A_s Cross-sectional area of reinforcement

E_{lcm} Secant modulus of elasticity of concrete

E_s Design value of modulus of elasticity of reinforcing steel

EI Bending stiffness

F Load

I Moment of inertia

L Length of beam

M Bending moment

T_c Compressive resultant force from the concrete

S Tensile resultant force from the reinforcement

V Shear force

W Weight of beam

Latin lower case letters

b Width of a cross-section

c_{nom} Concrete cover

d Effective depth of a cross-section

h Height of the cross-section

h' Longitudinal reinforcement internal arm

f_{lc} Compressive strength of concrete

f_{lck} Characteristic compressive cylinder strength of concrete at 28 days

f_{lcm} Mean value of concrete cylinder compressive strength

f_{lctm} Mean value of axial tensile strength of concrete

f_{yk} Characteristic yield strength of reinforcement

n_b Number of bottom longitudinal bars

q Dead load

s Spacing of the reinforcement stirrups

z Lever arm of internal forces

Greek lower case letters

α_{lcc}	Coefficient for long term- and unfavourable effects on the compressive strength
δ	Deflection/Displacement
ε_{lcu3}	Ultimate compressive strain in the concrete (Bottom of cross-section)
$\varepsilon_{lcu3'}$	Ultimate compressive strain in the concrete (Top of cross-section)
ε_{yd}	Strain limit in the reinforcement
ε_s	Strain in the reinforcement
η_1	Coefficient for determining tensile strength for LWC
η_E	Conversion factor for calculating the modulus of elasticity for LWC
θ	Angle between the concrete compression strut and the beam axis perpendicular to the shear force
μ_ϕ	Curvature ductility
ρ	*Oven-dry density*
σ_2, σ_3	Effective lateral compressive stress
ϕ_b	Diameter of the bottom longitudinal reinforcement bars
$\phi_{s,w}$	Diameter of the reinforcement stirrups
ϕ_u	Curvature at ultimate limit
ϕ_y	Curvature at yielding of the tension reinforcement

Definitions

CMOD	Crack Mouth Opening Displacement
FRC	Fibre Reinforced Concrete
LWA	Lightweight Aggregate
LWC	Lightweight Concrete
LWAC	Lightweight Aggregate Concrete
NWC	Normal Weight Concrete

1 Introduction

Lightweight aggregate concrete (LWAC) is becoming more common in modern structures. Where the dead load of buildings is often the governing load since the need to build high rise buildings instead of more wide spread. And lightness of bridges is beneficial while the dynamic loads are not too large.

The purpose of this thesis is testing the effect of different type of fibre reinforcements to the compressive ductility of lightweight aggregate concrete (LWAC). Ductility is the ability of a material to be deformed without losing its entire load bearing capacity. The goal is modifying the stress-strain diagram of LWAC so that it looks more like the diagram for the fibre reinforced concrete shown in figure 1.1 here below.
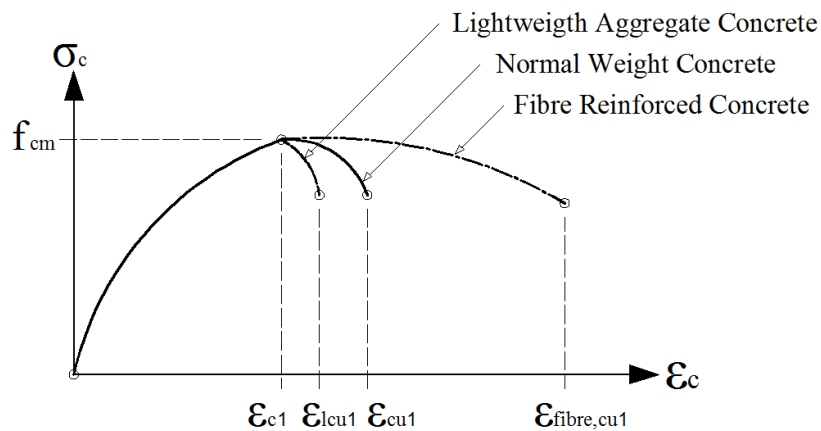
Figure 1.1. Stress-strain diagram for Lightweight Aggregate Concrete (LWAC), Normal Weight Concrete (NWC) and Fibre Reinforced Concrete (FRC).

To ensure the best possible effect from the fibres there must be equal distribution and orientation of the fibres over the whole cross section. The optimal direction of fibres to get the best effect on ductility in compression is transverse to the beams longitudinal direction, as shown in figure 1.2. Therefore is it very important to be very thorough when casting fibre reinforced concrete.
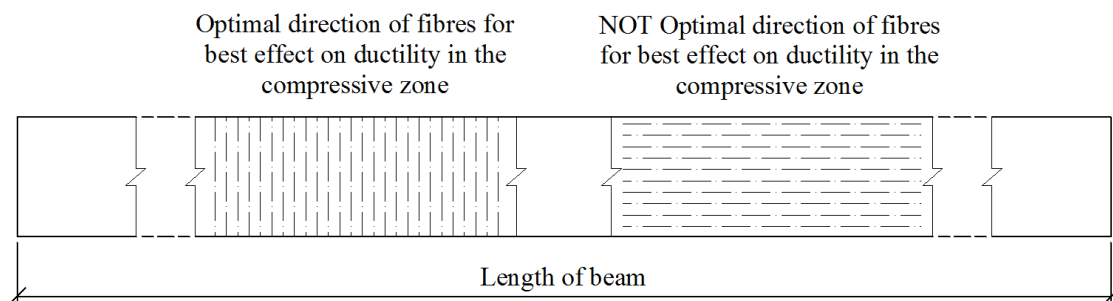
Figure 1.2. Different directions of fibres in a beam.

To improve LWAC's ductility is a very relevant task to make it a more attractive alternative to normal weight concrete and usable in constructions located on seismic active areas since they must be flexible enough to withstand the seismic forces.

The method used in this study is construction of eight full scale over-reinforced lightweight aggregate concrete beams with different type of fibres added. The beams are over-reinforced to ensure compressive failure of the beams. Two and two identical beams (twin beams) are casted where one set is without fibre reinforcement as the base point and then three sets of beams with different type of fibres. The beams were then tested in a four point bending until failure.

The structure of this project is divided in two major overlapping parts. The laboratorial work including fabrication of the beams and testing represent the first part. The second part of the project involves a literature study, beam design and evaluation of the test results.

This thesis is a continuation of previous testing where the goal was testing which effect fibre reinforcement in addition to traditional reinforcement stirrups had to the ductility of LWAC.

2 Literature

2.1 Ductility

Structural steel is a ductile material while concrete in itself is brittle. So when combined it can become a relatively ductile material. Ductility of structural concrete ensures visible indication of deformation if the applied loads become too large [1]. Ductility is especially important for constructions located in seismic active areas since the structures must have enough flexibility to withstand the seismic load.

> *"Ductility may be defined as the ability to undergo deformations without a substantial reduction in the flexural capacity of the member"* [2]

Ductility can be calculated by using the load-deflection or moment-curvature diagrams. For reinforced concrete sections it can be expressed in the form of curvature ductility, μ_ϕ:

$$\mu_\phi = \frac{\phi_u}{\phi_y} \tag{2.1}$$

Where ϕ_u is the curvature at ultimate when the concrete strain reaches a specified limiting value and ϕ_y is the curvature when the tension reinforcement first reaches the yield strength, see figure 2.1 [2]. Curvature can generally be determined by the expression:

$$\phi = \frac{\varepsilon_1 + \varepsilon_2}{h} \tag{2.2}$$

Where ε_1 and ε_2 are the strains at top and bottom of a section of height h.
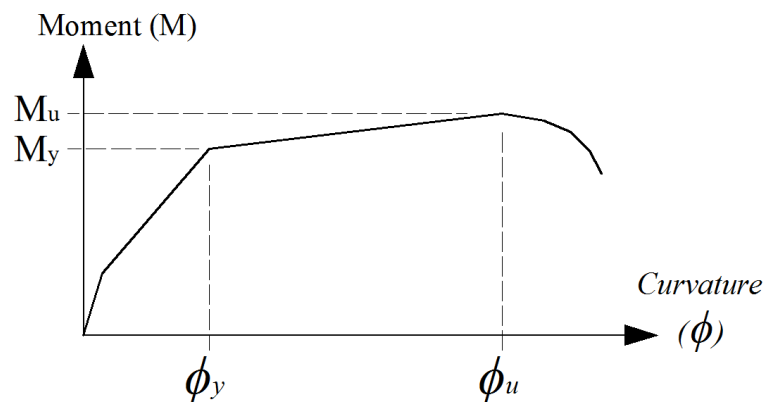
Figure 2.1. Definition of ductility [2].

2.1.1 Confined Concrete

Cylinder strength f_{lck} is used when defining concretes compressive strength. Eurocode 2 specifies in chapter 3.1.9 that confinement of concrete modifies the effective stress-strain relationship by achieving higher strengths and higher critical strains. Confinement is attained by applying lateral compressive stress of σ_2 ($=\sigma_3$) to the test cylinder in the transverse direction of the applied load as shown in figure 2.2.
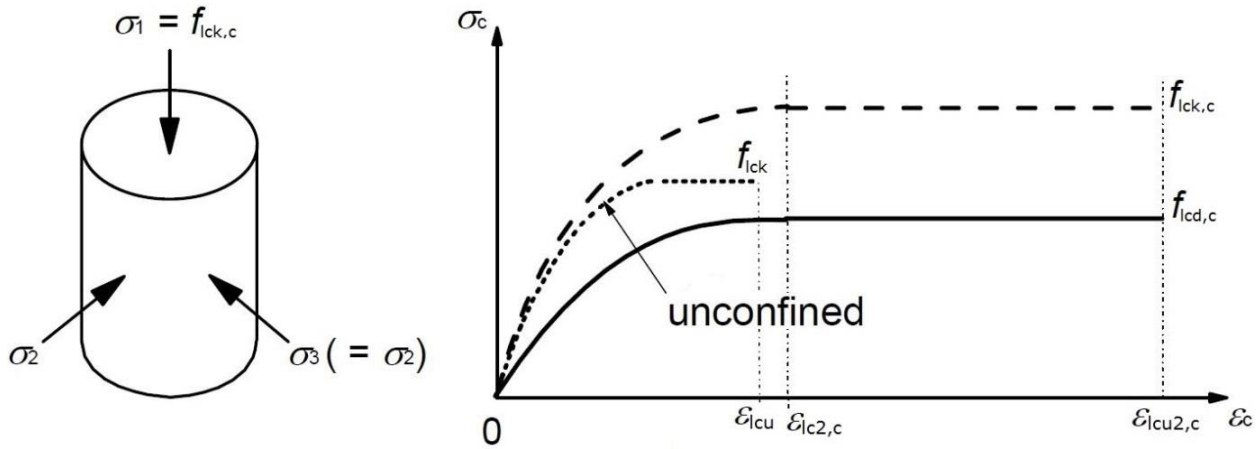
Figure 2.2. Stress-strain relationship for confined concrete[3, edited for LWC].

The confined characteristic strength and strains for lightweight aggregate concrete shown in figure 2.2 can be expressed by:

$$f_{lck,c} = f_{lck}\left(1,0 + k\,{}^{\sigma_2}\!\big/_{f_{lck}}\right) \tag{2.3}$$

Where k is an aggregate coefficient equal to 1,0 in the Norwegian National Annex for Eurocode 2 and the strains are expressed by:

$$\varepsilon_{lc2,c} = \varepsilon_{lc2}\left({}^{f_{lck,c}}\!\big/_{f_{lck}}\right)^2 \tag{2.4}$$

$$\varepsilon_{lcu2,c} = \varepsilon_{lcu2} + 0,2\,{}^{\sigma_2}\!\big/_{f_{lck}} \tag{2.5}$$

Confinement of concrete structures results in increased ductility of the cross-section. Confinement of high-strength concrete columns in high rise building with steel casing has become a common method to decrease the brittleness and increase ductility. Internal transverse reinforcement, e.g. stirrups, also has confining effect.

4

2.2 Lightweight Aggregate Concrete

2.2.1 Properties of Lightweight Concrete

Lightweight concrete (LWC) can be mixed with oven-dry density from 300 to 2000 kg/m^3, cube strength from approximately 1 to over 60 MPa and thermal conductivity of 0,2 to 1,0 W/mK. For normal weight concrete (NWC) these values correspond to 2100 to 2500 kg/m^3 density, 15 to over 100 MPa cube strength and 1,6 – 1,9 W/mK thermal conductivity.

Lightweight concrete can be categorized by different methods of production:

- By removing the finer fraction aggregates from the mix to create air-filled voids. This concrete is also known as *no-fines concrete*.
- By including gas bubbles in the cement paste to form a cellular structure which contains approximately 30–50% voids. This concrete is also known as *aerated concrete*.
- By replacing, either wholly or partially, natural aggregates in the mix with lightweight aggregates containing a large proportion of voids. This concrete is also known as *lightweight aggregate concrete* [4].

Lightweight aggregate concrete (LWAC) is the type of lightweight concrete used in this thesis.

The density is essentially decreased by the presence of voids, either in the aggregates, the mortar or in the interstices between the coarse aggregates. It is clear that these voids reduce the strength of the concrete, but high strength is not always essential. On the other hand the advantage of these pores is that they improve the insulating effect in the concrete, and sometimes that is a preferred quality [5].

Other properties that have to be taken into consideration in lightweight concrete are workability, absorption, drying shrinkage and moisture movement. To be able to get similar workability as normal weight concrete the lightweight aggregate concrete has to have lower slump and lower compacting factor because the work done by gravity is smaller. If higher workability is used then there is always the risk of segregation of the mix. The high water absorption is caused by porous nature of the lightweight aggregates. If the aggregate is dry at the time of mixing, it will rapidly absorb water and the workability will quickly decrease [5].

Some other interesting properties of lightweight aggregate concretes compared with normal weight concrete are for example 25-50% lower E-modulus of elasticity, better freeze/thaw resistance and more fire resistance [5].

2.2.2 Fresh concrete

When designing a concrete mix there are many things to consider. The increased absorption, decreased density and range of available lightweight aggregates amplify this problem for lightweight aggregate concrete. The increased water absorption is especially important to take into consideration [4].

> *"All aggregates, whether natural or manufactured, absorb water at a rate which diminishes with time. Such absorption is important in that for unsaturated or partially saturated aggregate it will influence such properties of fresh concrete as workability (including pumpability) and density and also affect such hardened properties as density, thermal insulation, fire resistance and freeze/thaw resistance."* [4, pp. 2/11]

The rate of water absorption is likely to be much higher for lightweight aggregates particles than for normally dense aggregates due to the relatively large pore volume. However the sintered shell around the expanded clay aggregates *(see 2.2.4 Norwegian Leca)* slows down the absorption process. Water absorption is usually expressed as the proportion of the oven-dry mass absorbed after 30 minutes and 24 hours. Lightweight aggregates generally absorb about 5-15% of the dry mass while most natural aggregates absorb about 0,5-2% in 24 hours.

Casting of lightweight aggregate concrete is no different from normal aggregate concrete. But it can be more tolerant to poor curing since the aggregates withhold some water [4].

2.2.3 History of Lightweight Aggregate Concrete

Lightweight concrete is not quite a new invention. Through the ages people have used the material at hand to build constructions where there has been used many aggregates of different types. Such as some lightweight aggregates (LWA) of volcanic natural origin like pumice, scoria, tuff etc. [6].

The use of lightweight concrete can be traced to as early as 3000 B.C. when the towns of Mohenjo-Daro and Harappa in Pakistan were built with porous clay bricks. Later the Greeks and Romans used pumice when building their constructions, which some of them still exist like St.

Sofia Cathedral (Hagia Sofia) in Istanbul and the Roman temple, the Pantheon and the Colosseum in Rome [6].

Lightweight aggregate can be categorized as naturally resourced aggregate or synthetic aggregates. The most common naturally resourced aggregates are volcanic originated as pumice and scoria aggregates. For example has pumice been used in local building industries in Iceland since 1928. Then there are organic aggregates such as palm oil shells which is a waste product of the palm oil industry.

Most synthetic aggregates are produced by thermal treatment of the materials which have the ability to expand. These materials are divided into three groups

- *Natural materials* such as perlite, vermiculite, clay, shale and slate.
- *Industrial products* such as glass.
- *Industrial by-products* such as fly ash, expanded slag cinder, bed ash etc.

The most common group is the natural materials, which includes the lightweight aggregate produced from expandable clay known as *Leca* (Light Expanded Clay Aggregate) and *Liapor*. Those made from fly ash are known as *Lytag* [6].

In modern time the demand of LWAC increased and the natural originated lightweight aggregates were not available everywhere so there was developed technology for producing LWA. It is assumed to have originated in Germany in the 19th century where porous clay pieces were produced by quick evaporation of water. Industrial use of natural lightweight aggregates in Germany began in 1845 with production of masonry blocks form pumice with burnt lime as binder. Then later in North America a contractor and brick maker named Stephen J. Hayden observed that clay bricks could expand up to 1/3 of its original size if placed too close to the burning fire. He then crushed these porous clay bricks and used them as aggregates. In 1920 the first commercial plant began operating producing "Haydite" expanded shale aggregates. In Europe the first commercial production of expanded clay began in Germany between 1935 and 1939. Denmark is however looked at as the European birthplace of expanded clay where production of Leca started in 1939 [6].

2.2.4 Norwegian Leca

Leca is produced by mixing clay and water into a paste. Then the paste is fed into the higher end the rotary kiln where it is broken into smaller granules by chains. The granules get burned in different sized spherical pellets with a glazed but porous skin, often called clinker, and then sieved to right size. Leca is produced in Norway and Sweden and are named Norwegian Leca and Swedish Leca, see figure 2.3.
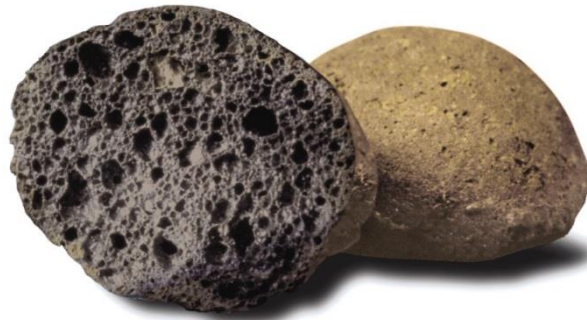
Figure 2.3. Cross-section of Leca pellet [7].

The Production of Norwegian Leca was started in1954 using one single kiln. The production capacity was less than 100.00 m^3 per year, while today's production capacity is nearly 1 million m^3 annually from four rotary kilns [6].

Other types of commonly used LWA are:

German Liapor: *"These are also expanded clay aggregates. The process of their manufacture is different from the production of Leca. They are first pressed into balls of a desired shape, dried and then burned. Thus, unlike Leca, their size and shape is very precise, there is no dust or 0-1 mm portion."* [6, pp. 403]

Lytag / Aardelite: *"Sintered fly ash aggregate, fly ash collected from the flue gas of thermal power stations is dampened with water and mixed with coal slurry in screen mixers. The material is then fed into rotating pans, known as pelletizers, to form special pellets. These are then sintered at a temperature of about 1400°C. This causes the ash particles to coalesce, without fully melting, to form a lightweight aggregate."* [6, pp. 401]

8

2.2.5 Use of Lightweight Aggregate Concrete in Norway

The main use of LWAC in Norway has been in the precast industry where the total amount of produced floor slabs and wall panels has varied between 100.000 m² and 200.000 m² each year. Then there have been constructed six major bridges since 1989 and some offshore constructions like Troll GBS (Gravity Based Structure), Troll West floating platform and Heidrun Tension Leg Platform. Concrete types used in these offshore construction varies from LC60 to LC75 (High strength Lightweight Concrete) with density of 1900 – 2250 kg/m^3 [6].

Two of these bridges, Bergsøysundet Bridge (opened in 1992) and Nordhordland Bridge (opened in 1994), see figure 2.4, are floating bridges that were the first structures of their kind in the world with pontoons made of LWAC. The Nordhordland Bridge is also partly a 368m long cable-stayed bridge which was the first structure of that kind using high-strength LWAC in Norway [6].
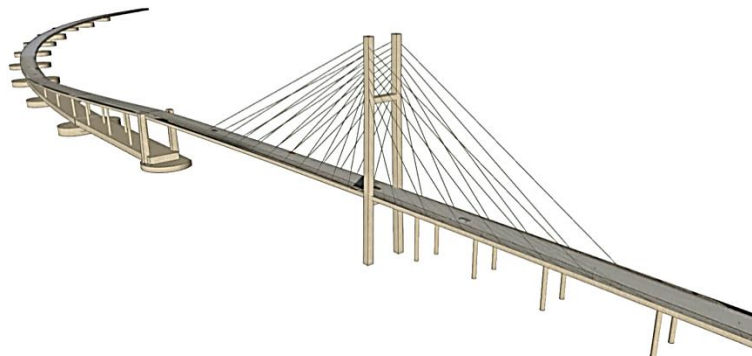
Figure 2.4. Nordhordland bridge, pontoons and cable deck casted with LWAC [8].

Stolmasundet Bridge (opened in 1998) and Raftsundet Bridge (opened earlier in 1998) are also world record cantilever bridges with the longest bridge span constructed with LWAC which made these long spans possible. The total length of Stolmasundet Bridge is 467m with a main span of 301m where of the middle 184m are made of LWAC. And the Raftsundet Bridge has a total length of 711m and a main span of 298m which is constructed with LWAC [9]. The typical concrete used in all of these bridges was LC55 and with density of approximately 1900 kg/m^3 [6].

2.3 Fibre Reinforcement

The purpose of fibre reinforcement is mainly to increase the tensile strength of the concrete and delay the formation of cracks and to increase toughness by transmitting stress across a cracked section so that much larger deformation is possible beyond the peak stress than without fibre reinforcement, see figure 2.5 [5].

"Fibres provide post-cracking ductility to the fibre reinforced concrete" [10]
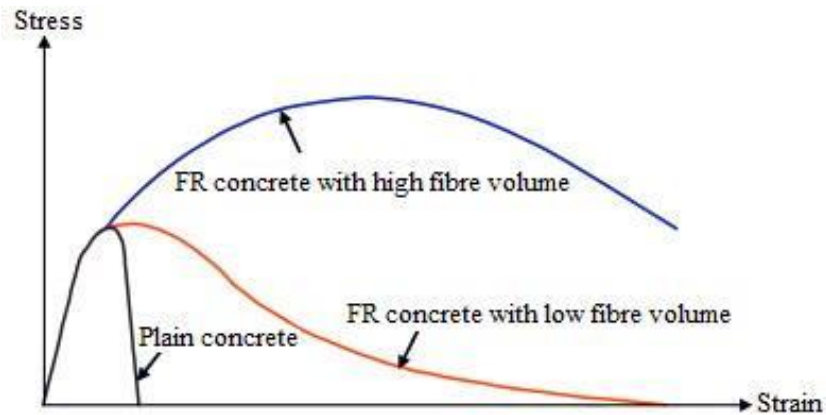
Figure 2.5. Stress-strain diagram for plain concrete vs. fibre reinforced concrete [11].

During the last decades fibre reinforced concrete has mostly been used in slabs on grade and shotcrete in tunnels with good results, but it is also possible to use fibre reinforced concrete as load bearing in pipes, culverts, foundations, walls, shells and slabs [12].

The most actual method for fibre reinforcement is when it is combined with normal reinforcement, especially in the sense of reducing or eliminating the amount of stirrups needed since the fibres cannot replace the longitudinal tension bars completely.

2.3.1 Properties of Fibres

Fibres can be made from natural material such as basalt and asbestos or be a manufactured product such as steel, glass, carbon and polymer, e.g. polypropylene [5]. The most common types used today are steel-, glass-, synthetic- and natural material fibres. Generally the length of fibres can vary from only few millimetres up to 80 mm and the diameter can be from tenth of a millimetre to 2 mm [12].

In this project there are used three types of fibres. Dramix 65/60 and Dramix 65/35 steel fibres, see figure 2.6, and 3rd generation basalt fibre reinforced polymer MiniBars, see figure 2.7. The

material properties of these fibres are shown in table 2.1. Data sheets for these fibre types are found in Appendix A.

Table 2.1. Material properties of the fibres [13, 14, 15].

Fiber	Young's modulus	Tensile strength	Density
	GPa	MPa	kg/m^3
Steel	210	1.160 / 1.345	7.850
Basalt, gen. 2	60	1.100	1.900

Production of steel fibres can generally be done by cutting wire, shearing sheet or from a hot melt extract [10]. Dramix fibres are made out of cold drawn wire which is deformed and cut to lengths. Dramix 65/60 has a length of 60 mm and a performance class of 65 which is based on the length-diameter ratio where the diameter is 0,90 mm. Corresponding for the Dramix 65/35 fibres with length of 35 mm and diameter of 0,55 mm [14, 15]

Figure 2.6. Dramix 65/60 glued steel fibres. The hooked shaped of the fibres increases the bondage with the concrete [16].

Basalt fibre reinforced polymer (BFRP) MiniBars are engineered to deliver high flexural toughness and energy absorption. It is made from basalt stone and treaded to thin basalt fibres and then coated with solution suitable for use in concrete, see figure 2.7 [13].

Basalt stone   Melted Basalt   Fiber   MiniBars ^{TM}
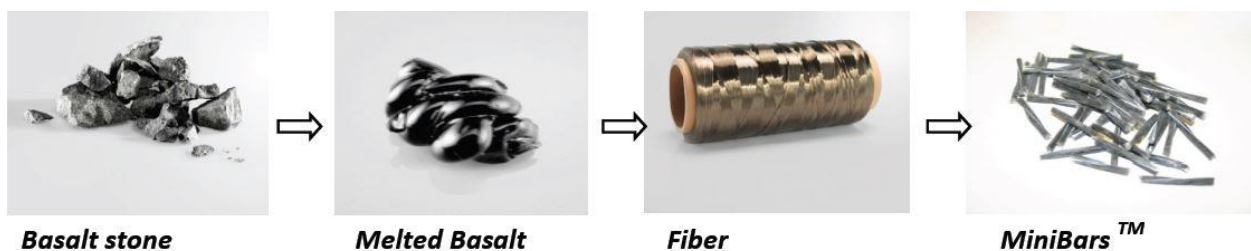
Figure 2.7 Production process for basalt fibre MiniBars [13].

2.3.2 Producing and Casting Fibre Reinforced Concrete

Concrete that includes fibres usually demands greater amount of finer aggregates (fines) and smaller aggregates then normal concrete. The reason for this is the long and thin shape of the fibre which increases the pores and reduces the workability of the concrete. This also increases the need for more water in the mix. Generally the workability decreases with increasing amount of fibres [12].

Casting of fibre reinforced concrete has to be planned and done in such a manner that possible obstacles like reinforcement steel or electrical piping don't create weakness zones with little amount of fibres that can weaken the concrete, see figure 2.8.
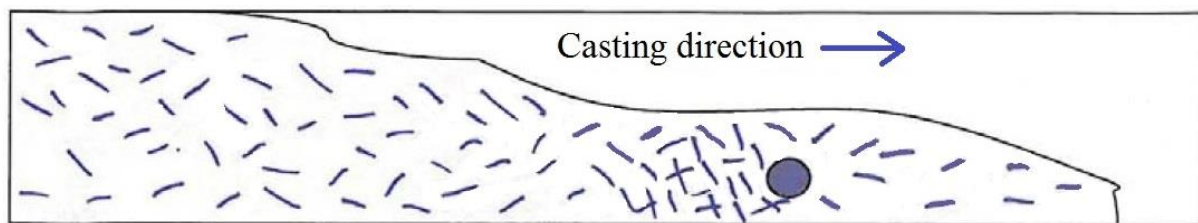
Figure 2.8. Fibre weakness zone behind reinforcement bar [5].

Achieving equal distribution and orientation of the fibres over the whole section is most important when casting fibre reinforced concrete since that is assumed in design of the reinforcement [12].

2.4 COIN (Concrete Innovation Centre)

COIN has been involved in the education of Master of Science (MSc) students at the Norwegian education institutions NTNU, UMB and Oslo University College for the last years. Several master theses have been written in this period. Some of the industrial partners that are involved in COIN have also been involved in supervision of master students [17].

> *"The vision of COIN is creation of more attractive concrete buildings and constructions. Attractiveness implies aesthetics, functionality, sustainability, energy efficiency, indoor climate, industrialized construction, improved work environment, and cost efficiency during the whole service life. The primary goal is to fulfil this vision by bringing the development a major leap forward by more fundamental understanding of the mechanisms in order to develop advanced materials, efficient construction techniques and new design concepts combined with more environmentally friendly material production."* [17, pp. 3]

3 Design of Concrete Beams

The purpose of this project was to test the effect of three different types of fibre reinforcement on the ductility in compression of lightweight aggregate concrete (LWAC) beams. These types of fibres are:

- Dramix 65/60 steel fibres; length 60 mm.
- Dramix 65/35 steel fibres; length 35 mm.
- Basalt fibre reinforced polymer MiniBars generation 3; length 45 mm.

To generate a compression zone on the top side of the beam two symmetric point loads are applied to form the four point bending test. This results in a mid-span between the loading points with constant bending moment and free for shear forces as shown in figure 3.1.
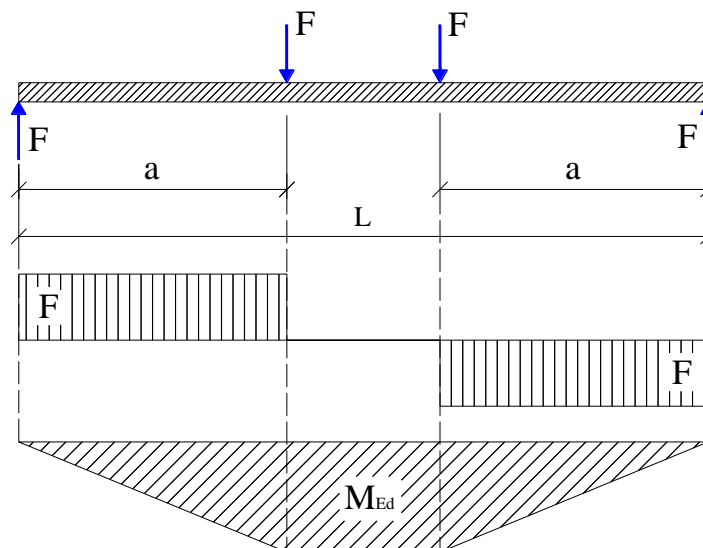
Figure 3.1. Static model for four point bending test.

3.1 Design

Previous years SINTEF has been researching and testing lightweight aggregate concrete (LWAC) in cooperation with NTNU. Therefore they have developed a mix of LWAC which has a density of about 1800 kg/m^3 and mean compressive strength of about 40 MPa, which will be used in this project. SINTEF decided to cast four twin beams (denoted A and B), all with the same geometry and traditional steel reinforcement. The only variation of the beams should be the fibre reinforcement since the purpose of the project was to test their effect on ductility in compression. An overview over the beams and the reinforcement is given in table 3.1.

Table 3.1. Fibre reinforcement in the beams.

Beam	1A 1B	2A 2B	3A 3B	4A 4B
Type of fiber	Only LWAC	Dramix 65/60	Dramix 65/35	Basalt gen. 3

The concrete mixer in NTNU's laboratory has a volume of about 800 litres and therefore was the cross-section chosen according to that by SINTEF. To be able to cast two beams and test specimens with one batch from the mixer it was decided to set the beams cross-section to 200x300 mm (WxH) and the total length of 4,2 meters, see figure 3.2. This means that one beam has the volume of 252 litres excluded the reinforcement and the total amount needed concrete, including the test specimens, is about 600 litres from one batch. Therefore we just had to calculate the required amount of reinforcement to make the beams over reinforced to ensure that the beams would fail in compression.

After some preliminary calculations it was decided to use 4Ø32 mm longitudinal reinforcement bars in the bottom of the beam and 2Ø8 mm longitudinal bars in the top with Ø8 mm stirrups with 100 mm spacing in the entire beam with exception of the mid-span between the two loading points. The longitudinal bars in the top are basically to support the stirrups since they are not present in the compressive mid zone, and are therefore not taken into consideration in the calculations. To utilize the cross-section the concrete cover was set as only 15 mm. This doesn't fulfil Eurocode's requirements but this is safe to do since the beams don't have to withstand any weathering influences. Figures 3.2 and 3.3 show the geometry and the reinforcement layout of the beams.
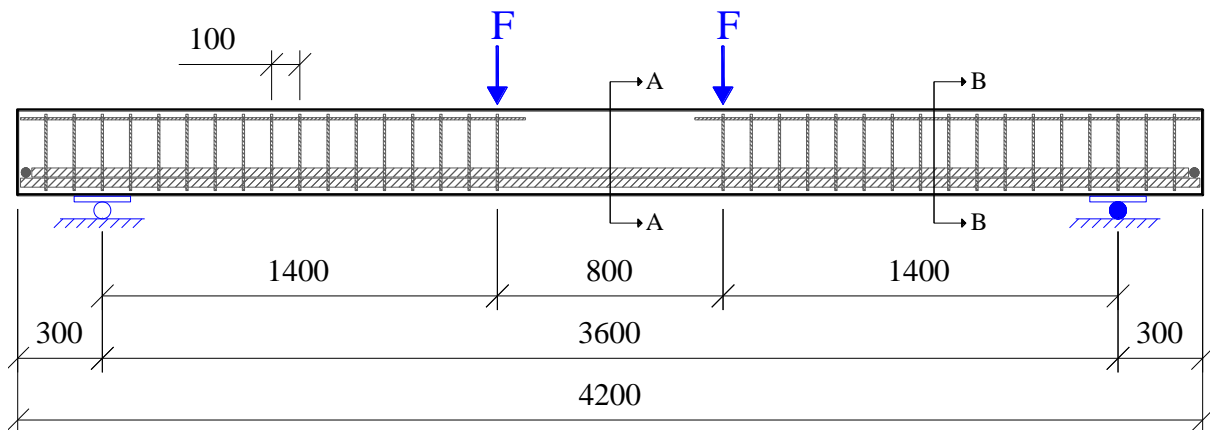
Figure 3.2. Geometry of the beams.

Section A-A   Section B-B

Ø8c100   Ø8c100
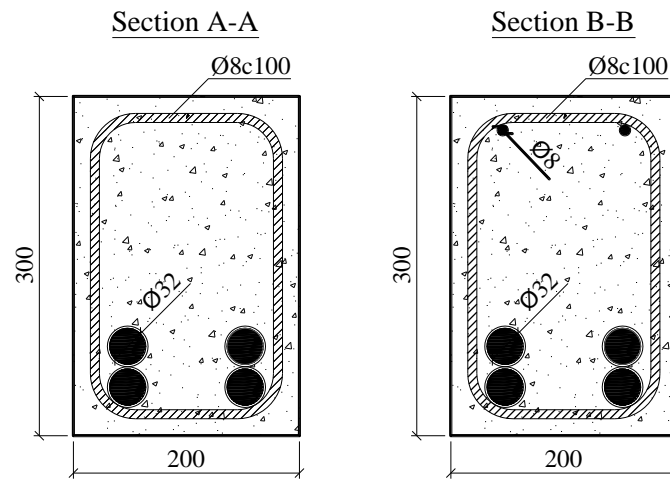
Figure 3.3. Cross-section of the beams.

Following is a table over the beams main geometry and cross section parameters used in calculations for the capacity of the beam.

Table 3.2. The beams geometry and cross-section.

Geometry			Cross-section		
Total Length =	4 200	mm	Beam width - b =	200	mm
L =	3 600	mm	Beam height - h =	300	mm
L_1 =	300	mm	Concr. cover - c_{nom} =	15	mm
L_2 =	1 400	mm	d =	239	mm
L_3 =	800	mm	z = 0,9d =	215	mm
Weight =	453,6	kg	h' =	209	mm

3.2 Calculations

Detailed calculations of the beam are shown in Appendix B where the capacity of the given beam is checked while the main results are presented on the following pages.

All calculations are done in accordance with *Eurocode 2: Design of concrete structures* [3], where chapter 11 is about Lightweight aggregate concrete structures, and *Betongkonstruksjoner; Beregning og dimensjonering etter Eurocode 2* by Svein Ivar Sørensen [18]. Cited formulas in the calculations in the appendix refer to *Eurocode 2* (EC2) and *Betongkonstruksjoner* (BK) where some equations are adapted to the concretes mean value of cylinder compressive strength f_{lcm} instead of f_{lck} (where l stands for lightweight concrete). The mean value strength is used since this is a laboratorial testing and the concrete batch is mixed in a more controlled way then when

the concrete is mixed at a concrete plant. The beams are then humidified while stored until tested in a controlled loading, i.e. optimal conditions for casting, storing and testing.

All partial and material factors are set as 1,0 in the calculations to get the most comparable results to the test results. Other material parameters for the LWAC and reinforcement are given in table 3.3.

Table 3.3. Material parameters for the LWAC and reinforcement.

Lightweight Aggregate Concrete			
Mean compr. strength	$f_{lcm} =$	40	N/mm^2
Oven dry density	$\rho =$	1 800	kg/m^3
Tensile strength	$f_{lctm} =$	3,1	N/mm^2
Modulus of elasticity	$E_{lcm} =$	23 430	MPa
Strain	$\varepsilon_{lcu3} =$	3,12	‰
LWAC coefficient for ε_{lcu3}	$\eta_1 =$	0,89	EC2-11.1
LWAC coefficient for E_{lcm}	$\eta_E =$	0,67	EC2-11.2
Reinforcement			
Characteristic yield strength	$f_{yk} =$	500	N/mm^2
Modulus of elasticity	$E_s =$	190 000	N/mm^2
Strain	$\varepsilon_s =$	2,63	‰
Bottom longitudinal bars	$\varnothing_b =$	32	mm
Number of bottom long. Bars	$n_b =$	4	mm
Stirrups	$\varnothing_{s,w} =$	8	mm
Stirrup spacing	$s =$	100	mm
Angle between the concrete compr. strut and the beam axis perpendic. to the shear force	$\cot(\theta) =$	2,5	EC2-6.7N

3.2.1 Moment Capacity

According to Eurocode 2 – 6.1(2)P [3]; When determining the ultimate moment resistance of reinforced cross-sections, the following assumptions are made:

- Plane sections remain plane (Navier's hypothesis is valid).
- Same strain in the concrete and the reinforcement (complete bond).
- Stress-strain relationship of the concrete according to EC2 - 3.1.7.
- The tensile strength of the concrete is ignored.

To find the moment capacity of the beam I start by determining the neutral axis of the cross section with axial equilibrium of the stress and strain distribution shown in figure 3.4.
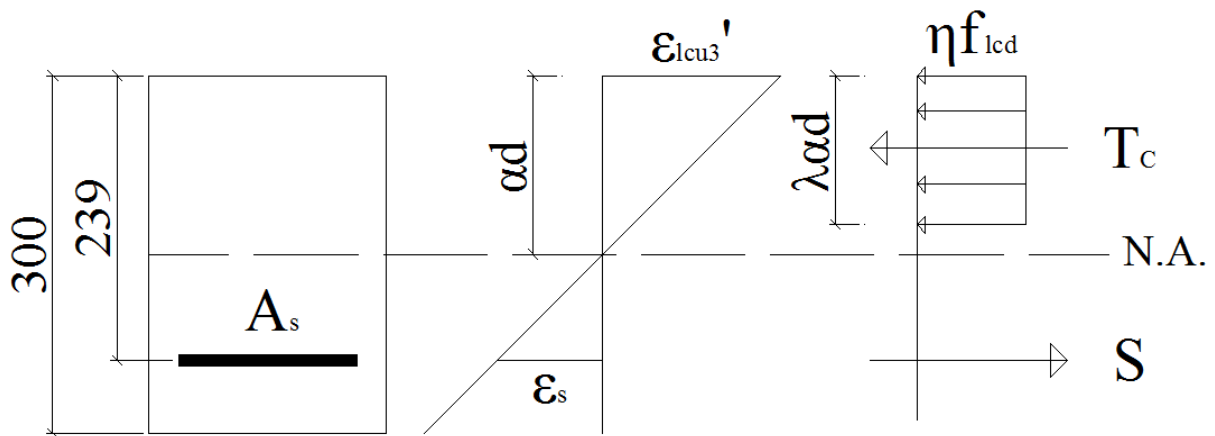
Figure 3.4. Stress and strain distribution.

Where
$$T_c - S = 0 \tag{3.1}$$

With the concrete force expresses by:

$$T_c = \lambda \eta f_{lcd} \alpha d b \tag{3.2}$$

And the force in the longitudinal reinforcement is given by:

$$S = \sigma_s A_s = E_s \varepsilon_s A_s \tag{3.3}$$

Then substitution of the reinforcement strain with concrete strain:

$$\varepsilon_s \frac{1}{(d - \alpha d)} = \frac{1}{\alpha d} \varepsilon_{lcu3}' \rightarrow \varepsilon_s = \varepsilon_{lcu3}' \frac{1 - \alpha}{\alpha} \tag{3.4}$$

Gives the neutral axis of αd = 157 mm, and then the moment capacity can be determined by:

$$M_{Rd} = \lambda\alpha(1-0,5\lambda\alpha)f_{lcm}bd^2 \tag{3.5}$$

So the moment capacity for the cross section is M_{Rd} = 176,8 kNm which means that the failure load should be F_{ult} = 123,3 kN when the beams dead weight and the weight of the load-distribution beam has been subtracted.

3.2.2 Shear Capacity

The shear capacity for the given reinforcement in the beam is determined by the smaller value of the following expressions:

$$V_{Rd,s} = \frac{A_{sw}}{s}zf_{yk}\cot\theta \tag{3.6}$$

and

$$V_{Rd,max} = \alpha_{cw}b_wzv_1\frac{f_{lcm}}{(\cot\theta+\tan\theta)} \tag{3.7}$$

Which means that the beam has a shear capacity of V_{Rd} = 222 kN and is sufficient to withstand the expected failure load of F_{ult} = 123,3 kN. The spacing of the stirrups is calculated to be at maximum 125 mm, which is fulfilled since the spacing is 100 mm in the beam.

3.2.3 Deflection

Calculations of the beam deflection are done according to methods in the Betongkonstruksjoner textbook by using bending stiffness of equivalent transformed uncracked (*Stadium I*) and cracked (*Stadium II*) cross-sections.

For stadium *I* when the cross-section is assumed to be uncracked the neutral axis is 177 mm from the top of the beam. The bending moment at cracking can be determined as M_{crack} = 15,1 kNm which means that the cracking force is F_{crack} = 9,1 kN and the beam should have deformed 1,2 mm at this stage.

Then for *Stadium II* when the beam has started cracking the neutral axis should move up to 151 mm from the top side of the beam and the deflection at failure load should be $\delta_{Failure}$ = 22,1 mm.

3.2.4 Strain

The strain in the longitudinal reinforcement and the top and bottom side of the concrete is checked at the expected failure point.

Reinforcement strain is expressed by:

$$\varepsilon_s = \frac{M(1-\alpha)d}{EI_{II}}$$

(3.8)

With input from the failure moment and neutral axis and bending stiffness from *Stadium II* calculations the strain is $\varepsilon_s = 1{,}53$ ‰.

Then the concrete strain at the top side is determined by:

$$\varepsilon_{lcu3}{}' = \frac{M \cdot \alpha d}{EI_{II}}$$

(3.9)

And the bottom side is found with:

$$\varepsilon_{lcu3} = \frac{M(h-\alpha d)}{EI_{II}}$$

(3.10)

Which gives the strains of $\varepsilon_{lcu3}{}' = 2{,}64$ ‰ at top and $\varepsilon_{lcu3} = 2{,}60$ ‰ at bottom.

4   Laboratory

Most of the work in the laboratory regarding fabrication of the beams took place during February month. But the testing of the beams, which is usually done after 28 days of hardening, had to be delayed due to Easter vacation in the end of Mars. The beams were therefore tested at age of 36 – 39 days of hardening.

4.1   Fabrication of Reinforcement Steel and Formwork

The reinforcement frame was quite simple to construct and there was no variation between the eight beams. All reinforcement steel was ordered pre-cut and bent in accordance with the cutting list which is to be found in Appendix C. The length of all the longitudinal bars was all within marginal error, so no cutting was necessary to make them fit within the formwork. But many of the stirrups needed some mending to make them fit.

The reinforcement frame was fabricated on benches where the frame was first turned upside down to start by fasten the stirrups to the Ø32 mm bottom longitudinal bars. Then the frame was turned and the Ø8 mm longitudinal bars in the top were placed to secure proper alignment of the stirrups.   Finally the upper bottom longitudinal bars were fitted.   Welded transverse reinforcement bar were added on the end of the bundled bottom bars to guaranty sufficient anchoring of the longitudinal tension bars, see figure 4.1.
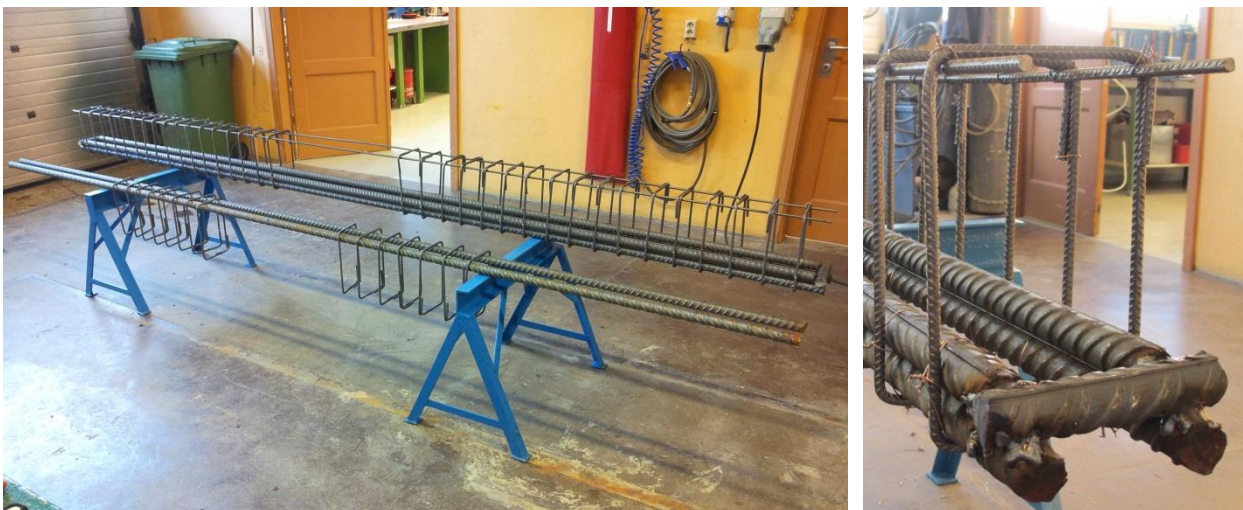
Figure 4.1. *Left:* **Reinforcement frames under production and completed.** *Right:* **Transverse anchoring bar on the end of longitudinal reinforcement.**

The formwork was re-used from previous year testing since those beams had the same length and the width could be easily adjusted. When the reinforcement had been placed in the framework it was decided to remove the longitudinal compressional reinforcement bars in the top at mid span between the horizontal stirrups, see figure 4.2. Doing this prevents the top bars increasing or accelerating the chance of the concrete spalling and affecting the ductility effects from the fibre reinforcement. This had to be done after positioning the reinforcement in the framework since the beams were lifted up on the stirrups and that would not have been possible if the longitudinal bars would have been removed on forehand.
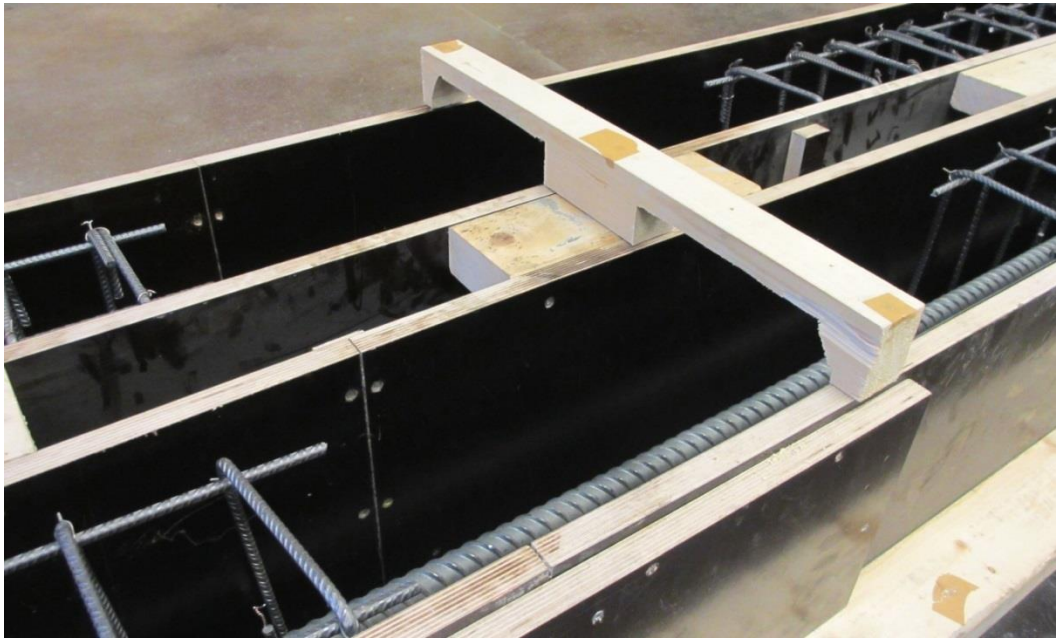
Figure 4.2. Side view of the reinforcement in the formwork with longitudinal top bars removed at mid-span.

4.2 Casting of the Concrete

As mentioned before each beam had a volume of 252 litres and the concrete mixer in the laboratory had a capacity of about 800 litres. Therefore it was possible to cast two beams (each concrete type, e.g. 1A and 1B) as well the test specimens in one batch from the mixer. Figure 4.3 shows an overview of the laboratory ready for casting.

The casting process took in all four days to complete with removal of the beams from the formwork one day after casting.

Figure 4.3. Overview of the laboratory with formwork for beams and test specimens ready for casting.

SINTEF was responsible for mixing all the concrete batches according to their own recipe which they have developed during the last years. Table 4.1 shows the ingredients used in the concrete mixes and the proportions they are mixed in.

Table 4.1. Materials in the concrete mixes.

Material	Recipe [kg/m^3]
Norcem Standard BP5/BP6	434,9
Elkem Microsilica 920 D	43,5
Limeston filler	4,3
Water	198,3
Absorbed water	10,7
Leca 2-4 mm (A-4048)	133,5
Leca 800 4-8 mm (A-4048)	237,8
0/8 mm NSBR (A-4045)	432,8
0/2 mm Filler sand (A-4045)	270,5
Sika FB2	7,8
Fibers (Varies in mixes)	-
• Dramix 65/60 - 1,0 % (Beams 2A & 2B)	78
• Dramix 65/35 - 1,0 % (Beams 3A & 3B)	78
• Basalt, gen. 3 - 1,0 % (Beams 4A & 4B)	19

The original recipes from SINTEF are presented in Appendix D. Beams 2A-2B, 3A-3B and 4A-4B all have two concrete recipes with different total volume of concrete. One set without fibres

and the other with fibres. This was done to improve the workability of the concrete when casting the bottom side of the beams with fibre-free concrete up to the upper side of the longitudinal bars where the concrete is theoretically in tension before adding the fibres in the concrete mix. Then the upper layer with fibre reinforced concrete was compacted well with the lower layer to secure good bonding between the layers. This should not have any effect on the test results since the critical area of the beam is the compression zone on the top side where the fibre reinforced concrete was placed. The first set of beams was casted with concrete skip but the last three sets of beams with the fibres the concrete was placed with wheelbarrows. After casting the beams they were covered in plastic to prevent drying shrinkage and cracking.

Figure 4.4. *Left:* **Casting of test cylinders on a vibrating table.** *Upper right:* **Slump test.** *Lower right:* **Formwork for the fibre test beams and cylinders.**

SINTEF also performed all testing of the fresh concrete, such as slump test, and casting of the test specimens and then subsequently the testing of them. For every set of beams there were made six test cylinders to test the compressive strength and oven dry density. Then for the beams with fibre reinforcement (i.e. beams 2A-2B, 3A-3B and 4A-4B) there were also made small-beam specimens to test the bending stiffness. Figure 4.4 shows these tests.

4.3   Removal of the Formwork and Storage of the Beams

The beams were removed from the formwork the day after casting when they had reached sufficient strength to carry their own weight. The beams were then moistened by placing soaking wet burlap sacks on top of the beams and then covered in plastic to keep them as humidified as possible, see figure 4.5. The test cylinders were also placed under the plastic with the main beams to keep them stored at the same conditions as the main beams.

Figure 4.5. *Left:* **Beams covered in plastic directly after casting.** *Right*: **Beams covered in burlap sacks after removal from the formwork and then covered in plastic again.**

5 Beam Testing

5.1 Set up

The testing took place in NTNU's laboratory testing hall in a testing rig mounted with HOWDEN 1000 kN hydraulic jack which was run by INSTRON 8800 operating console, see figure 5.1. The beams were fitted with in total seven inductive sensors on the exterior to measure the deflection and the strain in the upper and lower edges of the beam, see figure 5.1. In addition to this data, the load and the movement of the hydraulic jack was recorded in a testing log via Spider8 PC measurement electronics.

Figure 5.1. *Left*: **Testing rig in the laboratory with the beams north end on the left side on the picture and the south end on the right side of the picture.** *Upper right:* **Strain sensors on the beams west side.** *Lower right:* **Deflection sensors on the underside of the beam.**

5.2   Procedure

The beams were mounted on 180 mm wide thick (20 mm) steel plates and then on supporting solid steel rollers of diameter 50 mm. The support in North end was free to roll while the South support was fixed horizontally. On top of the concrete beam were comparable steel plates and steel rollers placed on wood fibre plates to form the loading roller support. The load from the hydraulic jack was then distributed by a strengthened HE260B steel beam onto the two loading points on the concrete beam to form the four point bending test as shown in figure 5.2.
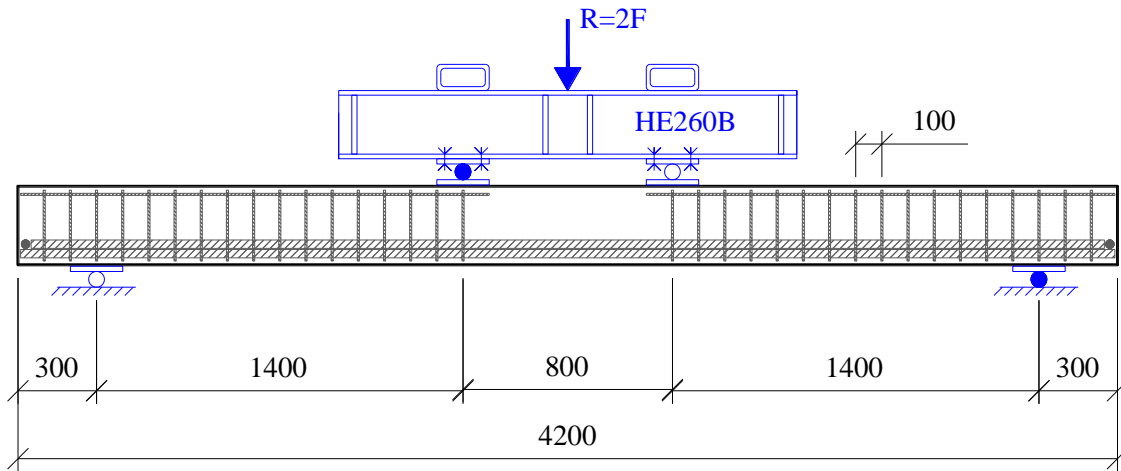
Figure 5.2. Loading set up of the test

Each beam was fitted with two inductive sensors parallel to the bottom side of the beam (IS1 and IS2), two inductive sensors parallel to the upper side of the beam (IS3 and IS4) to measure the concrete strain and then three inductive sensors were fitted perpendicular to the underside the beam to measure the deformation at the loading points (IS5 and IS7) and the middle of the beam (IS6). See the placement on figure 5.3 and cross-section of the bracket and sensors in figure 6.6.
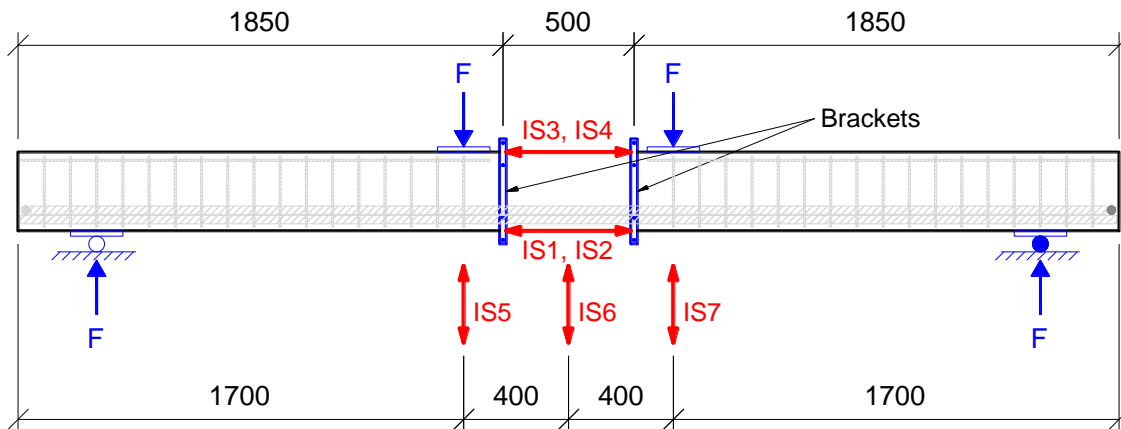
Figure 5.3. Placement of the inductive sensors (IS)

28

The loading was carried out in three levels, at 25 kN, 50 kN and 75 kN loading. Then run until failure and finally to test end. Test end was when the beams deflection had increased of 20 mm above the failure point.

Between the loading levels there was a five minute break to mark the cracks that had developed. This procedure was photographed from two angles, showing the north and south ends separately, see example of beam 1B in figure 5.4 for loading level 1 and the final position of the beam.

Figure 5.4. Example of the loading procedure for beam 1B from two angles. 25 kN load in the upper pictures and cracking at end of test in the lower picture.

Since it is so difficult the see the cracking development on the beams on these pictures, there will rather be shown pictures of the total loading procedure for beam 4B from the north-end angle in figure 5.5 on the following page. The cracking development was generally very similar on north and south end for all the beams, so it is enough to see one end of the beam.

Figure 5.5. Test procedure for beam 4B. The load at each loading level is indicated on the pictures but the last picture shows the cracking at mid span for the final load at the end of test.

6 Test Results

In this chapter the test results will be presented. First by comparing the loading time, deflection and concrete strain of all the beams. Then by describing the testing of every beam separately in the following sections.

Load forces in tables, diagrams and the main text corresponds to one of the two applied loads, defined as F in figure 5.3, e.g. not the total applied force from the hydraulic jack.

6.1 Loading Time

The loading procedure was almost identical for all the beams to loading level 3 at 75 kN pressure as the diagram in figure 6.1 shows. But then it differed about five minutes when the beams reached their failure load. Table 6.1 lists up the time until failure load for all eight beams.

Table 6.1. Time until failure load

Beam	1A	1B	2A	2B	3A	3B	4A	4B
	Only LWAC		Dramix 65/60		Dramix 65/35		Basalt gen. 3	
Time till failure [min]	46	45	50	49	47	49	48	49
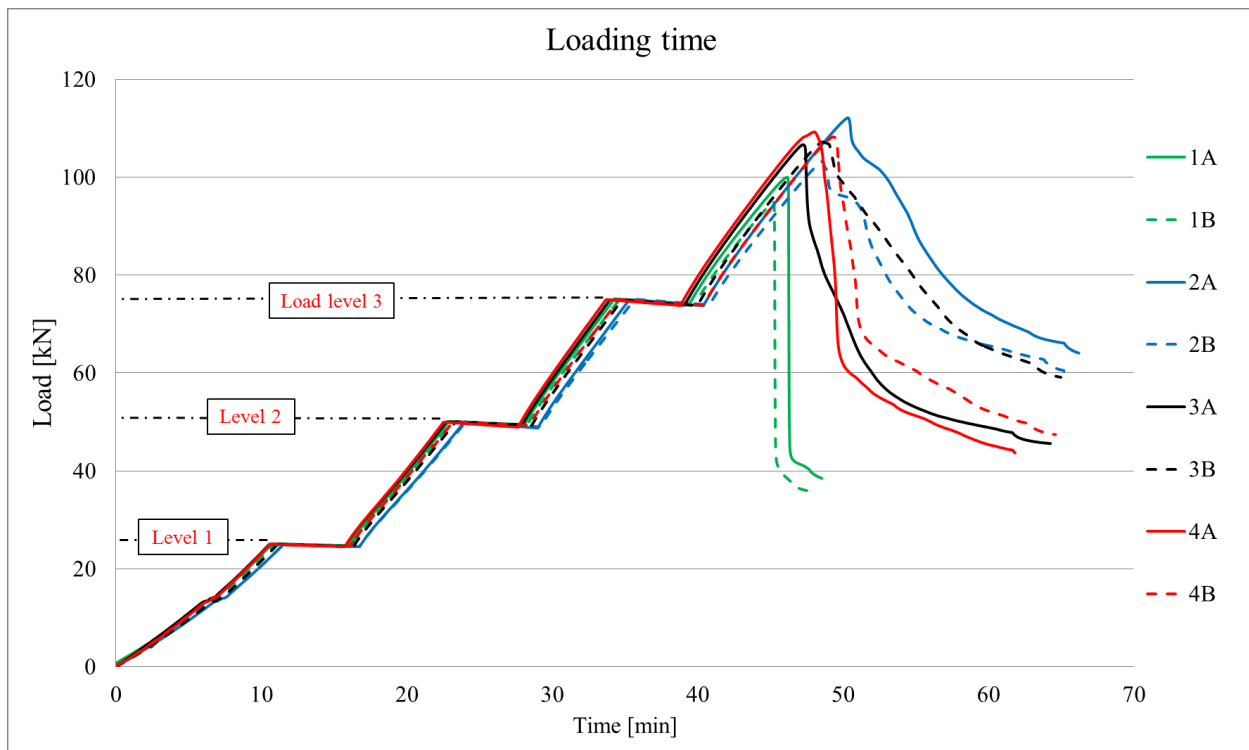
Figure 6.1. Loading time for all 8 beams.

6.2 Deflection

As mentioned before the deflection was measured at three points, below the two loading points and at the middle of the beam. Comparison of the three measuring points will be done for each beam in chapter 6.4. When comparing the deflection of the beams at the middle it is obvious that all the beams deflected in a very similar way until the failure load was reached. Then post-failure the fibres started affecting the deflection curve. The failure load and deflection at failure point are found in table 6.2 and figure 6.2 shows the deflection of all the beams at the middle, then a close-up of the failure point is shown in figure 6.3.

Table 6.2. Failure load and deflection at failure

Beam	1A	1B	2A	2B	3A	3B	4A	4B
Failure Load [kN]	100,0	94,9	112,2	103,2	106,6	107,2	109,2	108,2
Deflection at middle [mm]	22,3	21,1	25,2	23,3	22,6	23,4	24,5	23,9
Hardening time [days]	36	37	37	38	36	36	39	39
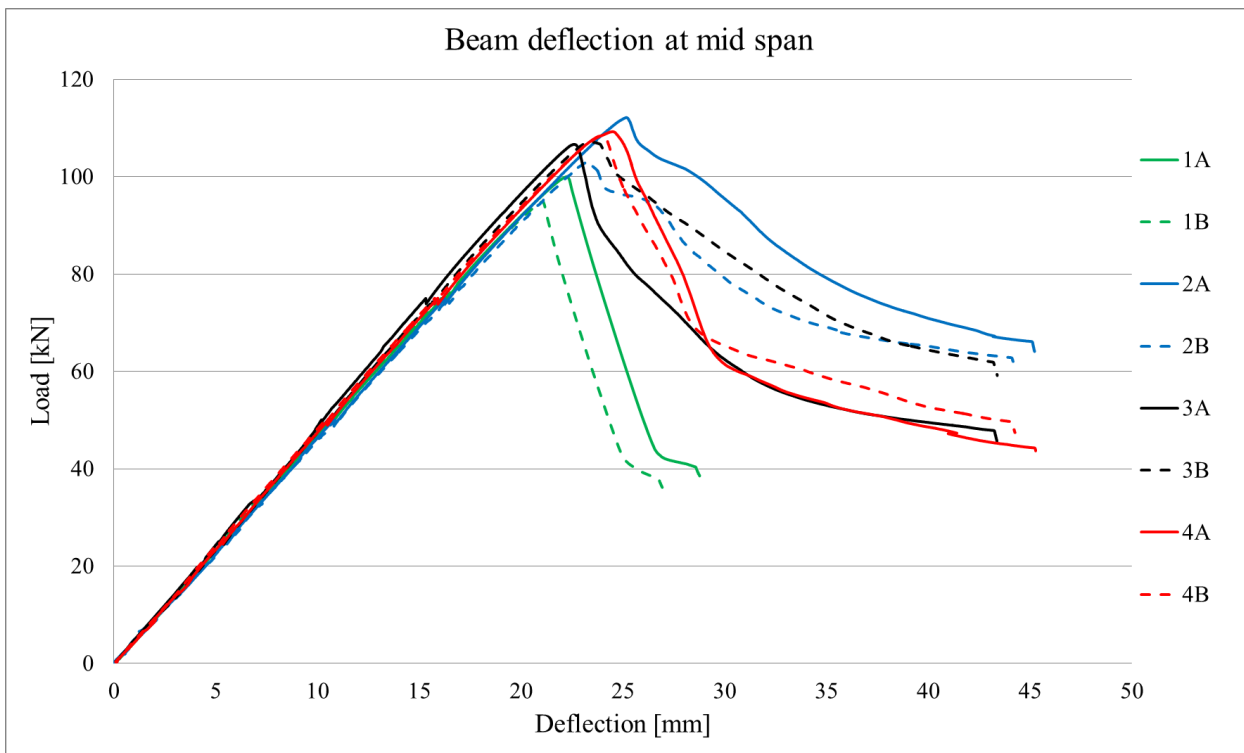
Figure 6.2. Deflection at mid span of all 8 beams

It is difficult to compare the effect from the different fibre types since the beams have different failure loads. Then it is possible to normalize the diagram to gather all the failure points in one point as done in figure 6.4 with close-up of the failure point and post-failure curves.
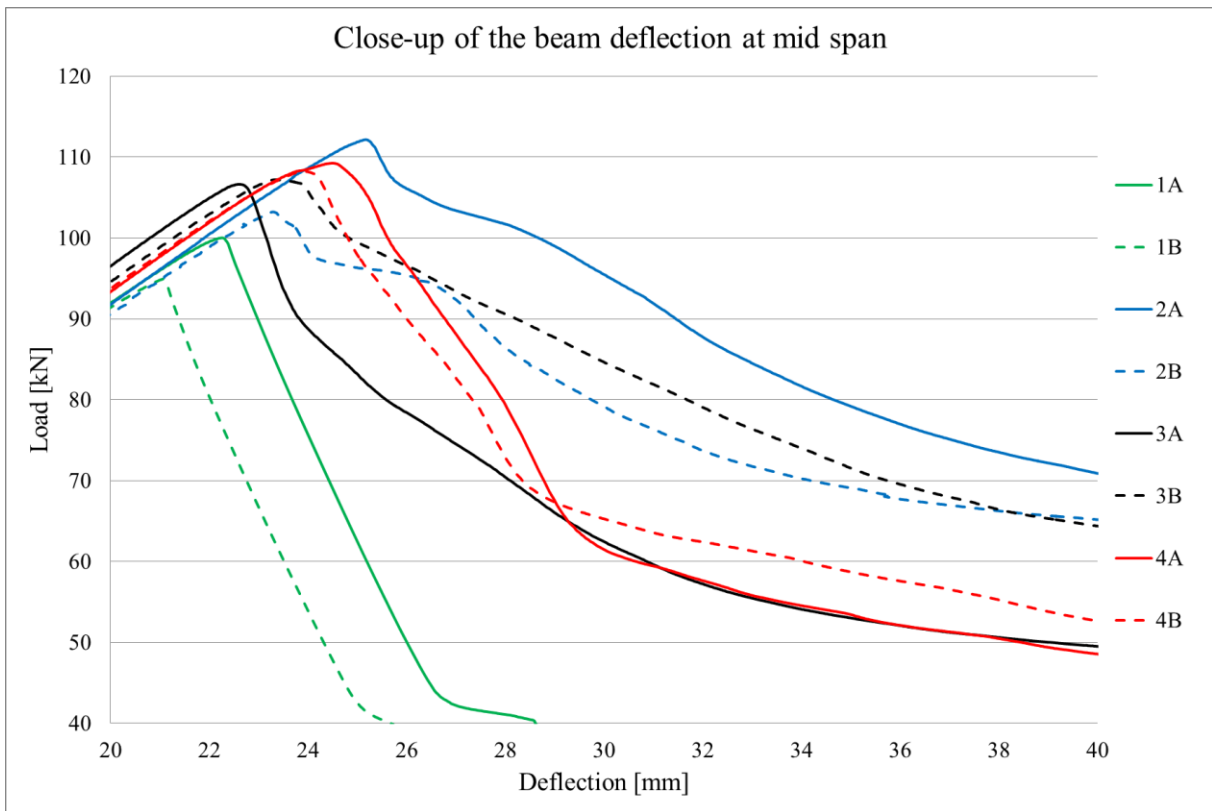
Figure 6.3. Close-up of the failure point
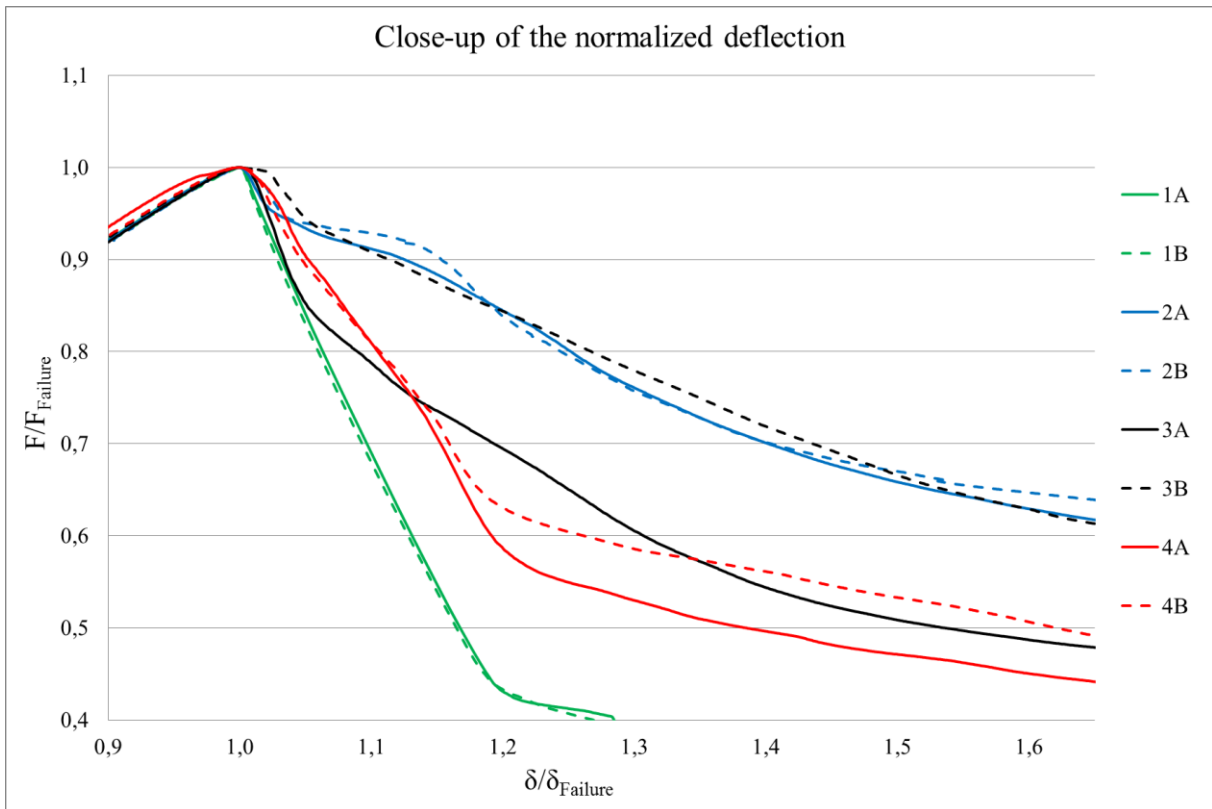
Figure 6.4. Close-up of the normalized deflection diagram

33

One possible method to measure the ductility of the beams it is to compare the load bearing capacity of the beams post failure point. To evaluate the loss of load bearing capacity post the failure point I find the value of deflection of the beams when the load bearing capacity has dropped down to 80% of the failure load post the failure point. Table 6.3 and figure 6.5 show this deflection and the deflection at each loading level (L.L.) before failure.

Table 6.3. Deflection at 80% of the load bearing capacity post-failure point.

Beam	1A	1B	2A	2B	3A	3B	4A	4B
Deflection at L.L. 1 [mm]	5,4	5,3	5,5	5,6	5,1	5,4	5,3	5,2
Deflection at L.L. 2 [mm]	10,7	10,5	10,8	10,9	10,2	10,5	10,5	10,4
Deflection at L.L. 3 [mm]	16,2	16,1	16,3	16,5	15,3	15,6	15,9	15,8
Deflection at failure point [mm]	22,3	21,1	25,2	23,3	22,6	23,4	24,5	23,9
Deflection at 80% Loading post-failure [mm]	23,7	22,3	31,5	29,0	24,6	29,6	27,1	26,5
ΔDeflection post-failure point [mm]	**1,4**	**1,3**	**6,3**	**5,7**	**2,0**	**6,3**	**2,6**	**2,5**
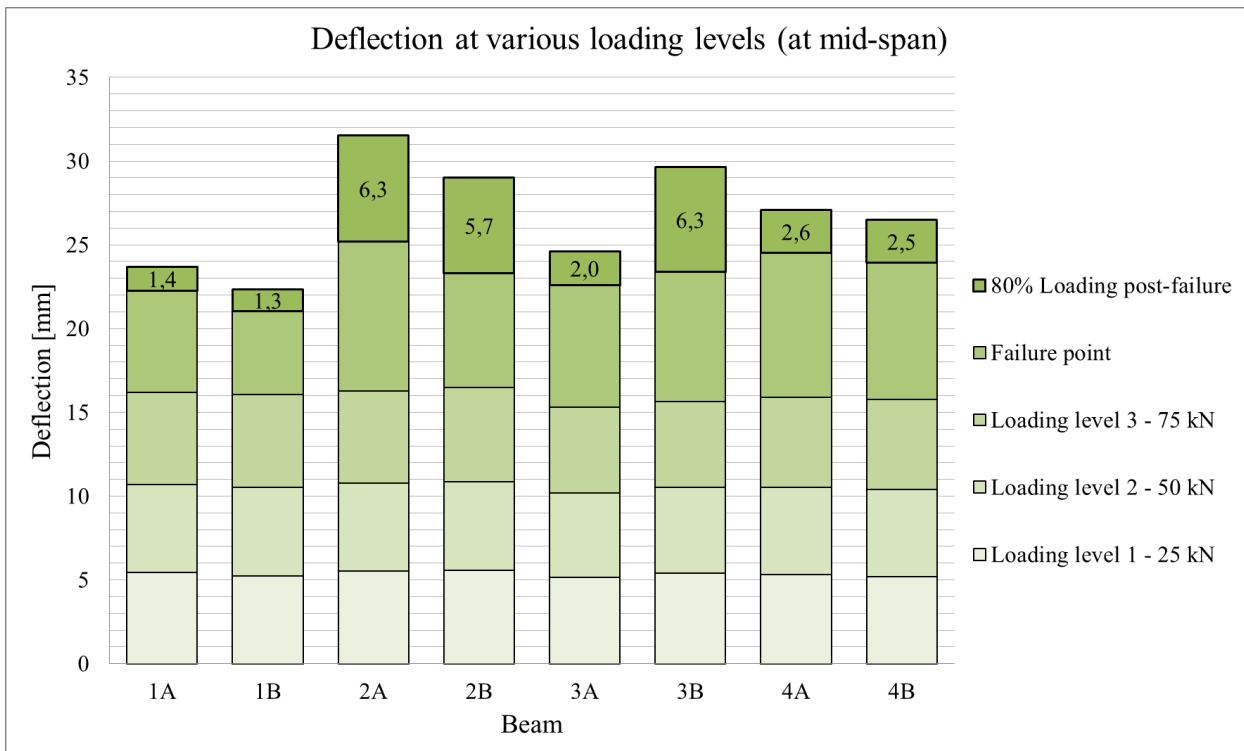
Figure 6.5. Deflection of the beams at 80% load bearing capacity post failure point.

6.3 Concrete Strain

The longitudinal concrete strain was measured with four inductive sensors located on the exterior of the beams. These sensors were placed on two brackets, each offset 250 mm from the centre line of the beam or 500 mm apart. The bottom sensors, IS1 and IS2, measured the elongation in the bottom while the sensors in the top, IS3 and IS4, measured the shortening in the top of the beam. IS1 and IS3 are on the east side and IS2 and IS4 are on the west side. Cross-section of the beam with brackets and sensors is shown in figure 6.6 and placement of the brackets was shown in figure 5.3.
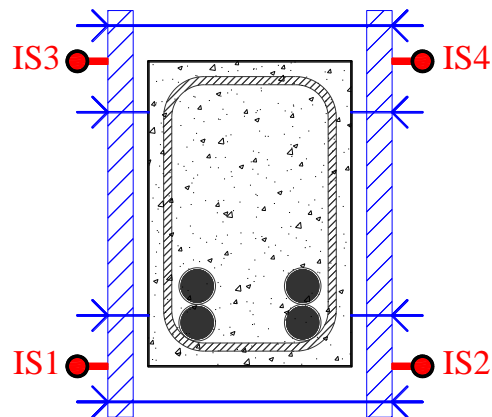
Figure 6.6. Cross-section of the beam showing the brackets and inductive sensors to measure the strain. IS1 and IS3 are on the east side and IS2 and IS4 are on the west side.

Two sensors are used on each edge of the beam to check for errors or misreading in the sensors. Much difference in the measurements on each edge of the beam could indicate if there was some warping of the beam if not just a misreading.

There were no abnormal differences in the readings from the top and bottom edge sensors so the results are presented with the average values of these measurements for all the beams. Which are plotted in figures 6.7 and 6.8 for the top and the bottom edge of the beam respectively.

The upper side of the beam has compressive strain and is therefore a negative value while the bottom side has tensile strain and has a positive value.

The diagram for strain at top edge corresponds very well with the Load-deflection diagram in figure 6.2.
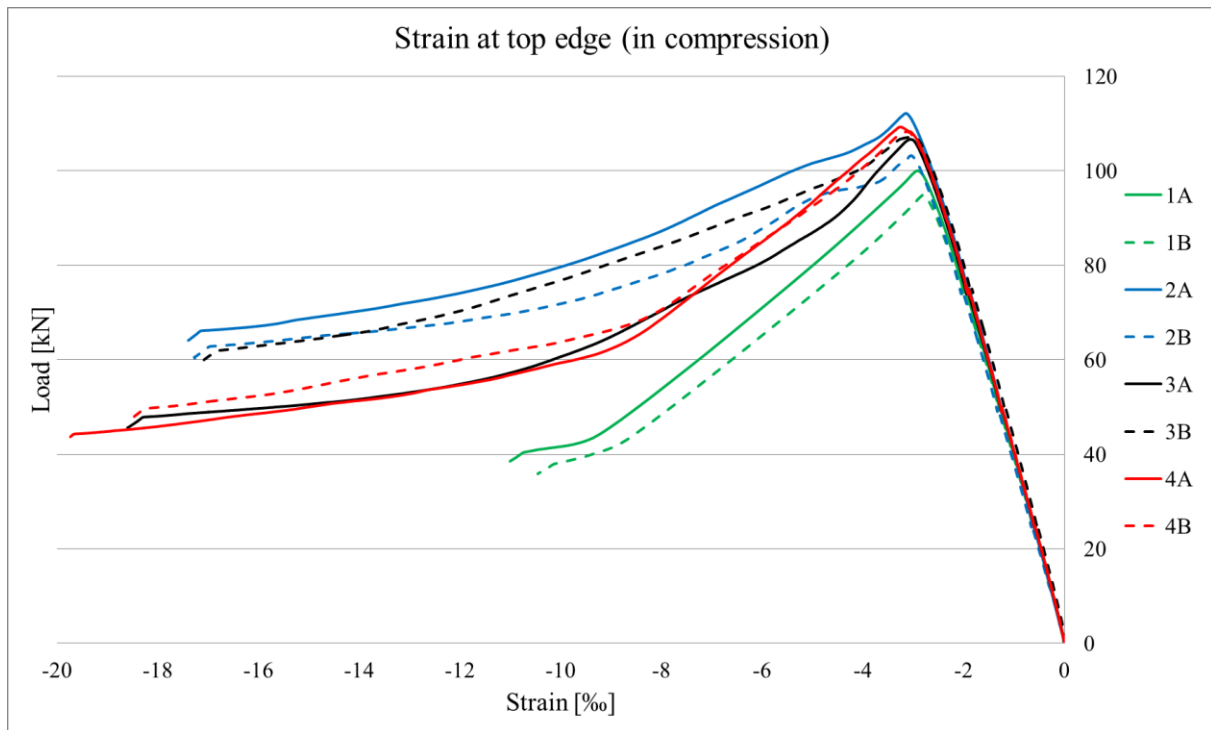
Figure 6.7. Strain at upper edge of all 8 beams.
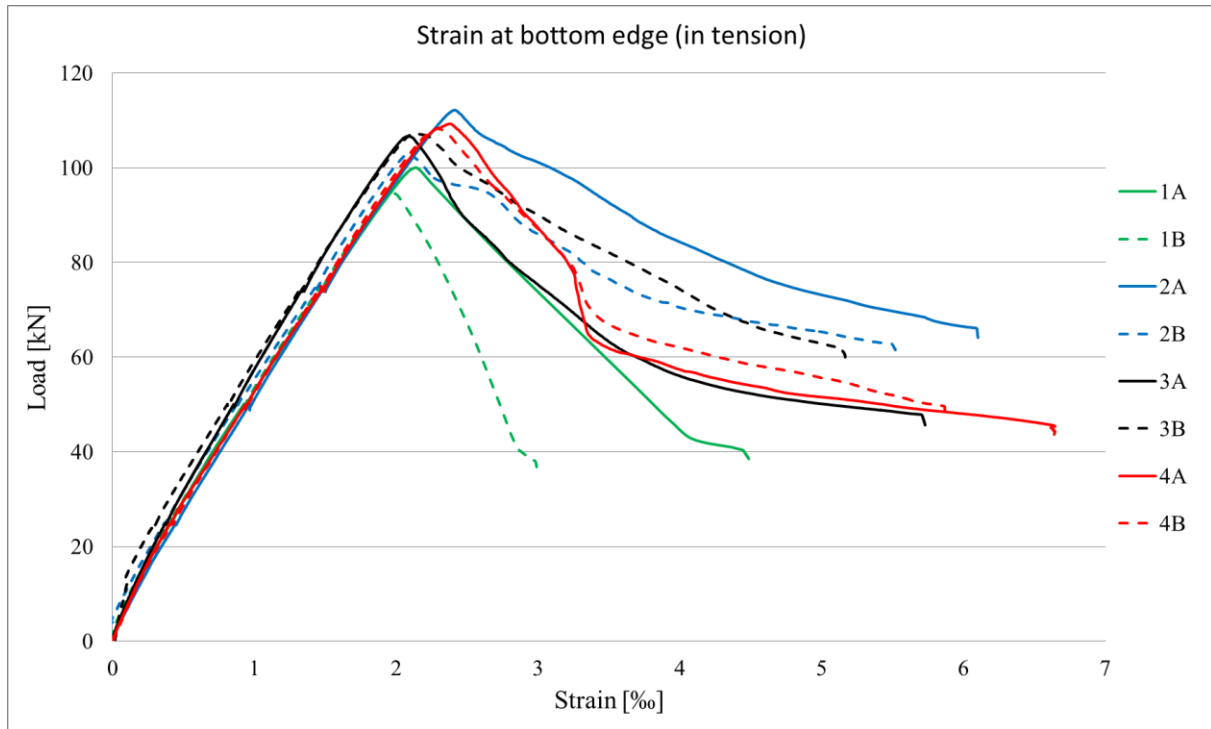
Figure 6.8. Strain at lower edge of all 8 beams.

36

6.4 Beams

Three sensors measured the deflection of the beams. One sensor was placed at mid span of the beam (called middle in the diagrams) and then there were two sensors placed directly below the loading points, or 400 mm away from the middle in both directions (called north and south in the diagrams).

Here will the test procedure for each beam be described. Two diagrams are shown for each beam. First the deflection measured by all the three sensors is plotted in a diagram in addition to the calculated deflection at the middle for comparison. Then the concrete strain in top and bottom of the beam is compared to the calculated values of the concrete strain.

The calculated values are found by input of the compressive strength and oven-dry density from the cylinder compression test (section 6.5.1) in the calculations that were done previously in chapter 3.2. Results of the calculations of the test beams are found in table 6.4.

Table 6.4. Tested and calculated values of failure load, deflection and concrete strain.

Beam	1A	1B	2A	2B	3A	3B	4A	4B
Type of fiber	**Only LWAC**		**Dramix 65/60**		**Dramix 65/35**		**Basalt gen. 3**	
Tested failure Load [kN]	100,0	94,9	112,2	103,2	106,6	107,2	109,2	108,2
Tested deformation at middle [mm]	22,3	21,1	25,2	23,3	22,6	23,4	24,5	23,9
Tested strain at top [‰]	-2,91	-2,80	-3,15	-3,05	-3,05	-3,01	-3,26	-3,13
Tested strain at bottom [‰]	2,13	1,97	2,42	2,09	2,09	2,13	2,38	2,29
Calculate failure load [kN]	**124,8**		**120,2**		**122,6**		**123,7**	
Calculated deformation at middle [mm]	**25,2**		**23,4**		**23,8**		**24,7**	
Calcualted strain at top - ε_{lcu3}' [‰]	**-3,19**		**-2,92**		**-2,96**		**-3,11**	
Calcualted strain at bottom - ε_{lcu3} [‰]	**2,79**		**2,64**		**2,69**		**2,75**	

6.4.1 Beam 1A and 1B

Beams 1A-1B are the only beams that were not fibre reinforced and are therefore the base point for the fibre reinforced beams. As expected these beams had the lowest failure load and lost all bearing capacity as soon as they reached the failure load.   The failure was very brittle and clean.

6.4.1.1 Beam 1A

Beam 1A started cracking at about 20 kN load and had failure load of 100,0 kN at 22,3 mm deflection at mid span when it immediately dropped down to about 42 kN load resistance in about 30 seconds. Figures 6.9 and 6.10 show the deflection and concrete strain and figures 6.11 and 6.12 show the final cracking of the beam at the end of the testing.

Figure 6.9. Load-deflection diagram at the three measuring points for beam 1A.

Figure 6.10. Top and bottom concrete strain of beam 1A.

38

Figure 6.11. Final cracking on the west side of beam 1A.
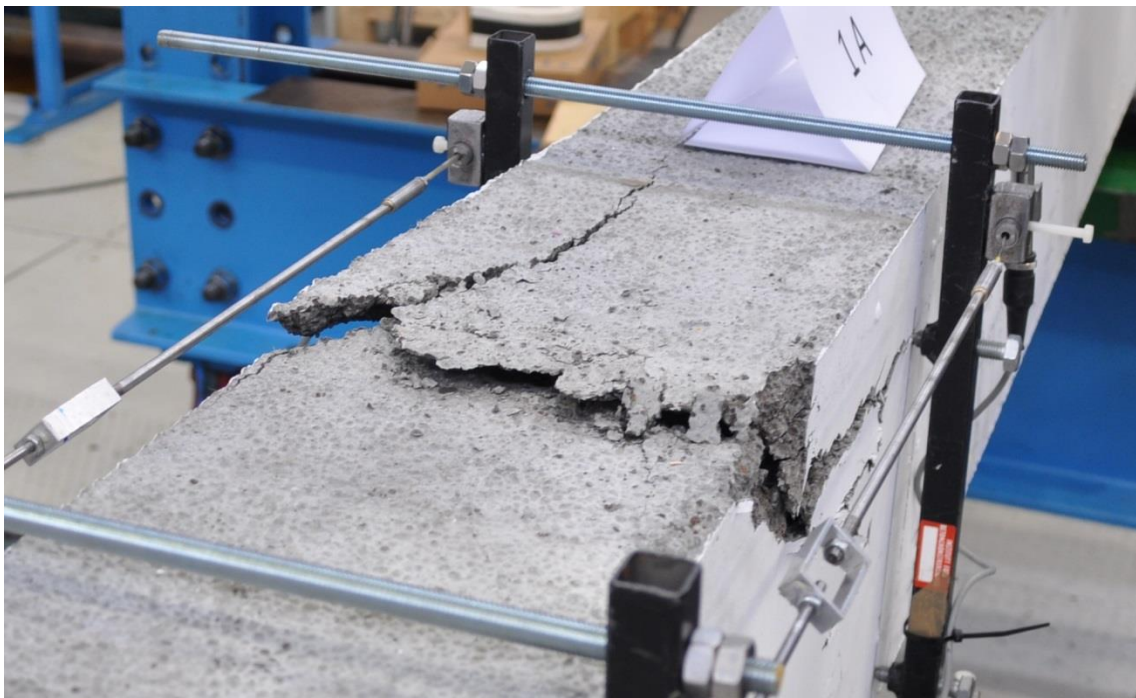
Figure 6.12. Spalling on the top of beam 1A.

6.4.1.2 Beam 1B

Beam 1B started cracking at about 20 kN load as well as beam 1A and had failure load of 94,9 kN at 21,1 mm deflection at the middle when it immediately dropped down to about 40 kN load resistance in about 30 seconds also. Figures 6.13 and 6.14 show the deflection and concrete strain and figures 6.15 and 6.16 show the final cracking of the beam at the end of the testing.
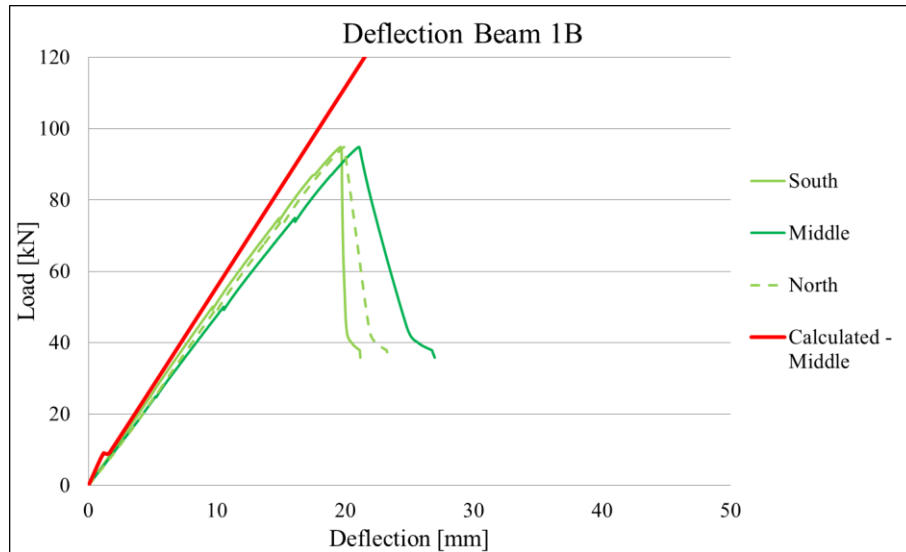
Figure 6.13. Load-deflection diagram at the three measuring points for beam 1B.
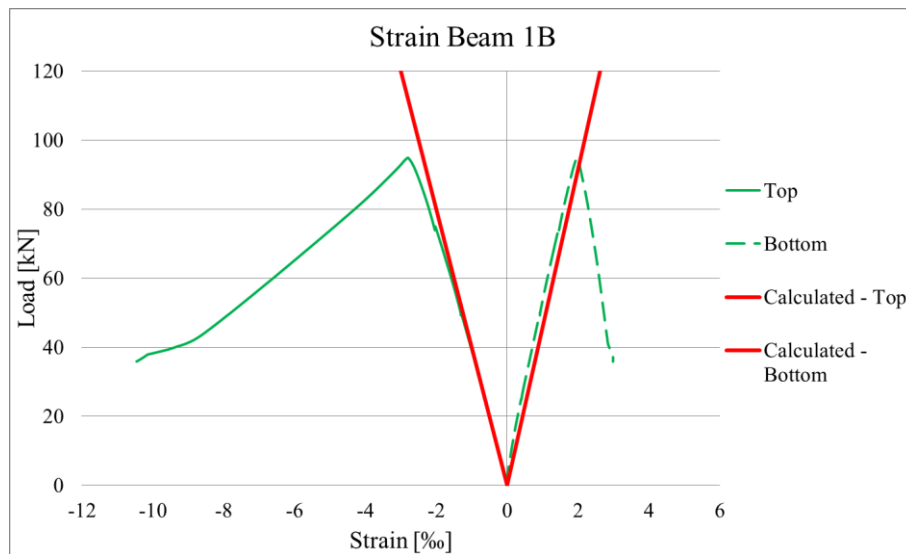
Figure 6.14. Top and bottom concrete strain of beam 1B.

Figure 6.15. Final cracking on the west side of beam 1B.

Figure 6.16. Piece of the top of beam 1B removed after testing.

6.4.2   Beam 2A and 2B

Beams 2A-2B had Dramix 65/60 steel fibres (1,0 volume%). The beams lost some load bearing capacity immediately at failure point, but then recovered soon some resistance to the loading. Testing was ended when the deflection had increased by 20 mm above the failure point.

6.4.2.1   Beam 2A

Beam 2A started cracking at about 21 kN load and had failure load of 112,2 kN at 25,2 mm deflection at the middle when it immediately dropped down to about 107 kN load resistance. Then it gradually levelled out and held some load resistance until the test ended at 64 kN. Figures 6.17 and 6.18 show the deflection and concrete strain and figures 6.19 and 6.20 show the final cracking of the beam at the end of the testing.
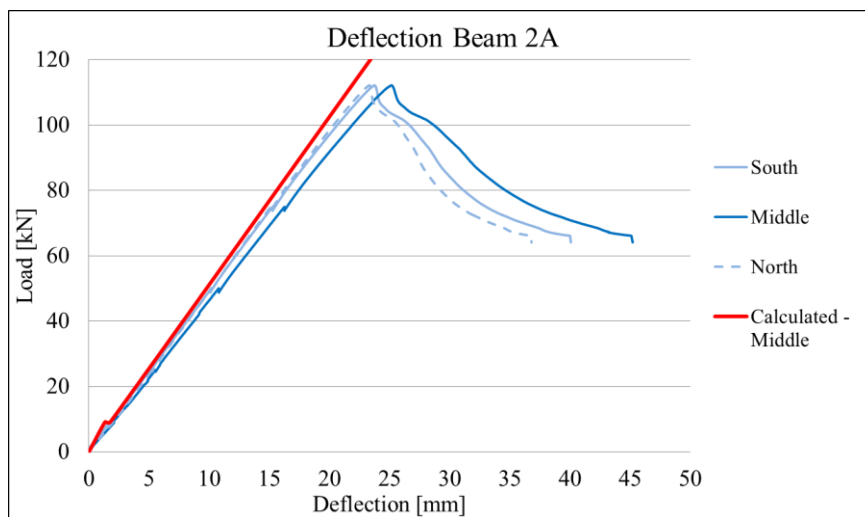
Figure 6.17.   Load-deflection diagram at the three measuring points for beam 2A.
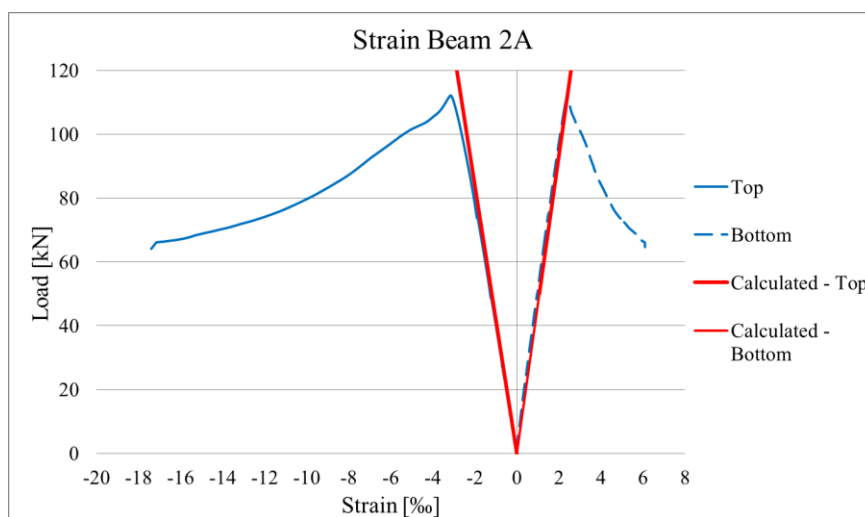
Figure 6.18.   Top and bottom concrete strain of beam 2A.

42
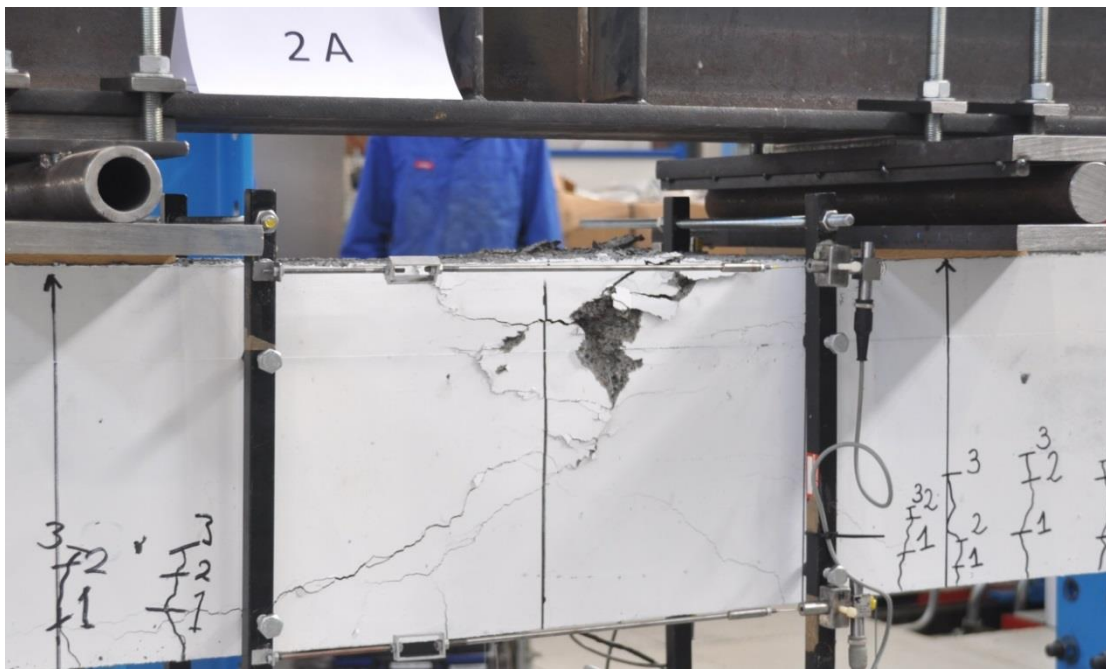
Figure 6.19. Final cracking on the west side of beam 2A.

Figure 6.20. Final cracking on the east side of beam 2A.

Comments to the testing:

- The failure mode and cracking of beams 2A - 2B was quite different from beams 1A - 1B
- Finer cracks
- Smaller spalling particles, more "chip" like
- More distortion at the sides of the beams

6.4.2.2 Beam 2B

Beam 2B started cracking at about 17,5 kN load and had failure load of 103,2 kN at 23,3 mm deflection at the middle when it immediately dropped down to about 97 kN load resistance. It had a very similar behaviour as beam 2A when it levelled out until the test ended at 60 kN. Figures 6.21 and 6.22 show the deflection and concrete strain and figures 6.23 and 6.24 show the final cracking of the beam at the end of the testing.
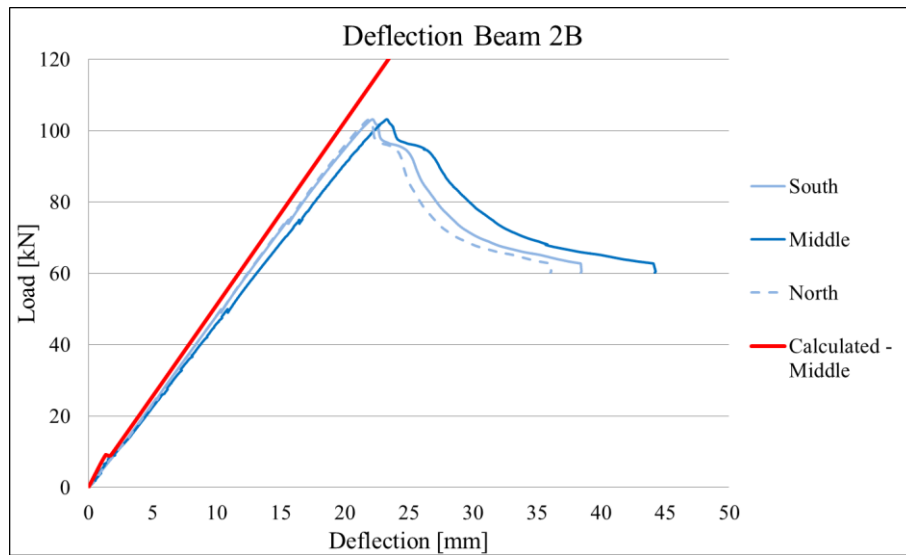
Figure 6.21. Load-deflection diagram at the three measuring points for beam 2B.
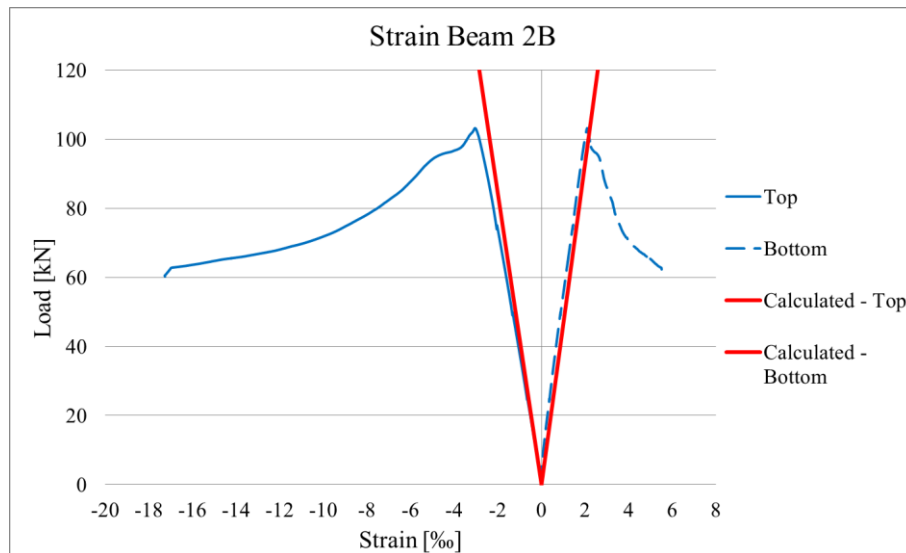
Figure 6.22. Top and bottom concrete strain of beam 2B.

44
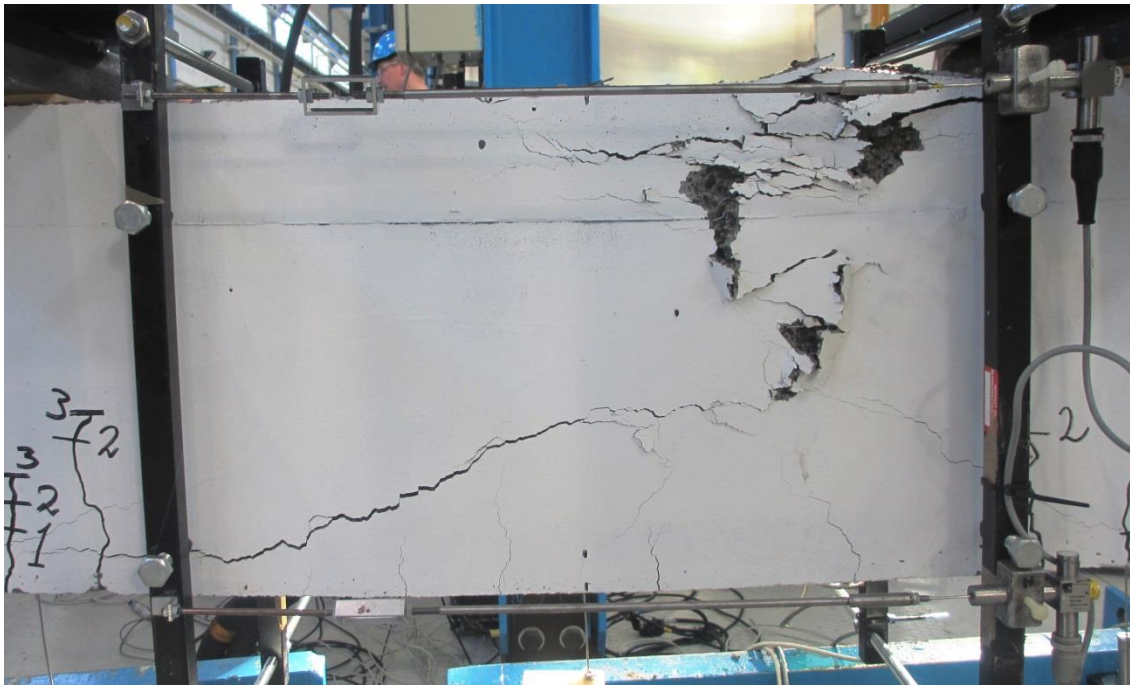
Figure 6.23. **Final cracking on the west side of beam 2B.**

Figure 6.24. **Final cracking on the top and west side of beam 2B.**

Comments to the testing:

- A restart was made after about three minute running time, or at 4,4 kN load because of a loose strain sensor at the lower edge of the beam.

6.4.3 Beam 3A and 3B

Beams 3A-3B had Dramix 65/35 steel fibres (1,0 volume%). These beams were expected to do somewhat worse than beams 2A-2B since they had smaller fibres. The results from these two beams varied the most out of all of the four beam types. Beam 3A lost much load bearing capacity really fast while beam 3B withheld much more of its capacity like beams 2A-2B. The beams had very similar failure load but beam 3A had about 15 kN lower load resistance then 3B at the end of the testing, when the beams had deflected 20 mm in excess of the failure deflection.

6.4.3.1 Beam 3A

Beam 3A started cracking at about 20,5 kN load and had failure load of 106,6 kN at 22,6 mm deflection at the middle when it dropped immediately down to about 93 kN load resistance. Then it continued to decrease much more than beams 2A-2B until it reached 60 kN when it started levelling out like beams 2A-2B had done until the ending of the testing at 46 kN. Figures 6.25 and 6.26 show the deflection and concrete strain and figure 6.27 shows the final cracking of the beam at the end of the testing.
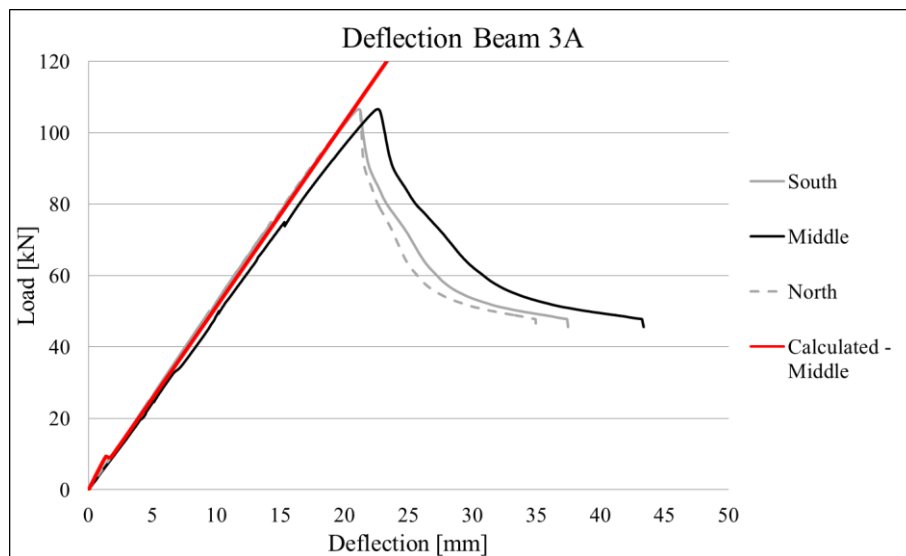
Figure 6.25. Load-deflection diagram at the three measuring points for beam 3A.

46
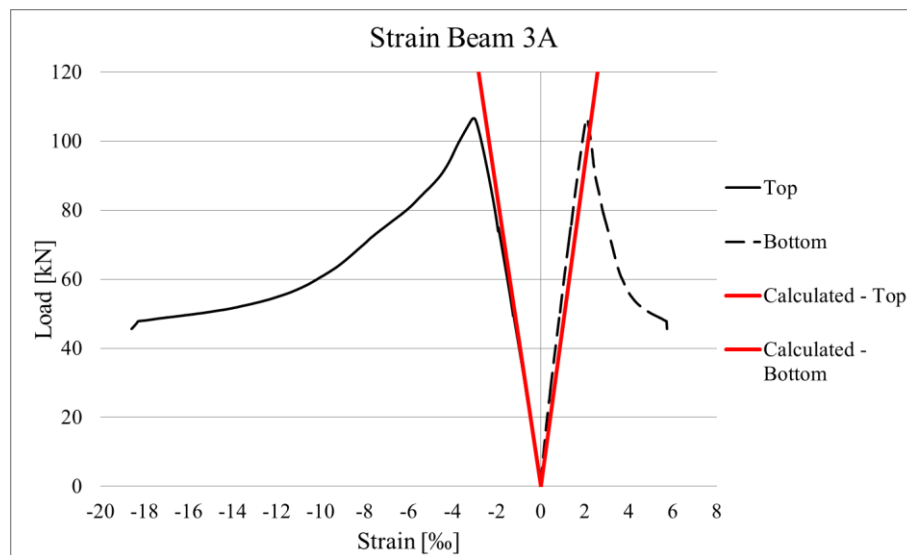
Figure 6.26. Top and bottom concrete strain of beam 3A.
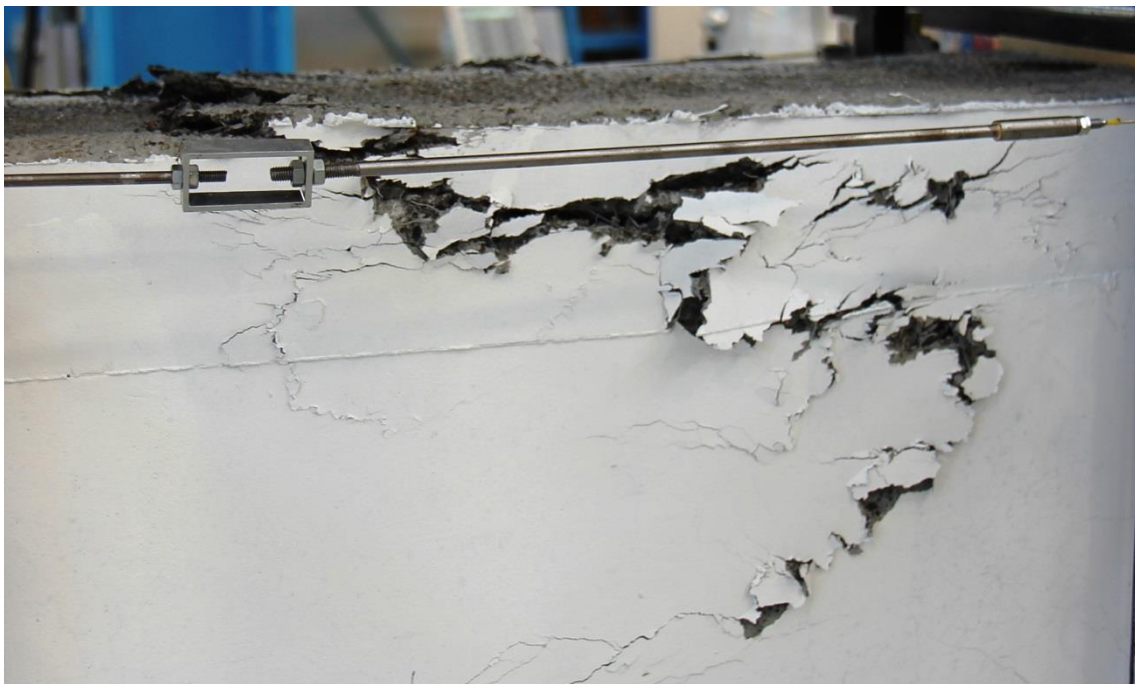
Figure 6.27. Final cracking on the top and west side of beam 3A.

47

6.4.3.2 Beam 3B

Beam 3B started cracking at about 16,5 kN load and had failure load of 107,2 kN at 23,4 mm deflection at the middle when it dropped immediately down to about 100 kN load resistance. Then it gradually levelled out in a similar way as beams 2A-2B and held some load resistance until the ending of the testing at 62 kN. Figures 6.28 and 6.29 show the deflection and concrete strain and figures 6.30 and 6.31 show the final cracking of the beam at the end of the testing.
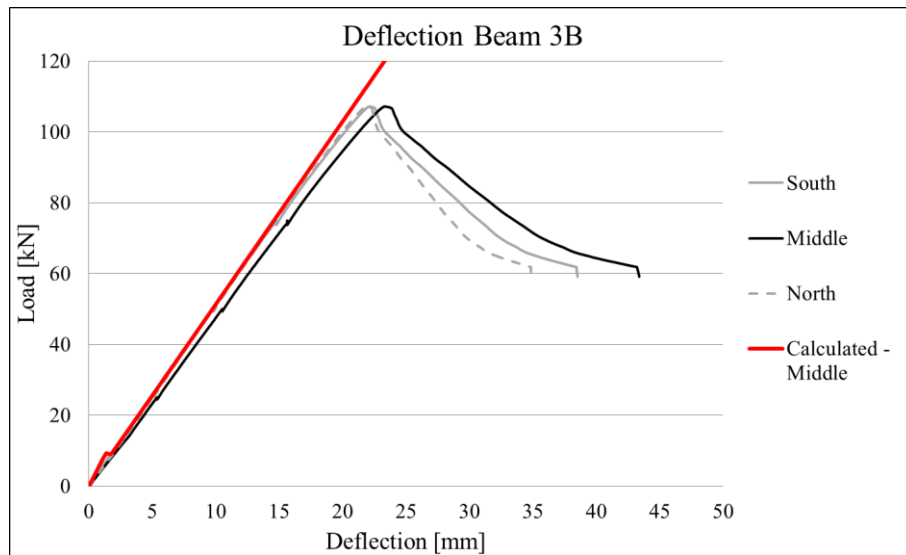
Figure 6.28. Load-deflection diagram at the three measuring points for beam 3B.
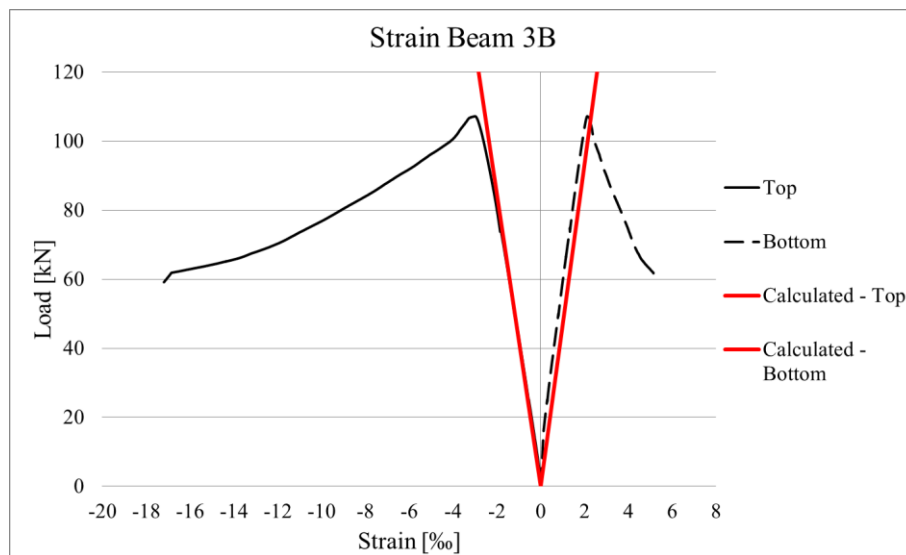
Figure 6.29. Top and bottom concrete strain of beam 3B.

48
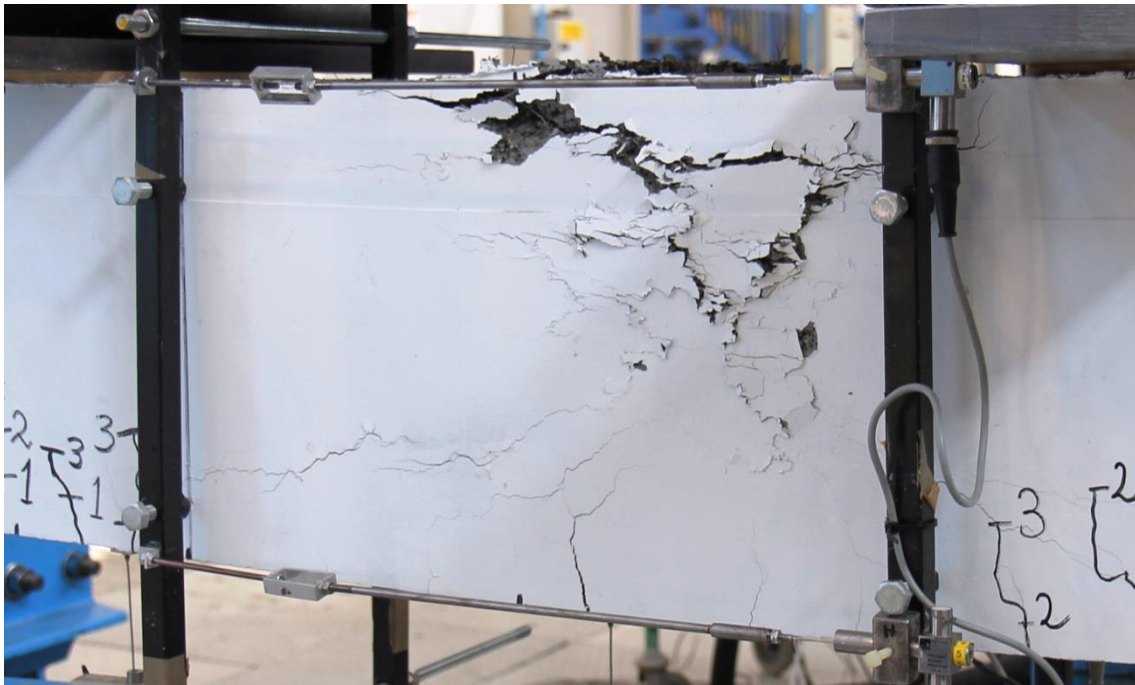
Figure 6.30. Final cracking on the west side of beam 3B.

Figure 6.31. Final cracking on the top and west side of beam 3B.

Comments to the testing:

- ◻ Loose strain sensor at the bottom west side of the beam was tightened at approximately 13 kN load.

6.4.4   Beam 4A and 4B

Beams 4A-4B had Basalt fibre MiniBars generation 3 (1,0 volume%). These beams had the most viscous failure peaks of all the beams. The load bearing capacity dropped very rapidly after the failure load like the non-fibre reinforced beams 1A-1B. Then they recovered at about 65-70 kN load resistance when they gradually levelled out until the end of the testing, which was as before when the deflection had increased by 20 mm above the failure deflection.

6.4.4.1 Beam 4A

Beam 4A started cracking at about 19 kN load and had failure load of 109,2 kN at 24,5 mm deflection at the middle when it dropped down to about 65 kN load resistance. Then it gradually levelled out and held some load resistance until the ending of the testing at 44 kN. Figures 6.32 and 6.33 show the deflection and concrete strain and figure 6.34 shows the final cracking of the beam at the end of the testing.
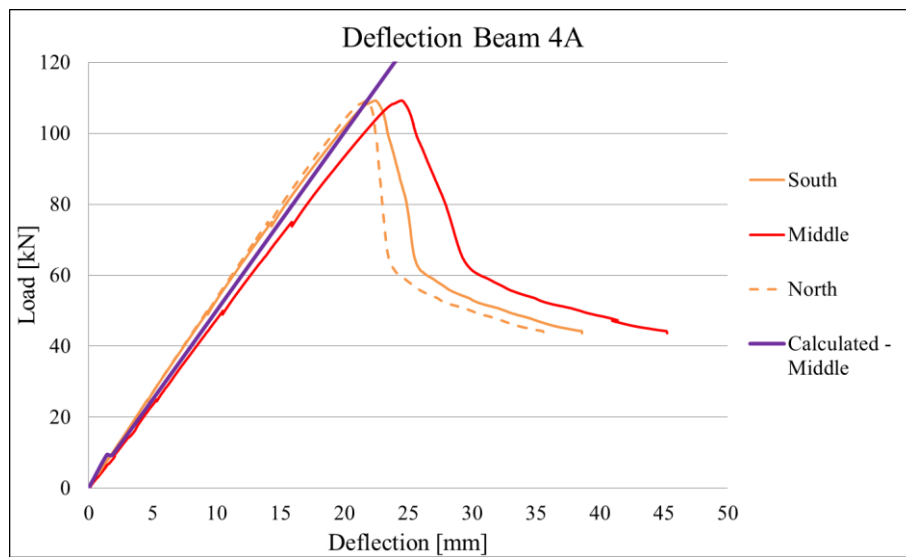
Figure 6.32. Load-deflection diagram at the three measuring points for beam 4A.
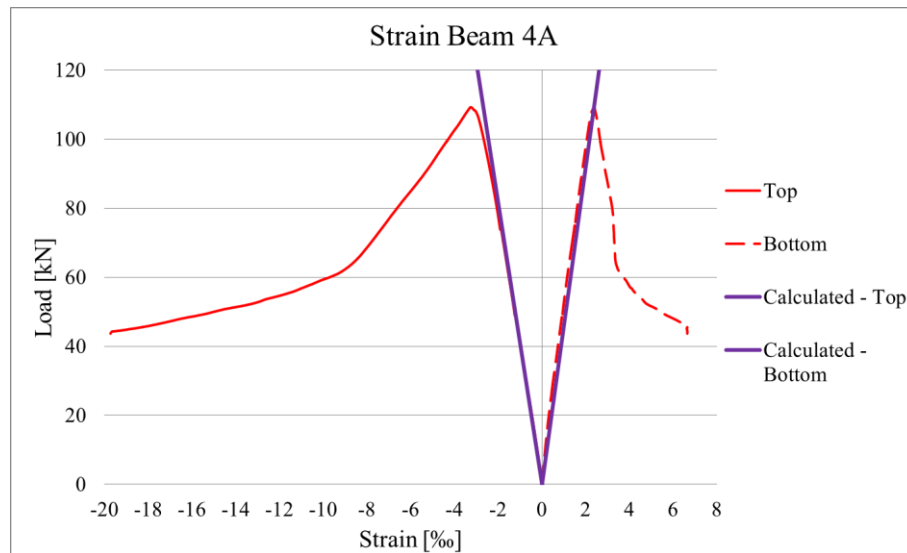
Figure 6.33. Top and bottom concrete strain of beam 4A.
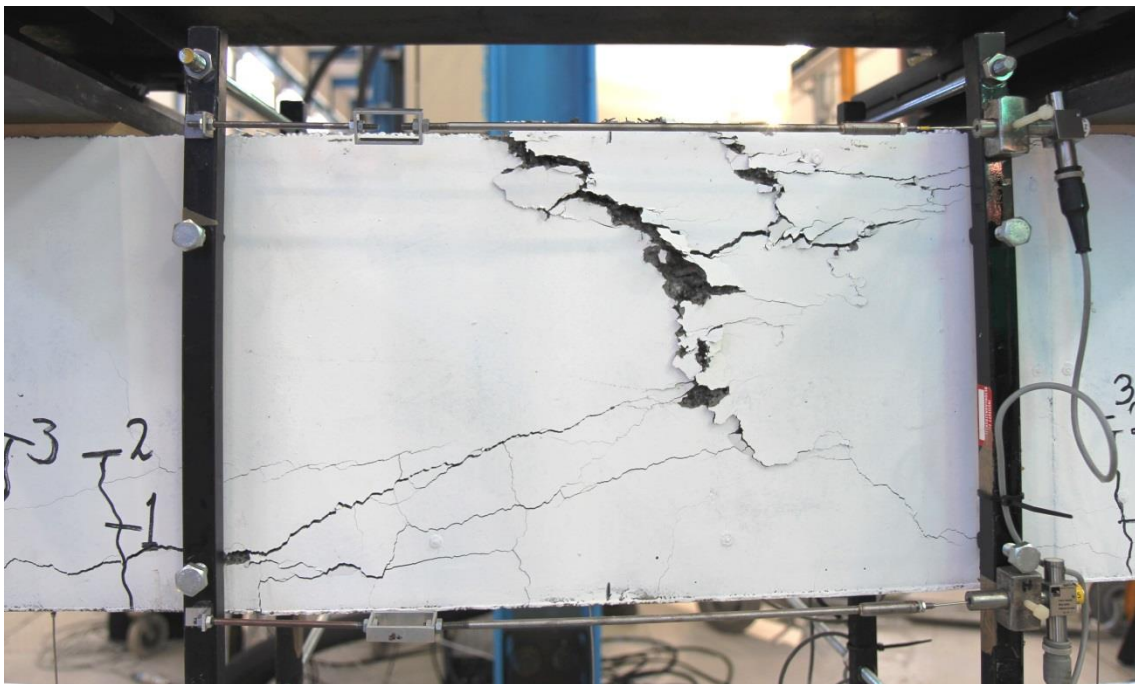
Figure 6.34. Final cracking on the west side of beam 4A.

6.4.4.2 Beam 4B

Beam 4B started cracking at about 16 kN load and had failure load of 108,2 kN at 23,9 mm deflection at the middle when it dropped down to about 68 kN load resistance. Then it levelled out and held some load resistance until the ending of the testing at 49 kN. Figures 6.35 and 6.36 show the deflection and concrete strain and figures 6.37 and 6.38 show the final cracking of the beam at the end of the testing.
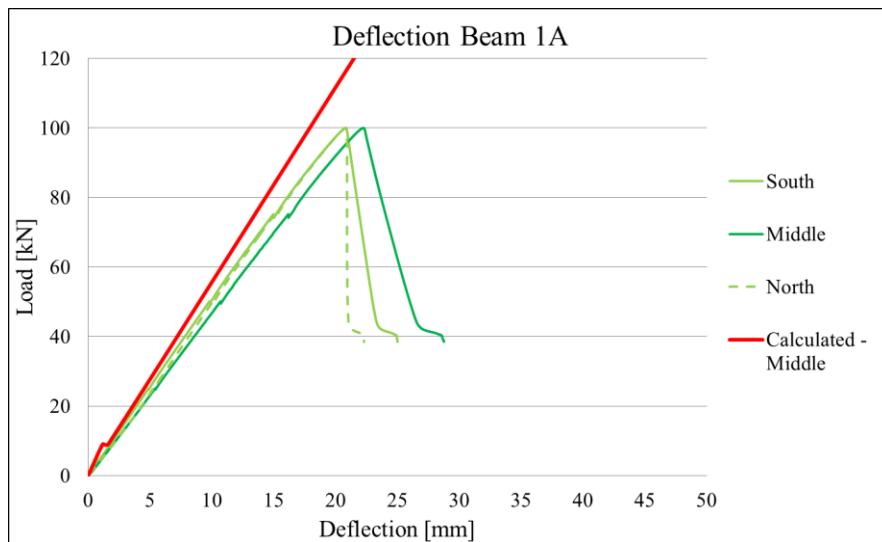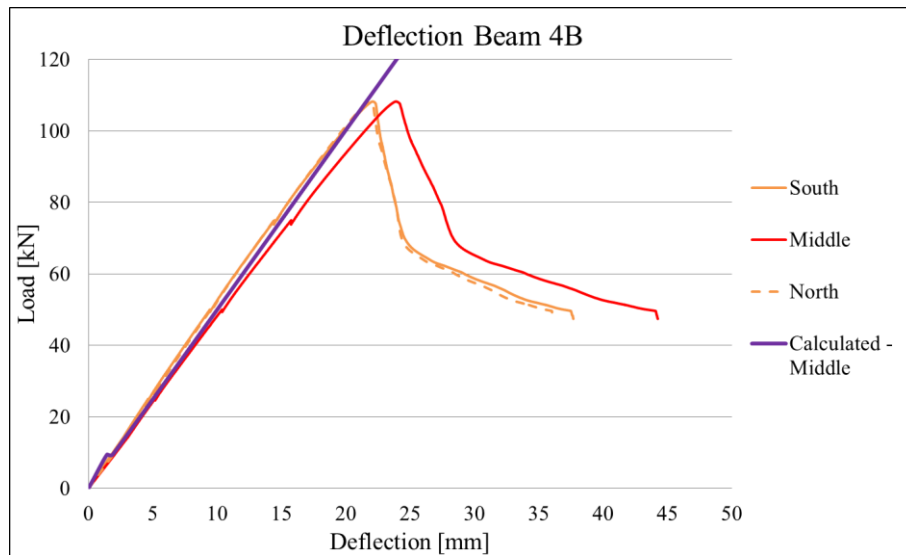

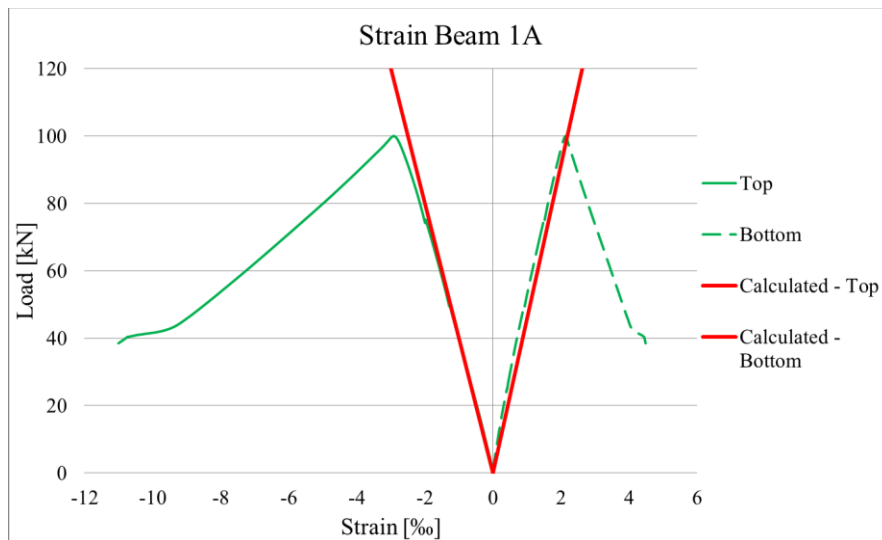**Figure 6.35. Load-deflection diagram at the three measuring points for beam 4B.**
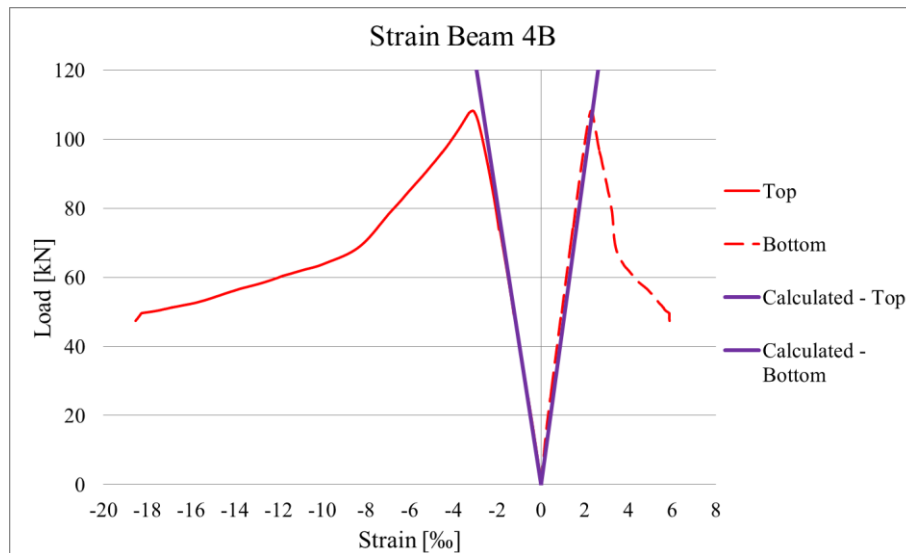
Figure 6.36. Top and bottom concrete strain of beam 4B.
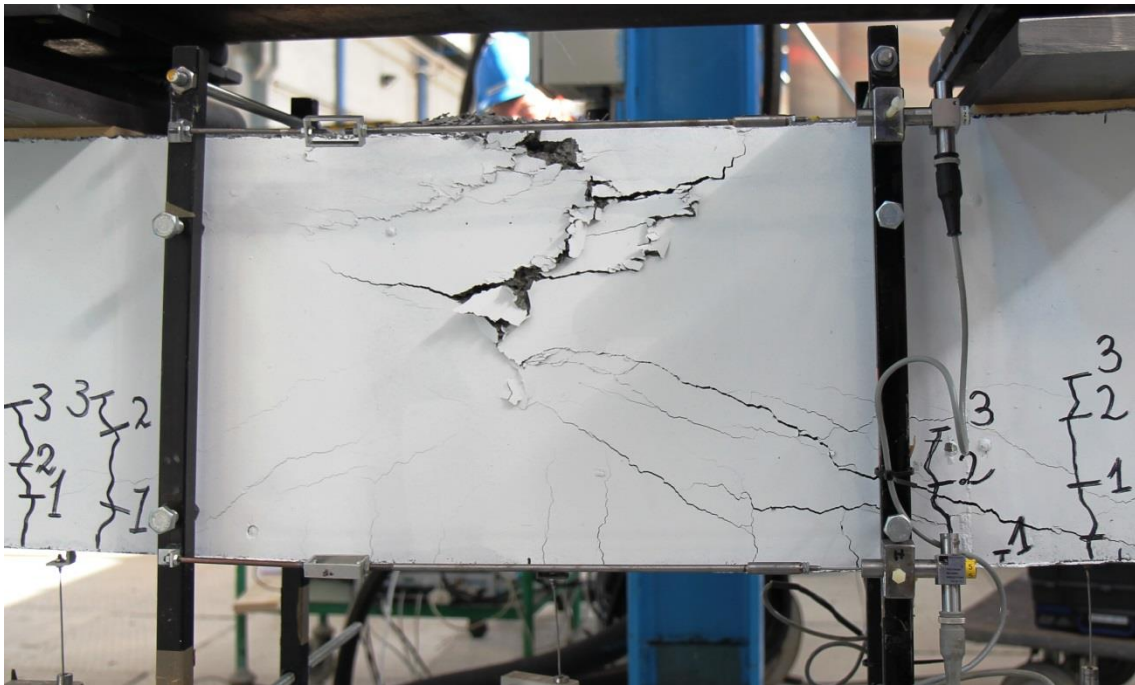
**Figure 6.37. Final cracking on the west side of beam 4B.**
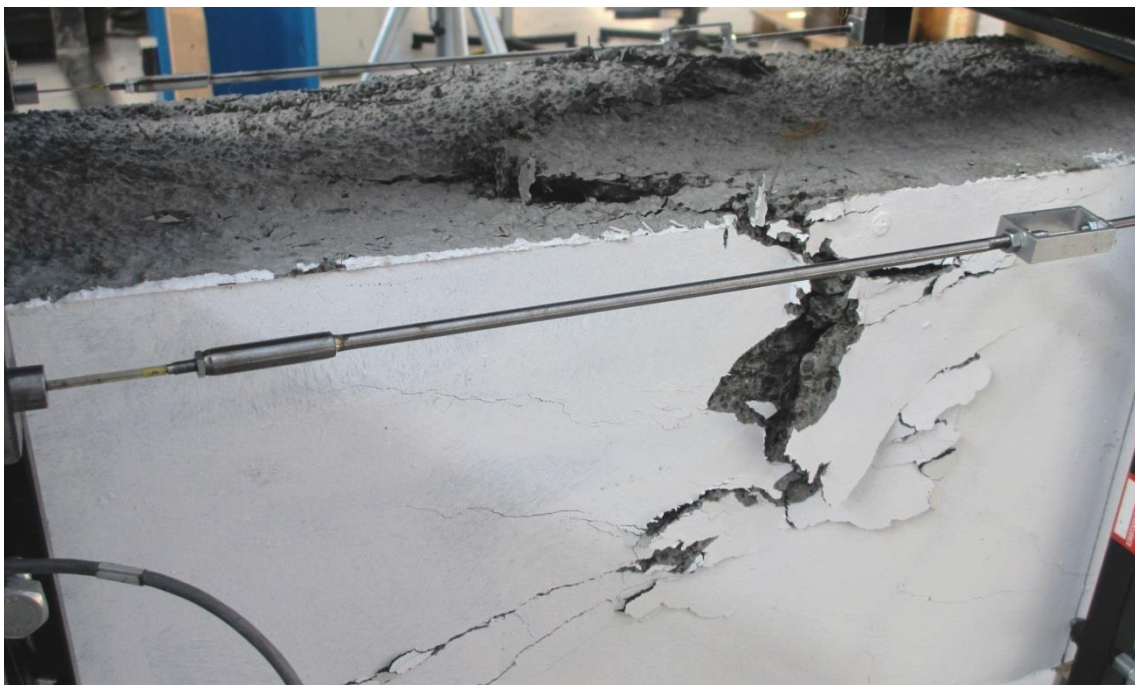
Figure 6.38. Final cracking on the top and east side of beam 4B.

Comments to the testing:

◙ Upper and lower strain sensors on the east side (IS1 and IS3) had to be refitted on the brackets before test start.

6.5   Concrete Cylinder and Small Beam Testing

6.5.1   Concrete Cylinder Test

Six cylinder specimens with diameter and height of 100 and 200 mm respectively were taken for each set of beams that were casted to test compressive strength and density of the concrete. Testing of the compressive strength was done according to NS-EN 12390-3: 2009 [19] in a Losenhausen B-52 hydraulic jack with 5000 kN compression capacity.

Since the test was performed by SINTEF only the results are presented in table 6.5 while the complete testing sheets are found in Appendix E. The compressive strength was tested on five of the six specimens, while the last one was used for measuring the oven-dry density of the mix.

Tore Myrland Jensen, SINTEF, recommended using oven-dry density of 150 kg/m^3 lower than the mean value of the measured bulk density (e-mail 04.25.2013), see Appendix F.

Table 6.5. Results from compressive strength and density testing

Specimens Fibre type	Hardening	Compressive Strength	Oven-dry test specimen		Mean Bulk Density	Used density
			Bulk Density	Oven-Dry Density		
	Days	MPa	kg/m^3	kg/m^3	kg/m^3	kg/m^3
1 - 6 (Mix 1A-1B) Only LWAC	35	41,0	-	-	1765	1615
11 - 16 (Mix 2A-2B) Dramix 65/60	36	39,1	1781	1659	1815	1665
21 - 26 (Mix 3A-3B) Dramix 65/35	35	40,0	1828	1686	1822	1672
31 -36 (Mix 4A-4B) Basalt fibre MiniBars	36	40,5	1785	1634	1782	1632

The compressive strength corresponds very well with the design strength of 40 MPa but the tested oven-dry density is considerably lower than the design value of 1800 kg/m^3.

6.5.2 Fibre Reinforced Test Beams.

For each set of fibre reinforced main beams SINTEF made six test-beam specimens with width and depth of 150 mm and length of 550 mm. Testing of these beams was done according to NS-EN 14651: 2005+A1: 2007 [20] in INSTRON 1332 hydraulic jack with capacity of 250 kN.

> "This European standard specifies a method of measuring the flexural tensile strength of metallic fibered concrete on moulded test specimen. The method provides for the determination of the limit of proportionality (LOP) and of a set of residual flexural tensile strength values." [20, pp. 4]

Before testing a 25 mm deep and 5 mm wide notch is sawn on the underside of the beam which is used to measure the *CMOD* (Crack mouth opening displacement) and to control where the beam starts to crack, see figure 6.39. But SINTEF performed a test on these beams where the deflection was measured with an inductive sensor on the underside of the beam, similar to the testing of the main beams.
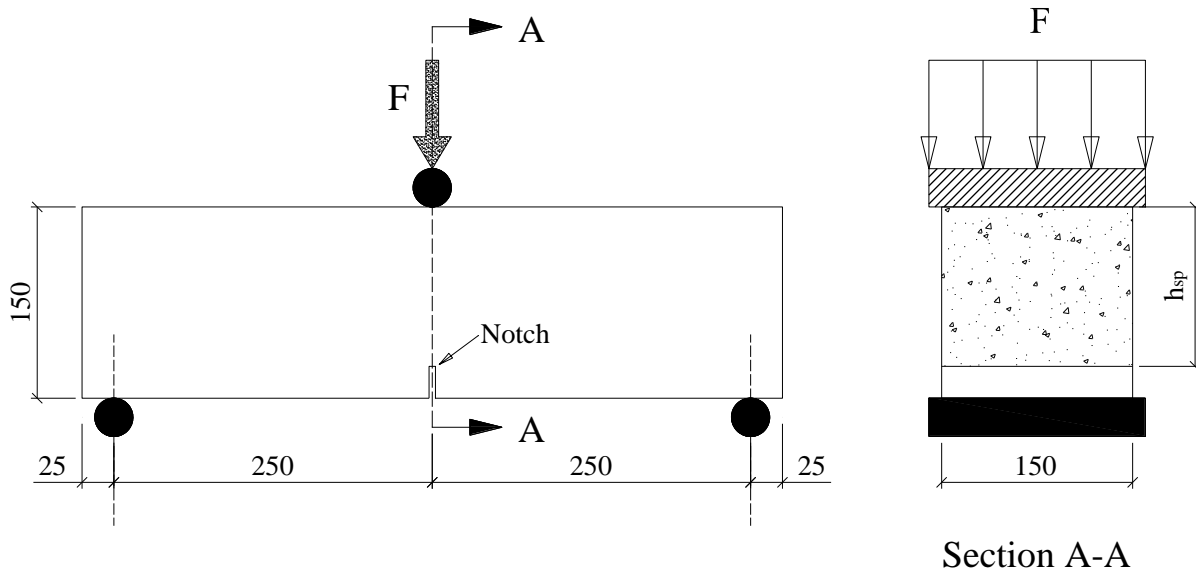
Figure 6.39. Test set-up for test-beams

CMOD and flexural tensile strength are usually used when designing structures with fibre reinforcement. Therefore is it possible to calculate the *CMOD* from the measured displacement δ by:

$$\delta = 0,85\,CMOD + 0,04 \qquad (3.11)$$

And then the residual flexural tensile strength $f_{R,j}$ is given by the expression:

55

$$f_{R,j} = \frac{3F_jl}{2bh_{sp}^2} \qquad (3.12)$$

Where F_j is the load corresponding with $CMOD_j$, see figure 6.40, l is the span length [mm], b is the width of the specimen [mm] and h_{sp} is the distance between the top of the notch and the top of the specimen.

CMOD (mm)	δ (mm)
0,05	0,08
0,1	0,13
0,2	0,21
0,5	0,47
1,5	1,32
2,5	2,17
3,5	3,02
4,0	3,44
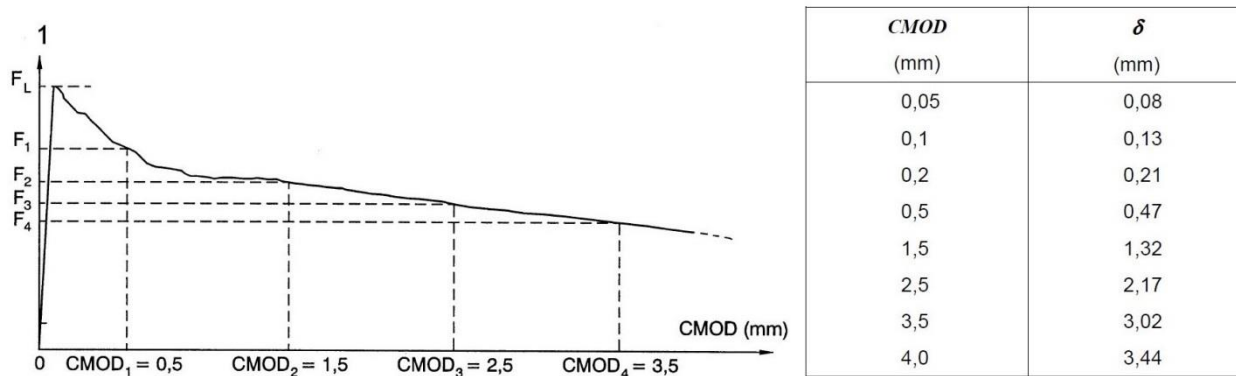
Figure 6.40. Load F_j and relationship of CMOD and deflection.

Complete results with deflection and *CMOD* diagrams for each test specimen is shown in Appendix G but the average values for every three test specimens is shown in figures 6.41 and 6.42 which give a pretty good indication of the results.
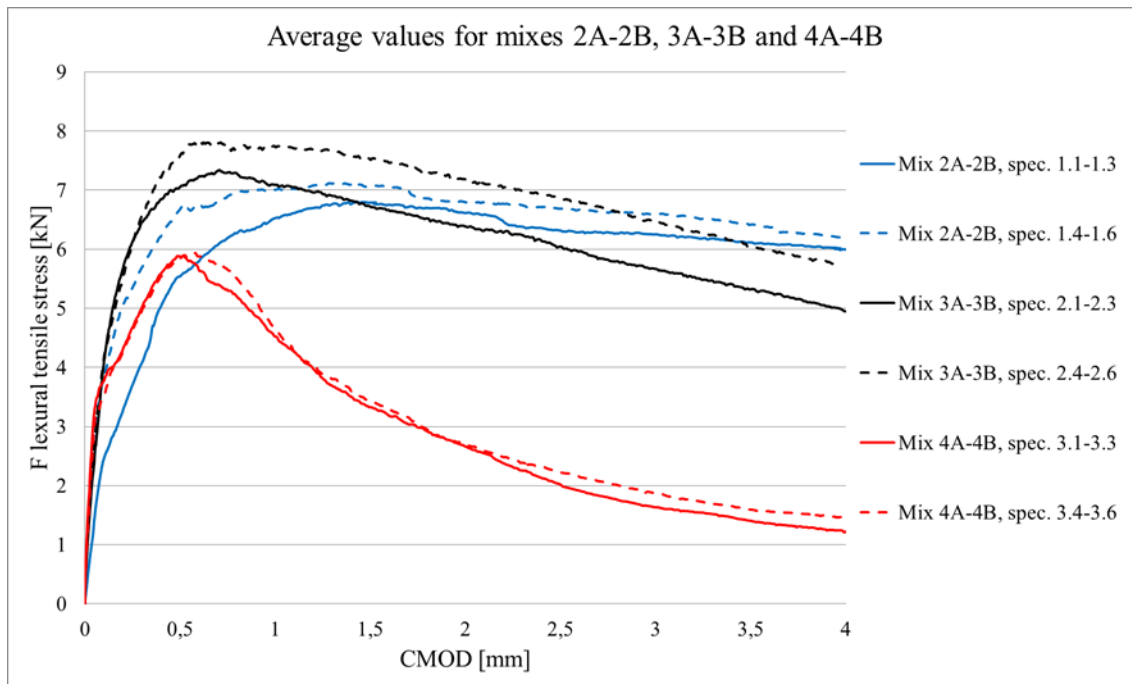
Figure 6.41. Average CMOD for every three test beams (in total six specimens for each mix).

56
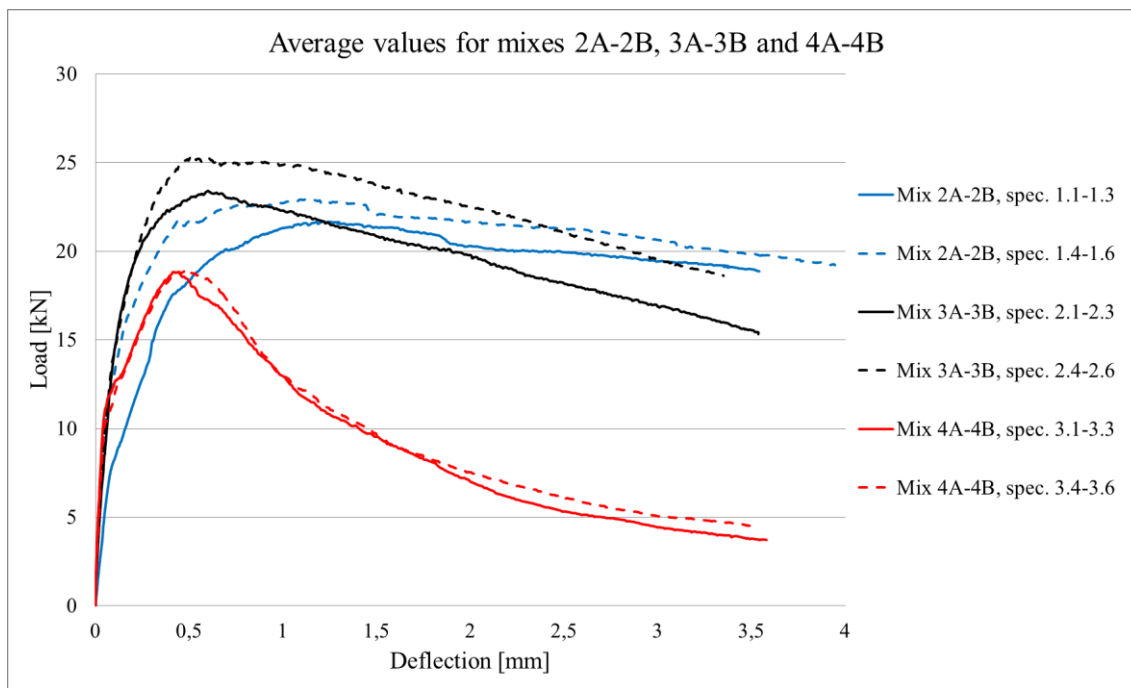
Figure 6.42. **Average deflection for every three test beams (in total six specimens for each mix).**

Good distribution of the fibres is very important to get the best possible effect from the fibres. To get an indication of the distribution of the fibres in a cross-section a fibre count was done on cross-section pieces from the fibre test beams. These were 50 mm thick specimens cut from the middle of the test beams right next to the notch.   The fibres were market with dots on a transparent foil which was scanned and the dots counted in a computer program.

The complete results from these counting's are in Appendix H, but the average values for each concrete mix (with fibres) are listed up in table 6.6 and a column chart in figure 6.43.

Table 6.6. **Average values and relative standard deviation (CoV) of number of fibres in each mix**

Number of fibres	Average values					
	Mix 2A-2B		**Mix 3A-3B**		**Mix 4A-4B**	
	Mean	**CoV**	**Mean**	**CoV**	**Mean**	**CoV**
Upper	74	22 %	160	26 %	55	25 %
Middle	68	39 %	164	34 %	65	25 %
Lower	90	26 %	176	20 %	55	42 %
Total	231	11 %	499	25 %	175	28 %
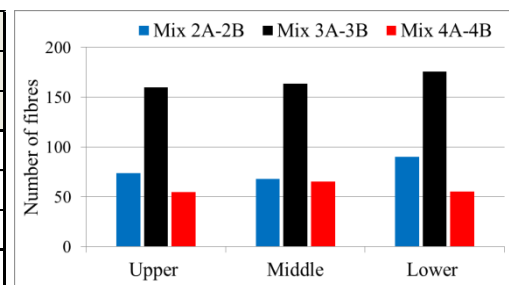
Figure 6.43. **Column chart of the mean values of number of fibres in each concrete mix**

7 Analysis of Test Results

The test results were generally really good and each beam set had very good correlation with exception of beams 3A and 3B which will be discussed later on in section 7.3.

The steel fibres, both Dramix 65/60 and Dramix 65/35, increase the ductility fairly more than the basalt fibres. This different effect from the fibres is pretty much as expected with regard to the different material properties of the fibres, where the modulus of elasticity is about three times higher for the steel fibres than the basalt fibres and the shape of the hooked steel fibres indicates that they should have more anchorage in the concrete. This will be addressed in section 7.4.

7.1 Comparison of Tested and Calculated Results

Same calculations as were done previously in chapter 3.2 were redone for each set of beams with input values from the concrete cylinder testing, i.e. compressive strength and oven dry density. The results are shown in table 7.1 with the test results. Increase of compressive strength due to the fibre reinforcement was not accounted for in the calculations.

Table 7.1. Main results from testing and calculations.

	Beam	1A	1B	2A	2B	3A	3B	4A	4B
	Type of fiber	Only LWAC		Dramix 65/60		Dramix 65/35		Basalt gen. 3	
Tested values	Failure Load [kN]	100,0	94,9	112,2	103,2	106,6	107,2	109,2	108,2
	Failure deformation at middle [mm]	22,3	21,1	25,2	23,3	22,6	23,4	24,5	23,9
	Strain at top [‰]	-2,91	-2,80	-3,15	-3,05	-3,05	-3,01	-3,26	-3,13
	Strain at bottom [‰]	2,13	1,97	2,42	2,09	2,09	2,13	2,38	2,29
SINTEF	Compressive strength [MPa]	41,0		39,1		40,0		40,5	
	Oven-dry density [kg/m^3]	1615		1665		1672		1632	
Calculated values	Failure moment [kNm]	178,5		172,2		175,6		177,1	
	Failure load [kN]	**124,8**		**120,2**		**122,6**		**123,7**	
	Failure deformation at middle [mm]	**25,2**		**23,4**		**23,8**		**24,7**	
	Strain at top - ε_{lcu3}' [‰]	-3,12		-2,86		-2,89		-3,04	
	Strain at bottom - ε_{lcu3} [‰]	2,73		2,58		2,63		2,69	
	Strain in long. bottom reinf. - ε_S [‰]	1,54		1,48		1,50		1,52	

The calculated deflection curve and strain curves from table 7.1 has been plotted in the deflection and strain diagrams for each beam in chapter 6.4 for visualization.

7.2 Evaluation of α_{lcc}

α_{lcc} is the coefficient for long term- and unfavourable effects on the compressive strength and is often also called construction compression strength coefficient. The value of α_{lcc} was set as 1,0 in the calculations since the beams were tested after only 1 month from casting in controlled loading.

According to the Norwegian National Annex for Eurocode 2 the value for α_{lcc} is supposed to be equal to 0,85 [12]. It is therefore interesting to find which value of α_{lcc} gives the same result as the test results. This is shown is table 7.2.

$$f_{lc} = \alpha_{lcc} \cdot f_{lcm} \tag{7.1}$$

Table 7.2. Coefficient for long term and unfavourable effects - α_{lcc}.

Beam	1A	1B	2A	2B	3A	3B	4A	4B
Type of fiber	**Only LWAC**		**Dramix 65/60**		**Dramix 65/35**		**Basalt gen. 3**	
Tested failure Load [kN]	100,0	94,9	112,2	103,2	106,6	107,2	109,2	108,2
Calculate failure load [kN]	124,8		120,2		122,6		123,7	
f_{lc} - Compressive strength giving tested failure load [MPa]	31,7	29,8	36,1	32,7	34,0	34,2	35,0	34,6
f_{lcm} - Tested compressive strength giving calculated failure load [MPa]	41,0		39,1		40,0		40,5	
α_{lcc} - Long term effect coefficient	**0,77**	**0,73**	**0,92**	**0,84**	**0,85**	**0,86**	**0,86**	**0,86**

The average value for all the eight beams is $\alpha_{lcc} = 0,84$, while the average value for the six fibre reinforced beams is $\alpha_{lcc} = 0,86$. This shows that the test results for the failure load correspond very well with the standard value of $\alpha_{lcc} = 0,85$.

7.3 Discussion of Beam 3A

Beams 3A and 3B had very similar failure loads, 106,6 kN and 107,2 kN, and failure deflections of 22,6 mm and 23,4 mm. Generally the same deformation process until failure. Then directly post-failure beam 3A falls down in the deflection curve at the same rate as the un-fibre reinforced beams 1A and 1B as figure 7.1 shows very clearly.

The Δdeflection of the 80% post-failure column chart in figure 7.2 shows how little resistance the beam has to the loading and falls almost at the same rate as beams 1A and 1B. This means that beam 3A has just deflected 2,0 mm while resisting 80% of the failure load, or about 85,3 kN. While beam 3B had deflected 6,3 mm when still resisting 80% of the failure load, or about 85,8 kN. More deflection means more ductile behaviour in this case.

And if we look at how much load beam 3A was resisting when it had deflected ~6 mm as beam 3B had at the 80% post-failure deflection then it was only supporting about ~63% of its failure load, or about 67 kN. Which is almost 20 kN less load bearing capacity than beam 3B at that same deflection.
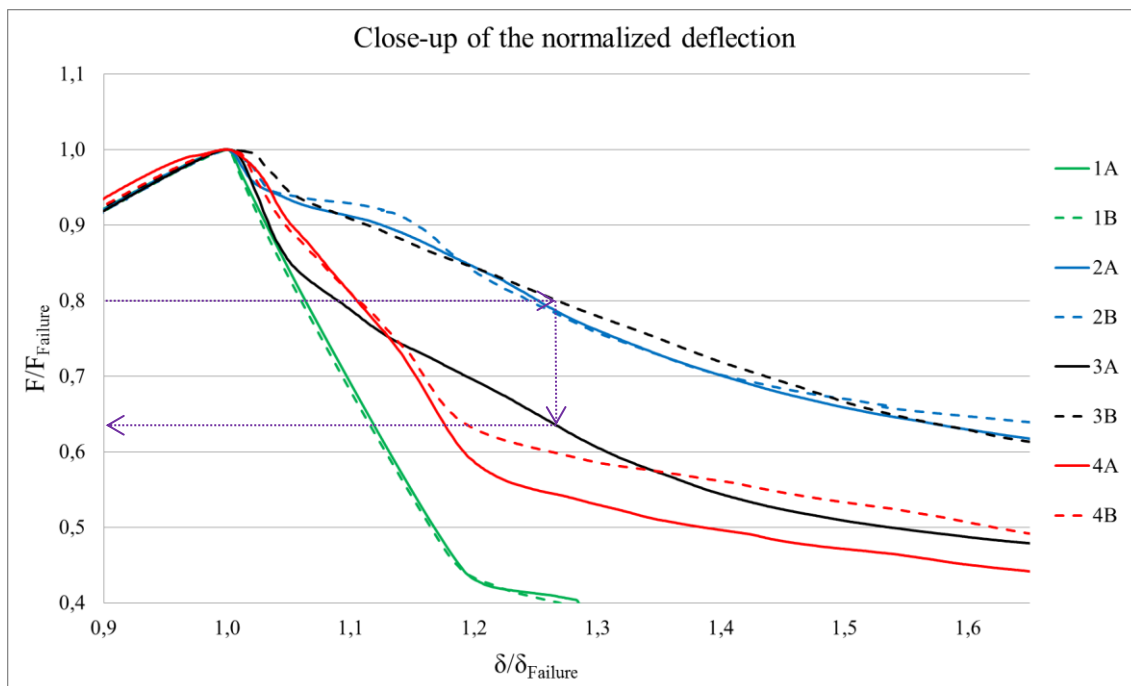
Figure 7.1. Deflection diagram as shown in figure 6.4. Close-up of the normalized deflection.
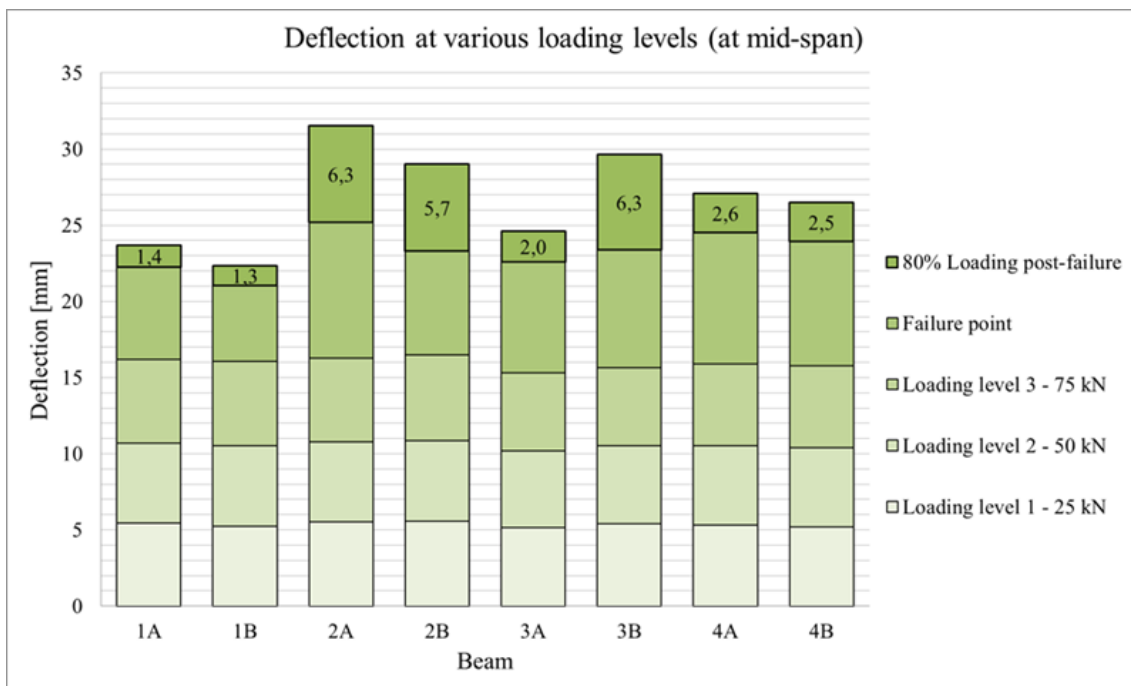
Figure 7.2. Column chart as shown in figure 6.5. Deflection of the beams at 80% post-failure point.

Subsequently the diagrams for the loading time, figure 6.1, and the diagrams for the top and bottom strains, figures 6.7 and 6.8, show that beams in beam set 3 had the biggest variation of the beam sets. It is very unlikely that the concrete batch itself was poorly mixed since the failure loads are similar to the other beams and the results from the compressive strength, table 6.5 and Appendix E also show that concrete batch should have been consequent. But the results from the fibre test beam deflection, see figure 6.42 and Appendix G also show more variation for beam set 3 than the other sets. This is pretty strange since the specimens were taken at the same time and of course from the same batch because there was only one batch for each set of beams.

I would argue that the deformation curve of beam 3B is more as it should be for beam set 3 rather than the curve for beam 3A. This is basically based on how little the beam deflected post-failure point and was more similar to beam sets 1 and 4 directly after the failure point.

7.4 Discussion of the Basalt Fibre Beams 4A-4B

The purpose of the fibre reinforcement is to confine the concrete by applying internal transverse stress, as shown in figure 2.2, and minimize the transverse expansion of the compression zone and thereby making the concrete more ductile in compression.

Since the modulus of elasticity of the basalt fibres is only about 30 % of the steel fibres, as shown in figure 7.3, then the transverse internal pressure applied from the basalt fibres to the concrete is much lesser then from the steel fibres. Then the concrete with the basalt fibres has to expand much more and at higher strains than the steel fibre reinforced concrete to get the same confining effect.
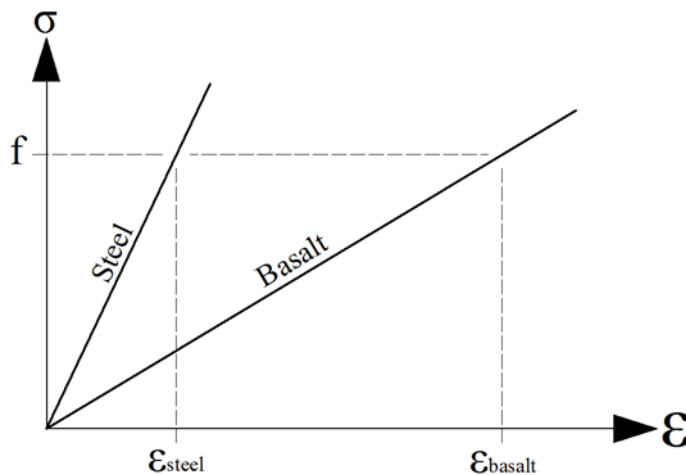
Figure 7.3. E-modulus of steel- and basalt fibres

This is why the basalt fibre beams (4A-4B) got poorer result in load-deflection diagram in figures 7.1 (and figures 6.2-6.4). They started dropping very rapidly directly post the failure point, but then they started levelling out at a similar rate as the steel fibre beams (beams 2A-2B and 3B). The presumably worse anchorage of the basalt fibres can also have affected these results.

7.5   Importance of Good Fibre Distribution

When the fibres are equally distributed in all directions they have confining effect similar to traditional reinforcement in transverse direction. This improves the ductility of the beam and helps keeping the cross-section undamaged as long as possible to withhold the compressive strength of the concrete. Therefore is it critical that the casting of fibre reinforced concrete is done in a proper way.

This indicates that there must have been some error in casting of beam 3A. It is possible that the direction of majority of the fibres in the compressive zone was not optimal, i.e. in the longitudinal direction, see figure 7.4.
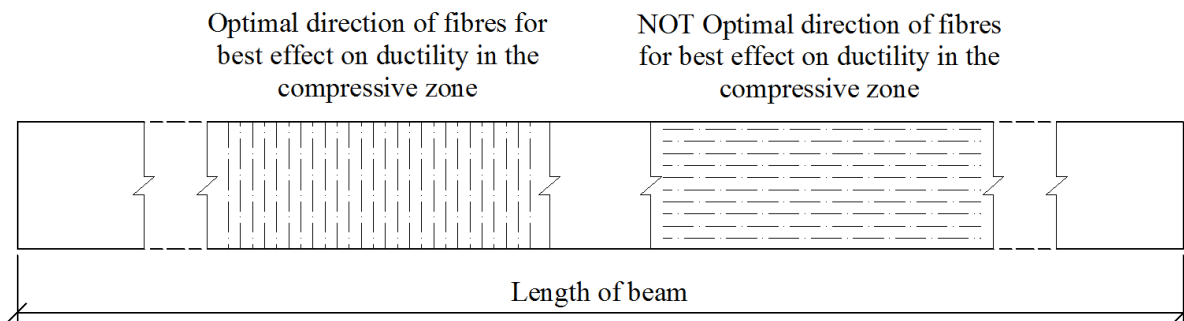
Figure 7.4. Different directions of fibres in a beam.

Good anchorage is also more important than the tensile strength of the fibre. The fibres must of course bond with the concrete to be able to transfer the tensile forces.

8 Conclusion

Eight full scale lightweight aggregate concrete (LWAC) beams were casted to test the effect of different types of fibre reinforcement to the compressive ductility. Test results of these beams were compared to calculations with input values from testing of the compressive strength and oven-dry density from cylinder testing. Comparison of tests and calculations results showed a generally good compliance.

This test indicated clear difference in effect of the steel fibres versus the basalt fibres to the compressive ductility. The steel fibres seemed to have almost immediate effect post the failure point, with exception of beam 3A. While the basalt fibres took longer time to affect the load bearing capacity of the beams post-failure due to lower E-modulus. This project also emphasized how important it is to be thorough when casting fibre reinforced concrete to achieve good fibre orientation and distribution.

Comments to the testing:

- ⊡ It is possible that the small magnitude of the beams, 200x300 mm, resulted in the similarity of the effect from the steel fibres. Was the cross-section of the beams to small?
- ⊡ It would have been very better to have casted three beam specimens, especially of the fibre reinforced beams, in case of a poor correlation of one set of beams as in set 3.

Recommendations of continuation on the topic.

Both types of the steel fibres, with length of 35 mm and 65 mm, gave very similar results in the testing. It is therefore possible to recommend further testing and use of the smaller type of fibres (Dramix 65/35) with regards of better workability of the fresh concrete and that the fibres are meant as an additive to the structure and not as load-bearing.

It could also be interesting to compare the Dramix 3D type which was used in this project with the newer 4D and 5D types which have even more effective end-hooks for concrete anchorage. But on the other hand it doesn't necessarily result in more ductility in compression since they are more relevant for load bearing usage.

9 References

[1]   Gere J.M., 2004. *Mechanics of Material, 6th ed*. London U.K.; Thomson Learning.

[2]   Olivia, M., & Mandal, P., 2005. *Curvature Ductility of Reinforced Concrete Beam*. Journal of Civil Engineering, 6, no. 1.

[3]   CEN, 2004+NA: 2008. NS-EN 1992-1-1:2004+NA: 2008, *Eurocode 2: Design of Concrete Structures - Part 1-1: General rules for buildings + National Annex 2008*. Oslo; Standard Norge.

[4]   Newman, J. & Choo, B.S. (Eds.), 2003. *Advanced concrete technology 3 – Processes*. Oxford U.K.; Elsevier Butterworth-Heinemann.

[5]   Neville, A.M. & Brooks, J.J., 2001. *Concrete Technology, revised edition*. Essex U.K.; Pearson Education Limited.

[6]   Chandra, S. & Berntsson, L., 2003. *Lightweight Aggregate Concrete: Science, Technology and Applications*. Norwich N.Y.; Noyes Publications/William Andrews Publishing.

[7]   Wikimedia Commons. *Leca Pellets*. [Retrieved from: http://upload.wikimedia.org /wikipedia/commons/8/82/Leca_pellets.jpg – found 05.13.2013].

[8]   Henning Van Duffel, 2013. *Nordhordland bridge model*. [Sketcup 3D model, recieved 05.21.2013].

[9]   Jahren, P., 2011. *Concrete, History and Accounts*. Trondheim; Tapir academic press.

[10]   Mindess S., Young J. F. & Darwin D., 2003. *Concrete, 2nd ed*. Upper Saddle River N.J.; Pearson Education, Inc.

[11]   Ellobody, E., 2013. *Numerical modelling of fibre reinforced concrete-filled stainless steel tubular columns*. Thin-Walled Structures, 63, 1-12.

[12]   Kanstad, T. et al., 2011. *Forslag til retniningslinjer for dimensjonering, utførelse og kontroll av fiberarmerte betongkonstruksjoner, COIN Project report 29 -2011*. Trondheim; SINTEF Building and Infrastructure.

[13]   ReforceTech Product data sheet, 2013. *Basalt Fiber Reinforced MiniBars.* [Retrieved from: http://reforcetech.com/solutions_technology_3/products/ - found 05.02.2013]. Reforce-Tech, Basalt Fiber Reinforcement Technology.

[14]   Dramix Product data sheet. *Dramix 3D 65/35.* [Retrieved from: http://www.bosfa.com /docs/accordions/3D_6535BB.pdf – found 05.29.2013]. BOSFA.

[15]   Dramix Product data sheet. *Dramix 3D 65/60.* [Retrieved from: http://www.bosfa.com /docs/accordions/3D_6560BG.pdf– found 05.29.2013]. BOSFA.

[16]   New Construction Group. *Dramix 65/60 steel fibre.* [Retrieved from: http://ncg-bg.com/en/products/materials-for-industrial-floors/concrete-fibres/dramix-65-60.html - found 05.13.2013].

[17]   COIN, 2013. *Annual Report 2012.* [Retrieved from: http://www.coinweb.no - found 05.14.2013]. SINTEF Building and Infrastructure.

[18]   Sørensen, S.I., 2010. *Betongkonstruksjoner, Beregning og dimensjonering etter Eurocode 2.* Trondhiem; Tapir academic press.

[19]   CEN, 2009. *NS-EN 12390-3, Testing hardened concrete – Part 3: Compressive strength of test specimens.* Oslo, Standard Norge.

[20]   CEN, 2007. *NS-EN 14651: 2005+A1: 2007, Test method for metallic fibre concrete – Measuring the flexural tensile strength (limit of proportionality (LOP), residual).* Oslo, Standard Norge.

10 List of Appendices

Appendix A

Fibre Reinforcement Data Sheets.

Dramix®

Data Sheet

Aspect ratio Length Bright Belt

3D Dramix® **65/35BB**

CE
0749-CPD
EN 14889-1

Conforms to
ASTM A820

DRAMIX® 3D

Dramix® 3D is the reference in steel fibre reinforcement. Combining high performance, durability and ease-of-use, 3D provides you with a time-saving and cost-efficient solution for most common applications.

> original anchorage
> standard tensile strength

Dramix® 3D is a cost efficient solution for
> flooring
> tunnel applications
> precast
> residential applications

Bekaert supplies all of the support you need for your project. We help you determine the most suitable fibre types, calculate optimal dosages, select the right concrete quality. Contact your local support.

Go to www.bekaert.com/dosingdramix for our recommendations on handling, dosing and mixing.

Modifications reserved.
All details describe our products in general form only.
For detailed information, product specifications available on request.

PERFORMANCE

Material properties

Tensile strength: $R_{m,nom}$: 1.345 N/mm²
Tolerances: ± 7,5% Avg
Young's Modulus: ± 210.000 N/mm²

Geometry

Fibre family	**3D**	
Length (l)	35 mm	
Diameter (d)	0,55 mm	
Aspect ratio (l/d)	65	80 **65** 55 45

Fibre network

8,0 km per m³ (for 15 kg/m³)
14.531 fibres/kg

Dramix® range

5D 4D **3D**

Tensile strength	
Wire ductility	
Anchorage strength	

PRODUCT CERTIFICATES

CE
0749-CPD
EN 14889-1

Conforms to
ASTM A820

Dramix® is certified for structural use according to EN 14889-1 (system '1'). Detailed information is available on request.

SYSTEM CERTIFICATES

ISO 9001
BUREAU VERITAS
Certification
1828

ISO 14001
BUREAU VERITAS
Certification
1828

All Dramix® plants are ISO 9001 and ISO 14001 certified.

PACKAGING

BELT
(paper bags 250 gr)

STORAGE

KEEP DRY

NO STACKING

Dramix®

Data Sheet

Aspect ratio   Length   Bright   Glued

3D Dramix®   **65/60BG**

CE
0749-CPD
EN 14889-1

Conforms to
ASTM A820

DRAMIX® 3D

Dramix® 3D is the reference in steel fibre reinforcement. Combining high performance, durability and ease-of-use, 3D provides you with a time-saving and cost-efficient solution for most common applications.

> original anchorage
> standard tensile strength

Dramix® 3D is a cost efficient solution for
> flooring
> tunnel applications
> precast
> residential applications

Bekaert supplies all of the support you need for your project. We help you determine the most suitable fibre types, calculate optimal dosages, select the right concrete quality. Contact your local support.

Go to www.bekaert.com/dosingdramix for our recommendations on handling, dosing and mixing.

Modifications reserved.
All details describe our products in general form only.
For detailed information, product specifications available on request.

PERFORMANCE

Material properties

Tensile strength: $R_{m,nom}$: 1.160 N/mm^2
Tolerances: ± 7,5% Avg
Young's Modulus: ± 210.000 N/mm^2

Geometry

Fibre family	**3D**	
Length (l)	60 mm	
Diameter (d)	0,90 mm	
	80 **65** 55 45	
Aspect ratio (l/d)	65	
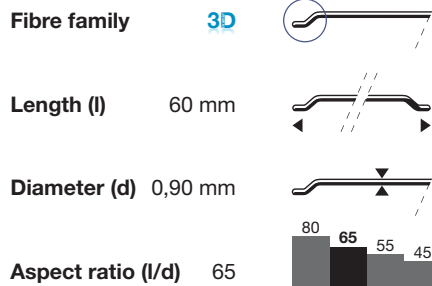
Fibre network

3,0 km per m^3 (for 15 kg/m^3)
3.183 fibres/kg
Minimum dosage:
15 kg per m^3 (according to CE)

Dramix® range

5D 4D **3D**

Tensile strength			
Wire ductility			
Anchorage strength			

PRODUCT CERTIFICATES

CE
0749-CPD
EN 14889-1

Conforms to
ASTM A820

Dramix® is certified for structural use according to EN 14889-1 (system '1'). Detailed information is available on request.

SYSTEM CERTIFICATES

ISO 9001
BUREAU VERITAS
Certification

ISO 14001
BUREAU VERITAS
Certification

All Dramix® plants are ISO 9001 and ISO 14001 certified.

PACKAGING

BAGS 20 kg   **BIG BAG** 1100 kg

STORAGE

KEEP DRY   NO STACKING

71.22.05 - 09/2012

BFRP MiniBars™
Patent Pending

PRODUCT DESCRIPTION

ReforceTech Basalt Fiber Reinforced Polymer BFRP MiniBars™ are an engineered macro fiber reinforcement designed to improve concrete structural strength through uniform distribution throughout the concrete matrix.

Concrete reinforced with RFT MiniBars™ has demonstrated very good flexural toughness and energy absorption capability after cracking when tested using ASTM C78 and C1399 and EN16451.

Testing demonstrates that MiniBars™ satisfy the relevant residual strength requirements based on ASTM C1609 tests (as specified in ACI 318-08 for steel fiber reinforced concrete) using MiniBars™ as shear reinforcement in reinforced concrete slabs and beams.

ReforceTech BFRP MiniBars™ are engineered to deliver high flexural toughness and energy absorption in concrete in conjunction with a proven alkali resistance and bond strength.

Det Norske Veritas (DNV) testing has demonstrated that the unique ReforceTech process delivers a strong bond between the concrete and the BFRP bars. Further testing with the University of Akron demonstrated results of Flexural Tensile Strength (ASTM C78-07) enabling the increase from 4.5 MPa (653 psi) for normal concrete up to 17 MPA (2465 psi) depending on volume fraction of MiniBars™. Testing Average Residual Strength (ASTM C1399) has developed ARS from zero in normal concrete up to over 15 MPa (2175 psi) depending on the volume fraction of MiniBars™ and the mix design.

From volcanic basalt stone thin basalt fibers are combined in ReforceTech's patented process to create unique and strong MiniBars™. The MiniBars™ are engineered to create the optimal mechanical bond and cut to the prescribed length 30 to 60 mm (1.18" to 2.36") to achieve the desired concrete products performance.

FROM BASALT TO STRUCTURAL PRE-REINFORCED CONCRETE

Basalt stone   *Melted Basalt*   *Fiber*   *MiniBars™*   *Pre-Reinforced Concrete*
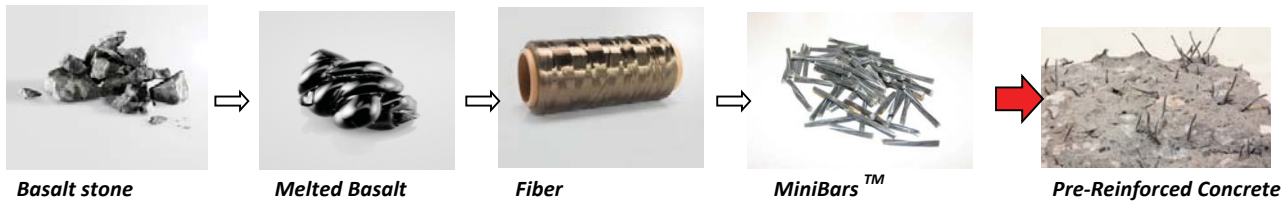
UNIQUE ENABLING FEATURES TO REDUCE PROJECT COSTS

- Corrosion Free allows thinner structures
- Zero Conductivity, eliminates galvanic corrosion
- Greatly Improved Flexural and Average Residual Strength of Concrete allowing design freedom, elimination or reduction of normal reinforcement
- Compatible Specific Gravity – 1.9 g/cm3 means uniform distribution, MiniBars™ do not settle or float and are easily mixed. Due to the large surface area, some large aggregate may need to be reduced or fine aggregates increased.
- No bars protrude from Concrete; no MiniBars™ are visible on the surface.
- Excellent distribution in mixing, suitable for on site mixing, pre-caster and use in dry concrete

- Longer lifetime, lower life cycle costs
- Improved freeze thaw resistance
- Increased chemical resistance with reduction of shrinkage cracks
- Diameter – 0.5 to 10mm (0.02" to 0.39")
- Length – 20 to 200mm (0.79" to 7.87")
- Savings of labor costs and faster construction
- Improved abrasion resistance
- Improves safety on site by eliminating handling of traditional steel reinforcement
- Uniform distribution
- Eliminates concerns related to proper position of reinforcment and thickness of concrete for flow of concrete

---

BFRP MiniBars™
Patent Pending

ReforceTech
Basalt Fiber Reinforcement Technology

IMPROVED CONCRETE PROPERTIES

Flexural Strength	Average Residual Strength	FTS vs VF%
ASTM C78-07	ASTM C1399	ASTM C78

Figure 4 — Flexural Tensile Strength of High Strength Concrete with 20 mm Maximum Size Aggregate (New Tests)

Figure 5 — Average Residual Strength of High Strength Concrete with 20 mm Maximum Size Aggregate (New Tests)

Cost Summary	Min Reinforcement		
	Steel Nets	MiniBars	
Reinforcement	100	10% higher	
Form Work	100	100	Same
Bar or Net Fixing	100	100% saved	Eliminated
Stool or Chair Fixing	100	100% saved	Eliminated plus no visible marks
Concrete	100	20% saved	Thinner walls
Comparative Costs	100	67	
	Total	**33% Savings**	

APPLICATIONS

o   *Greatly increases the toughness and strength of concrete*
o   *Enables thinner sections, lower weight products, easier installation and transportation*
o   *Suitable for aggressive chloride environments*
o   *Acts as minimum reinforcement to lower cost*
o   *Transforms concrete from a brittle material requiring steel reinforcement to a ductile concrete with tensile strength capacity*
o   *Enables innovative applications to take advantage of the Basalt MiniBars to reduce cost*

MiniBars Properties	Gen1	Gen2
Diameter	2.1	1.1
Core Thread	4800BF	1200BF
Helix Thread	Poly	200BF
BF %	70	76 to 80
Specific Gravity	1.9	1.9
Water Absorption	None	None
E modulus	45GPa	60GPa
Tensile Strength	1000	1100
Melting Point BF deg C	1000	1000
HDT VE Deg C	115	115
Alkaline Resistance	Excellent	Excellent
VF Range	1.5 to 8 %	0.5 to 10%

o   **Thinner Precast Facades Elements**
o   **Submersed Concrete**
o   **Low Cost Structural Slab on Grade**
o   **Lower Cost Inner walls**
o   **Highway Slabs & Bridge Decks**
o   **Floating Infrastructure**
o   **Agricultural Products**
o   **Drainage systems**
o   **Grout Systems**

DOSAGE AND MIX DESIGN

- **Specific applications can be developed as a custom engineered solution**
- **Up to 10 % by volume mixes well in concrete. Engineering reports available.**

ReforceTech AS
Luftveien 4
3440 Røyken
Norway
Phone: +47 66 76 77 80
www.reforcetech.com

ReforceTech Qatar
P.O.Box 3889,
Doha
Qatar
Phone +974 77 44 7732
www.reforcetech.com

Basalt Products Group LLC
2285 Botanica Circle
Melbourne, FL 32904-7340
USA
Phone +321 537 1810
www.basaltproducts.com

Appendix B

Detailed Calculations of the Design Beam.

Beam Design

All calculations are done in accordance with Eurocode 2: Design of concrete structures and Betong-konstruksjoner, beregning og dimensjonering etter Eurocode 2 (BK) by Svein Ivar Sørensen. Formulas that include concrete compressive strength used in these calculations are adapted to mean value of concrete cylinder compressive strength. All partial factors are set as 1.
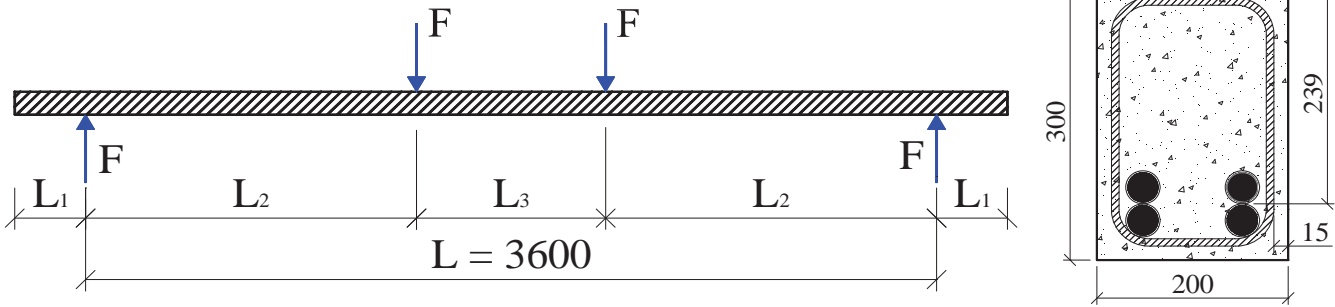
Geometry

Span Length - L =	3 600	mm
L_1 =	300	mm
L_2 =	1 400	mm
L_3 =	800	mm
Total length of beam =	4 200	mm
Weight of beam - W=	453,6	kg
Q =	4,45	kN
Dead load - q =	1,06	kN/m

Cross Section

Beam width - b =	200	mm
Beam height - h =	300	mm
Concrete cover - c_{nom} =	15	mm
d =	239	mm
z =0,9d =	215	mm
h' =	209	mm
A_c =	60 000	mm^2

LightWeight Aggregate Concrete

f_{lcm} =	40	N/mm^2
α_{lcc} =	1	
γ_c =	1	
f_{lctm} =	3,1	N/mm^2
ρ =	1 800	kg/m^3
ε_{cu3} =	0,0035	
η_1 =	0,89	
ε_{lcu3} =	0,00312	

$$\eta_1 = 0,40 + 0,60 \rho/2200 \quad (11.1)$$

E_{cm} =	35000	Mpa
η_E =	0,67	
E_{lcm} =	23 430	Mpa

$$\eta_E = \left(\rho/2200\right)^2 \quad (11.2)$$

λ =	0,8	for $f_{ck} \leq 50$ Mpa
η =	1	for $f_{ck} \leq 50$ Mpa

Reinforcement

f_{yk} =	500	N/mm^2
γ_s =	1	
f_{yd} =	500	N/mm^2
E_s =	190 000	N/mm^2
ε_s =	0,00263	
Stirrups =	8	mm
s =	100	mm
A_{sw} =	101	mm^2
Bottom =	32	**mm**
quantity =	4	
A_s =	3217	mm^2
Top =	8	mm
cot(θ) =	2,5	
cot(α) =	0	

Moment capacity

EC2 - 6.1(2)P:

When designing the ultimate moment resistance of reinforced cross sections, the following assumptions are made:

- Navier's hypothesis is valid. Plane sections remain plane.
- Complete bond between reinforcement and concrete. Same strain in concr. and reinforcement.
- Stress/Strain relationship of the concrete according to EC2 - 3.1.7.
- The tensile strength of the concrete is ignored.

Tensional strain

$$\varepsilon_s \frac{1}{(d-\alpha d)} = \frac{1}{\alpha d}\varepsilon_{lcu3}'$$

$$\Rightarrow \varepsilon_s = \varepsilon_{lcu3}'\frac{1-\alpha}{\alpha}$$

$Axial - equilibrium:$
$T_c - S = 0$
$where:$
$T_c = \lambda \eta f_{lcd}\alpha db$
$S = \sigma_s A_s = E_s \varepsilon_s A_s$
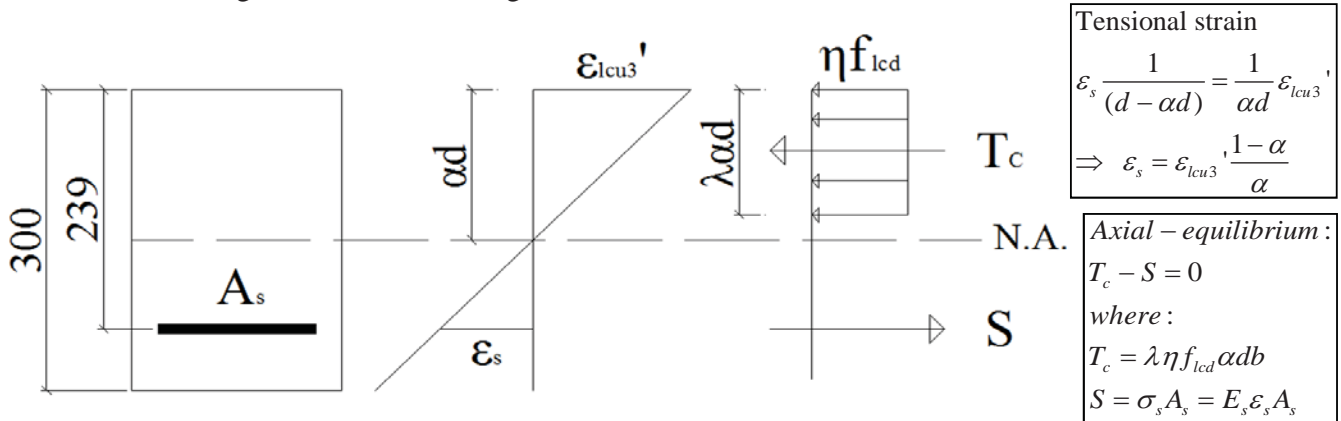
Solve the ABC formula to find the neutral axis of the beam:

A =	3,66E+08	Nmm
B =	4,56E+08	Nmm
C =	-4,56E+08	Nmm

so	α =	0,655	
and get:	αd =	157	mm

$Axial - equilibrium:$

$$\lambda \eta f_{lcm}\alpha db - E_s\frac{(1-\alpha)}{\alpha}\varepsilon_{lcu3}'A_s = 0$$

$$\lambda \eta f_{lcm}\alpha db - E_s\varepsilon_{lcu3}'A_s\frac{d}{\alpha d} + E_s\varepsilon_{lcu3}'A_s = 0$$

$Multiply \ with \ \alpha d:$

$$\lambda \eta f_{lcm}\alpha^2 d^2 b - E_s\varepsilon_{lcu3}'A_s d + E_s\varepsilon_{lcu3}A_s\alpha d = 0$$

$$\alpha^2(\lambda \eta f_{lcm}d^2 b) + \alpha(E_s\varepsilon_{lcu3}'A_s d) - E_s\varepsilon_{lcu3}'A_s d = 0$$

$$A = \lambda \eta f_{lcm}d^2 b$$

$$B = E_s\varepsilon_{lcu3}'A_s d \qquad \alpha = \frac{-B \pm \sqrt{B^2 - 4AC}}{2A}$$

$$C = -E_s\varepsilon_{lcu3}'A_s d$$

Then the Moment capacity can be found with:

M$_{Rd}$ =	**176,8**	**kNm**

$$M_{Rd} = \lambda \alpha(1 - 0,5\lambda\alpha)f_{lcm}bd^2 \qquad \text{(BK 4.14)}$$

Check the strain in the bottom reinforcement:

$$\varepsilon_s = \quad 0,0016$$

$$\varepsilon_s = \varepsilon_{lcu3}'\frac{1-\alpha}{\alpha}$$

where | **ε$_{yd}$ =** | **0,0026** | > | ε$_s$ = | 0,0016 | OK, the reinforcement is elastic

To determine compatible failure load with the test-results I have to subtract the dead weight of the beam and the load-distribution steel beam placed on top of the concrete beam under loading

Beam dead load: $M_{Ed,q} = $ 2,3 kNm

$$M_{Ed,q} = \frac{q \cdot L^2}{8}$$

Load-distribution beam: $M_{Ed,HEB} = $ 1,79 kNm
(260 kg total)

$$M_{Ed,HEB} = Q \cdot L_2$$

$M_{Ed,Dead} = $ **4,1** **kNm**

The statical model for the beam with 2 point loads:
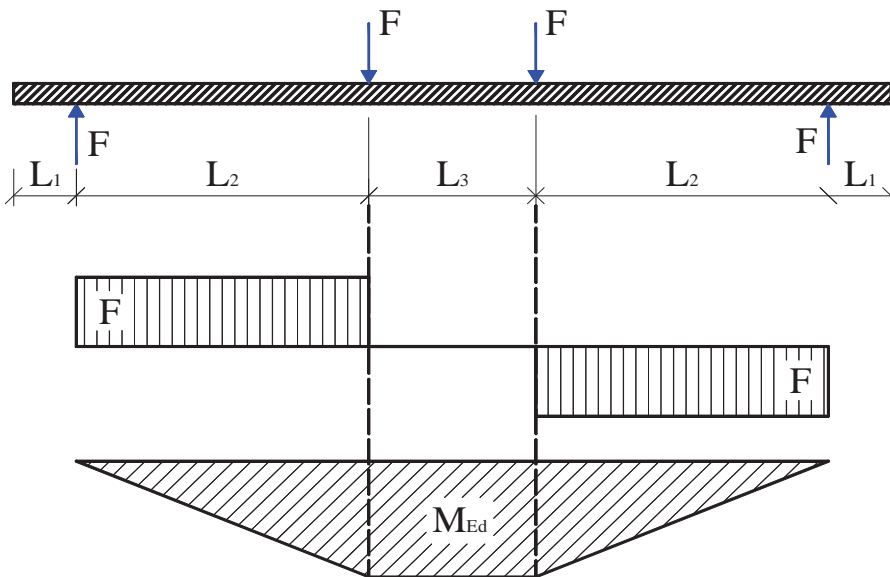
$$M_{Ed} = M_{Ed,F} + M_{Ed,Dead} = M_{Rd}$$
$$M_{Ed,F} = M_{Rd} - M_{Ed,Dead} = F \cdot L_2$$

$$\Rightarrow \quad F = \frac{M_{Rd} - M_{Ed,q}}{L_2}$$

where the failure load can be found by:

F$_{ult}$ = **123,3** **kN**

Shear resistance

Even though there isn't any shear reinforcement at mid-span, there is reinforcement in the rest of the beam.
Check if assumed Ø8c100 shear reinforcement is sufficient.

$V_{Rd,s}$ =   270,3   kN

$$V_{Rd,s} = \frac{A_{sw}}{s} z f_{yk} \cot \theta \qquad (6.8)$$

υ_1 =   0,3742

$$\nu_1 = 0{,}5\eta_1 \left(1 - \frac{f_{lcm}}{250}\right) \qquad (11.6.6N)$$

$V_{Rd,max}$ =   222,0   kN

$$V_{Rd,max} = \alpha_{cw} b_w z \nu_1 \frac{f_{lcm}}{(\cot \theta + \tan \theta)} \qquad (6.9)$$

So the shear resistance of the cross section is the smaller value of $V_{Rd,s}$ and $V_{Rd,max}$:

V_{Rd} =   222,0   kN   OK, this resistance is sufficient

Minimum stirrup spacing according to EC2.

$\rho_{w,min}$ =   0,0013

$$\rho_{w,min} = 0{,}1 \frac{\sqrt{f_{cm}}}{f_{yk}} \qquad (NA.9.5N)$$

s_{min} =   397   mm

$$s_{min} = \frac{A_{sw}}{\rho_{w,min} b_w} \qquad (9.4)$$

s_{max} =   125   mm   OK

$$s_{max} = 0{,}6 h'(1 + \cot \alpha) \qquad (9.6N)$$

Anchorage (with welded transverse bar)

Values for calculating the anchorage:

EC2 - 8.4.4(1)

$c_d =$	25	mm
$\alpha_1 =$	1	
$\alpha_2 =$	1,03	
$\alpha_3 =$	1	
$\alpha_4 =$	1	
$\alpha_5 =$	1	

EC2 - 8.4.2(2)

$\eta_1 =$	1	good bond, see fig. 8.2
$\eta_2 =$	1	for ø $\leq$ 32 mm

EC2 - Table 11.3.1 (and Table 3.1)

$f_{lck} =$	32	N/mm2
$\eta_1 =$	0,89	
$f_{lctk,0.05} =$	1,89	N/mm2
$f_{lctd} =$	1,89	N/mm2

The longitudinal bars are bundled two and two together in the bottom of the beam so the equivalent diameter of these two bars can be used.

$\varnothing_n =$	45	mm	$\phi_n = \phi\sqrt{n_{bundle}} \ \leq \ 55mm$	(8.14)
$\sigma_{sd} =$	47,9	Mpa	$\sigma_{sd} = \dfrac{\Delta F_{td}}{A_s} = \dfrac{0,5 V_{Ed}(\cot\theta - \cot\alpha)}{A_s}$	(6.18)
$f_{lbd} =$	4,2	Mpa	$f_{lbd} = 2,25\eta_1\eta_2 f_{lctd}$	(8.2)
$l_{b,rqd} =$	127,8	mm	$l_{b,rqd} = \left(\dfrac{\phi}{4}\right)\left(\dfrac{\sigma_{sd}}{f_{lbd}}\right)$	(8.3)
$l_{bd} =$	132,0	mm	$l_{bd} = \alpha_1\alpha_2\alpha_3\alpha_4\alpha_5\, l_{b,rqd} \geq l_{b,min}$	(8.4)
$l_{b,min} =$	**320**	**mm**	$l_{b,min} = \max\{0,3 l_{b,rqd}\,;\, 10\phi\,;\, 100mm\}$	(8.7)

Even though the requirement is l $_{b,min}$ = 320 mm and the available anchoring length is only 285 mm that shouldn't be a problem because the beam has a welded transverse end bar.

Deflection

Calculations of the beam deflection is done according to methods in the Betongkonstruksjoner book by using bending stiffness (second moment of area OR moment of inertia) of equivalent transformed Uncracked (Stadium I) and Cracked (Stadium II) cross-sections. Since the cross section does not have longitudinal reinforcement in the top formula can be used directly from the textbook.
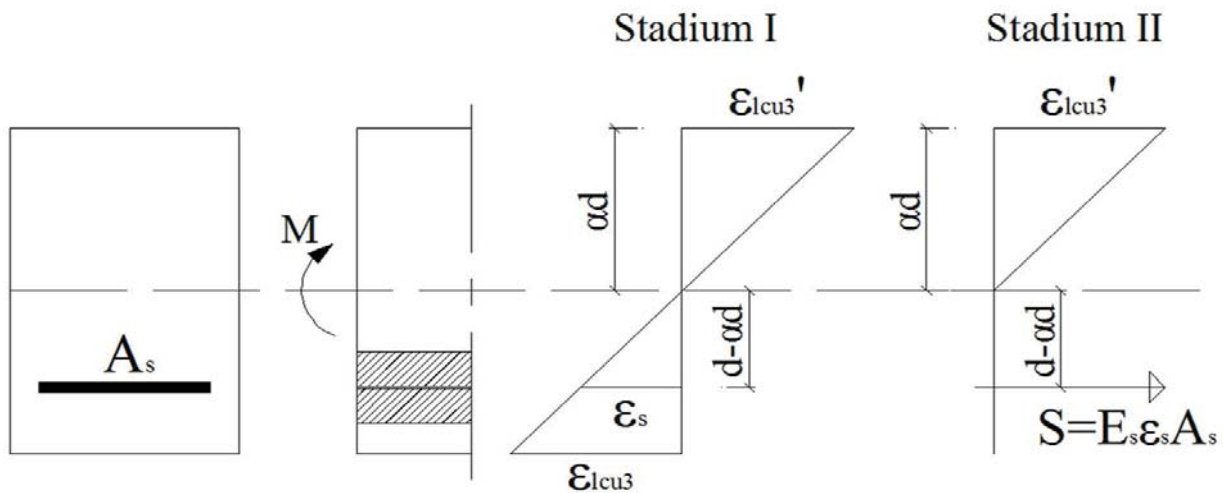
Stadium I. Now the section is uncracked and therefore the whole section is active.

$\eta =$ 8,11

$$\eta = \frac{E_s}{E_{lcm}}$$

$\alpha d =$ 177   mm

$$\alpha d = \frac{A_c \, h/2 + \eta A_s d}{A_c + \eta A_s}$$ (B.K. 5.13)

$I_{c,I} =$ 4,94E+08   mm^4

$$I_{c,I} = \frac{bh^3}{12} + A_c (\alpha d - h/2)^2$$ (BK 5.14)

$I_{s,I} =$ 1,24E+07   mm^4

$$I_{s,I} = A_s (d - \alpha d)^2$$ (BK 5.15)

$EI_I =$ 1,39E+13   Nmm^2

$$EI_I = E_{lcm} I_{c,I} + E_s I_{s,I}$$ (BK 5.16)

$M_{crack} =$ **15,1**   **kNm**

$$M_{crack} = \frac{I_{c,I} + \eta I_{s,I}}{h - \alpha d} \cdot f_{lctm}$$ (BK 5.20)

$F_{crack} =$ **9,1**   **kN**

$$F_{crack} = \frac{M_{crack} - M_{Ed,q}}{L_2}$$

$\delta_{crack,I} =$ **1,2**   **mm**

$$\delta_{crack,I} = \frac{F_{crack} L_2}{24 EI_I} (3L^2 - 4L_2^2)$$

Stadium II. Now the cross section is started cracking and the concrete only contributes to the compression, so it is only activ in the compression zone.

$\rho =$ 0,0673

$$\rho = \frac{A_s}{bd}$$

$\alpha =$ 0,63

$\alpha d =$ 151   mm

$$\alpha = \sqrt{(\eta\rho)^2 + 2\eta\rho} - \eta\rho \qquad \text{(BK 5.5)}$$

$I_{c,II} =$ 2,31E+08   mm^4

$$I_{c,II} = \frac{b(\alpha d)^3}{12} + b(\alpha d)\left(\frac{\alpha d}{2}\right)^2 = \frac{b(\alpha d)^3}{3} \qquad \text{(BK 5.6)}$$

$I_{s,II} =$ 2,48E+07   mm^4

$$I_{s,II} = A_s(d - \alpha d)^2 \qquad \text{(BK 5.7)}$$

$EI_{II} =$ 1,01E+13   Nmm^2

$$EI_{II} = E_{lcm}I_{c,II} + E_s I_{s,II} \qquad \text{(BK 5.8)}$$

Deflection right after cracking:

$\delta_{\text{crack,II}} =$ **1,6**   **mm**

$$\delta_{crack,II} = \frac{F_{crack}L_2}{24EI_{II}}(3L^2 - 4L_2{}^2)$$

Deflection at failure point

$\delta_{\text{Failure}} =$ **22,1**   **mm**

$$\delta_{Failure} = \frac{F_{Failure}L_2}{24EI_{II}}(3L^2 - 4L_2{}^2)$$

Strain

The curvature of the cracked cross-section in the figure on the previous page is expressed by:

$$\kappa = \frac{M}{EI_{II}} = \frac{\varepsilon_s}{(1-\alpha)d}$$ so the stress in the reinforcement is $$\sigma_s = E_s\varepsilon_s = E_s\frac{M(1-\alpha)d}{EI_{II}} \qquad \text{(BK 5.55)}$$

then the Reinforcement strain at failure:

$\varepsilon_s =$ **0,00153**

$$\varepsilon_s = \frac{M(1-\alpha)d}{EI_{II}}$$

and Concrete Strain at failure

Top $\varepsilon_{\text{lcu3}}' =$ **0,00264**

$$\varepsilon_{lcu3}' = \frac{M \cdot \alpha d}{EI_{II}}$$
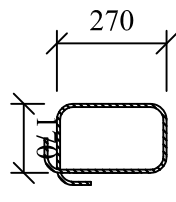
Bottom $\varepsilon_{\text{lcu3}} =$ **0,00260**

$$\varepsilon_{lcu3} = \frac{M(h - \alpha d)}{EI_{II}}$$

Appendix C

Cutting List.

Cutting list

Post	Diameter	Length [mm]	Quantity	Shape	Total Length [m]	Comment
1	32	4180	16	——	66,88	
2	32	4100	16	——	65,6	
3	32	170	16	——	2,72	
4	8	4180	16	——	66,88	
5	8	4180	304	270 / Ø170 shape	66,88	100 mm overlap in the corner. Bending diameter 32 mm

Appendix D

Concrete Recipe's from SINTEF.

10200 0442.8

Prosj./id.:	LWAC Bjelkestøp 2013_Bjelke 1A og 1B

Blandevolum:	720 liter
Dato:	26/2 - 13
Tidspunkt for vanntilsetning	10¹⁵
Ansvarlig:	GK/TMZ
Utført av:	KL/E7/GK.

Materialer	Resept kg/m³	Sats kg	Fukt* %	Korr. kg	Oppveid** kg	
Norcem Standard BP5/BP6	434,9	313,128			313,128	
Elkem Microsilica 920 D	43,5	31,313	0	0,000	31,313	
Kalksteinsmel	4,3	3,131	0	0,000	3,131	
Fritt vann	198,3	142,786		-34,417	108,369	116,050
Absorbert vann	10,7	7,681			7,681	
Leca 2-4 mm (A-4048)	133,5	96,091	0,0	0,000	96,091	
Leca 800 4-8 mm (A-4048)	237,8	171,200	0,0	0,000	171,200	
0/8mm NSBR (A-4045)	432,8	311,584	5,0	15,579	327,163	
0/2mm Fillersand (A-4045)	270,5	194,740	7,3	14,216	208,956	
0	0,0	0,000	0,0	0,000	0,000	
	0,0	0,000	0,0	0,000	0,000	
	0,0	0,000	0,0	0,000	0,000	
	0,0	0,000	0,0	0,000	0,000	
	0,0	0,000	0,0	0,000	0,000	
	0,0	0,000	0,0	0,000	0,000	
Sika FB2	7,8	5,636	82	4,622	5,636	5,193 kg
	0,0	0,000	100	0,000	0,000	
	0,0	0,000	100	0,000	0,000	
	0,0	0,000	100	0,000	0,000	
Stålfiber (Dramix 65/69)	78,0	56,160			56,160	
Basalt Gen 3	0,0	0,000			0,000	

*Se fotnote på delark "Proporsjonering"   ** NB! Våte mengder, også for pozzolaner og fillere

Fersk betong					
Tid etter vanntilsetning	ca. 15	ca. 25			
Synkmål					
Utbredelsesmål	490	470			
Luft					
Densitet		1772			

Prøvestykker (antall)					
Utstøpningstidspunkt					
Terninger					
150x300 sylindre					
100x200 sylindre	68stk. mh. "1-6 26/2" f(2stk på 8.16 7.8 26/2 v/7dg)				
100x200 sylindre					
Totalt tilsatt SP					

oppv. 6.810 kg 782

Prosj./id.:	LWAC Bjelkestøp 2013_Bjelke 2A og 2B	

Blandevolum:	720 liter /ca. 580ℓ
Dato:	26/2-13
Tidspunkt for vanntilsetning	13⁴⁰
Ansvarlig:	GK / TMJ
Utført av:	kk / cf / GK

Materialer	Resept kg/m³	Sats kg	Fukt* %	Korr. kg	Oppveid** kg	
Norcem Standard BP5/BP6	434,9	313,128			313,128	
Elkem Microsilica 920 D	43,5	31,313	0	0,000	31,313	
Kalksteinsmel	4,3	3,131	0	0,000	3,131	
Fritt vann	198,3	142,786		-31,846	110,940	118,621
Absorbert vann	10,7	7,681			7,681	
Leca 2-4 mm (A-4048)	133,5	96,091	0,0	0,000	96,091	
Leca 800 4-8 mm (A-4048)	237,8	171,200	0,0	0,000	171,200	
0/8mm NSBR (A-4045)	432,8	311,584	4,3	13,398	324,982	
0/2mm Fillersand (A-4045)	270,5	194,740	7,1	13,827	208,567	
0	0,0	0,000	0,0	0,000	0,000	
	0,0	0,000	0,0	0,000	0,000	
	0,0	0,000	0,0	0,000	0,000	
	0,0	0,000	0,0	0,000	0,000	
	0,0	0,000	0,0	0,000	0,000	
	0,0	0,000	0,0	0,000	0,000	
Sika FB2	7,8	5,636	82	4,622	5,636	4,730
	0,0	0,000	100	0,000	0,000	
	0,0	0,000	100	0,000	0,000	
	0,0	0,000	100	0,000	0,000	
Stålfiber (Dramix 65/69)	78,0	56,160			56,160	45,240 kg
Basalt Gen 3	0,0	0,000			0,000	

*Se fotnote på delark "Proporsjonering"   ** NB! Våte mengder, også for pozzolaner og fillere

Fersk betong		m/fiber		
Tid etter vanntilsetning	ca. 15	ca. 30		
Synkmål				
Utbredelsesmål	570	—		
Luft				
Densitet	1690	1727		

Tok ut ca. 140/150 ℓ til cannon Gjella deretter tilsatt 45,240 kg fiber til ca. 580 ℓ betong

Prøvestykker (antall)				
Utstøpningstidspunkt				
Terninger				
150x300 sylindre				
100x200 sylindre	6 stk. mrk: "11-16 26/2"			
150x150x550 bjelker	— u — "11-16 26/2"			
Totalt tilsatt SP				

Delark "Blandeskjema"

Prosj./id.: LWAC Bjelkestøp 2013_Bjelke 2A og 2B

Blandevolum:	580 liter
Dato:	
Tidspunkt for vanntilsetning	
Ansvarlig:	
Utført av:	

Materialer	Resept kg/m³	Sats kg	Fukt* %	Korr. kg	Oppveid** kg	
Norcem Standard BP5/BP6	434,9	252,242			252,242	
Elkem Microsilica 920 D	43,5	25,224	0	0,000	25,224	
Kalksteinsmel	4,3	2,522	0	0,000	2,522	
Fritt vann	198,3	115,022		-25,654	89,368	95,556
Absorbert vann	10,7	6,187			6,187	
Leca 2-4 mm (A-4048)	133,5	77,407	0,0	0,000	77,407	
Leca 800 4-8 mm (A-4048)	237,8	137,912	0,0	0,000	137,912	
0/8mm NSBR (A-4045)	432,8	250,998	4,3	10,793	261,791	
0/2mm Fillersand (A-4045)	270,5	156,874	7,1	11,138	168,012	
0	0,0	0,000	0,0	0,000	0,000	
	0,0	0,000	0,0	0,000	0,000	
	0,0	0,000	0,0	0,000	0,000	
	0,0	0,000	0,0	0,000	0,000	
	0,0	0,000	0,0	0,000	0,000	
	0,0	0,000	0,0	0,000	0,000	
Sika FB2	7,8	4,540	82	3,723	4,540	
	0,0	0,000	100	0,000	0,000	
	0,0	0,000	100	0,000	0,000	
	0,0	0,000	100	0,000	0,000	
Stålfiber (Dramix 65/69)	78,0	45,240			45,240	
Basalt Gen 3	0,0	0,000			0,000	

*Se fotnote på delark "Proporsjonering"   ** NB! Våte mengder, også for pozzolaner og fillere

Fersk betong					
Tid etter vanntilsetning					
Synkmål					
Utbredelsesmål					
Luft					
Densitet					

Prøvestykker (antall)					
Utstøpningstidspunkt					
Terninger					
150x300 sylindre					
100x200 sylindre					
100x200 sylindre					
Totalt tilsatt SP					

Delark "Blandeskjema"

A-27

Prosj./id.:	LWAC Bjelkestøp 2013_Bjelke 3A og 3B

Blandevolum:	720 liter / 580ℓ
Dato:	28/2-13
Tidspunkt for vanntilsetning	14:12
Ansvarlig:	GK/SMJ.
Utført av:	KL/EJ

Materialer	Resept kg/m³	Sats kg	Fukt* %	Korr. kg	Oppveid** kg	
Norcem Standard BP5/BP6	434,9	313,128			313,128	✓
Elkem Microsilica 920 D	43,5	31,313	0	0,000	31,313	✓
Kalksteinsmel	4,3	3,131	0	0,000	3,131	✓
Fritt vann	198,3	142,786		-35,585	107,201	114,882 ✓
Absorbert vann	10,7	7,681			7,681	
Leca 2-4 mm (A-4048)	133,5	96,091	0,0	0,000	96,091	✓
Leca 800 4-8 mm (A-4048)	237,8	171,200	0,0	0,000	171,200	✓
0/8mm NSBR (A-4045)	432,8	311,584	4,5	14,021	325,605	✓
0/2mm Fillersand (A-4045)	270,5	194,740	8,7	16,942	211,682	
0	0,0	0,000	0,0	0,000	0,000	
	0,0	0,000	0,0	0,000	0,000	
	0,0	0,000	0,0	0,000	0,000	
	0,0	0,000	0,0	0,000	0,000	
	0,0	0,000	0,0	0,000	0,000	
	0,0	0,000	0,0	0,000	0,000	
Sika FB2	7,8	5,636	82	4,622	5,636 4,909	
	0,0	0,000	100	0,000	0,000	
	0,0	0,000	100	0,000	0,000	
	0,0	0,000	100	0,000	0,000	
Stålfiber (Dramix 30/35)	78,0	56,160			56,160 45,240	✓
Basalt Gen 3	0,0	0,000			0,000	

*Se fotnote på delark "Proporsjonering"   ** NB! Våte mengder, også for pozzolaner og fillere

Fersk betong		m/fiber			
Tid etter vanntilsetning	15	20	25		
Synkmål					
Utbredelsesmål	560				
Luft		·			
Densitet		1789	1875		

Prøvestykker (antall)					
Utstøpningstidspunkt	1450				
Terninger					
150x300 sylindre					
100x200 sylindre	6 stk. nuh:	21-26	28/2		
150x150x550 Gjelbar	—«—	—«—	21-26	28/2	
Totalt tilsatt SP					

Delark "Blandeskjema"

Prosj./id.:	LWAC Bjelkestøp 2013_Bjelke 3A og 3B

Blandevolum:	580 liter
Dato:	
Tidspunkt for vanntilsetning	
Ansvarlig:	
Utført av:	

Materialer	Resept kg/m³	Sats kg	Fukt* %	Korr. kg	Oppveid** kg	
Norcem Standard BP5/BP6	434,9	252,242			252,242	
Elkem Microsilica 920 D	43,5	25,224	0	0,000	25,224	
Kalksteinsmel	4,3	2,522	0	0,000	2,522	
Fritt vann	198,3	115,022		-28,666	86,356	92,544
Absorbert vann	10,7	6,187			6,187	
Leca 2-4 mm (A-4048)	133,5	77,407	0,0	0,000	77,407	
Leca 800 4-8 mm (A-4048)	237,8	137,912	0,0	0,000	137,912	
0/8mm NSBR (A-4045)	432,8	250,998	4,5	11,295	262,293	
0/2mm Fillersand (A-4045)	270,5	156,874	8,7	13,648	170,522	
0	0,0	0,000	0,0	0,000	0,000	
	0,0	0,000	0,0	0,000	0,000	
	0,0	0,000	0,0	0,000	0,000	
	0,0	0,000	0,0	0,000	0,000	
	0,0	0,000	0,0	0,000	0,000	
	0,0	0,000	0,0	0,000	0,000	
Sika FB2	7,8	4,540	82	3,723	4,540	
	0,0	0,000	100	0,000	0,000	
	0,0	0,000	100	0,000	0,000	
	0,0	0,000	100	0,000	0,000	
Stålfiber (Dramix 30/35)	78,0	45,240			45,240	
Basalt Gen 3	0,0	0,000			0,000	

*Se fotnote på delark "Proporsjonering"   ** NB! Våte mengder, også for pozzolaner og fillere

Fersk betong					
Tid etter vanntilsetning					
Synkmål					
Utbredelsesmål					
Luft					
Densitet					

Prøvestykker (antall)					
Utstøpningstidspunkt					
Terninger					
150x300 sylindre					
100x200 sylindre					
100x200 sylindre					
Totalt tilsatt SP					

Delark "Blandeskjema"

Prosj./id.:	LWAC Bjelkestøp 2013_Bjelke 4A og 4B

Blandevolum:	720 liter *1580l*
Dato:	*28/2 - 13*
Tidspunkt for vanntilsetning	*1030*
Ansvarlig:	*GK/TMJ*
Utført av:	*KL/GT*

Materialer	Resept kg/m³	Sats kg	Fukt* %	Korr. kg	Oppveid** kg	
Norcem Standard BP5/BP6	434,9	313,128			313,128	
Elkem Microsilica 920 D	43,5	31,313	0	0,000	31,313	
Kalksteinsmel	4,3	3,131	0	0,000	3,131	
Fritt vann	198,3	142,786		-35,585	107,201	*114,882*
Absorbert vann	10,7	7,681			7,681	
Leca 2-4 mm (A-4048)	133,5	96,091	0,0	0,000	96,091	
Leca 800 4-8 mm (A-4048)	237,8	171,200	0,0	0,000	171,200	
0/8mm NSBR (A-4045)	432,8	311,584	4,5	14,021	325,605	
0/2mm Fillersand (A-4045)	270,5	194,740	8,7	16,942	211,682	
0	0,0	0,000	0,0	0,000	0,000	
	0,0	0,000	0,0	0,000	0,000	
	0,0	0,000	0,0	0,000	0,000	
	0,0	0,000	0,0	0,000	0,000	
	0,0	0,000	0,0	0,000	0,000	
	0,0	0,000	0,0	0,000	0,000	
Sika FB2	7,8	5,636	82	4,622	~~5,636~~	*4,833*
	0,0	0,000	100	0,000	0,000	
	0,0	0,000	100	0,000	0,000	
	0,0	0,000	100	0,000	0,000	
Stålfiber (Dramix 65/69)	0,0	0,000			0,000	
Basalt Gen 3	19,0	13,680			~~13,680~~	*11,020*

*Se fotnote på delark "Proporsjonering"   ** NB! Våte mengder, også for pozzolaner og fillere

Fersk betong			*m/fiber*		
Tid etter vanntilsetning	*15*	*25*	*40*		
Synkmål					
Utbredelsesmål	*550*		*—*		
Luft					
Densitet		*1794*	*1812*		

Prøvestykker (antall)					
Utstøpningstidspunkt	*1125*				
Terninger					
150x300 sylindre					
100x200 sylindre	*68stk.*	*merk:*	*31 - 36 28/2*		
150 x 150 x 550 Gjelker	*—a*	*—*	*31 - 36 28/2*		
Totalt tilsatt SP					

Delark "Blandeskjema"

Blandevolum:	580 liter
Dato:	
Tidspunkt for vanntilsetning	
Ansvarlig:	
Utført av:	

Materialer	Resept kg/m³	Sats kg	Fukt* %	Korr. kg	Oppveid** kg	
Norcem Standard BP5/BP6	434,9	252,242			252,242	
Elkem Microsilica 920 D	43,5	25,224	0	0,000	25,224	
Kalksteinsmel	4,3	2,522	0	0,000	2,522	
Fritt vann	198,3	115,022		-28,666	86,356	92,544
Absorbert vann	10,7	6,187			6,187	
Leca 2-4 mm (A-4048)	133,5	77,407	0,0	0,000	77,407	
Leca 800 4-8 mm (A-4048)	237,8	137,912	0,0	0,000	137,912	
0/8mm NSBR (A-4045)	432,8	250,998	4,5	11,295	262,293	
0/2mm Fillersand (A-4045)	270,5	156,874	8,7	13,648	170,522	
0	0,0	0,000	0,0	0,000	0,000	
	0,0	0,000	0,0	0,000	0,000	
	0,0	0,000	0,0	0,000	0,000	
	0,0	0,000	0,0	0,000	0,000	
	0,0	0,000	0,0	0,000	0,000	
	0,0	0,000	0,0	0,000	0,000	
Sika FB2	7,8	4,540	82	3,723	4,540	
	0,0	0,000	100	0,000	0,000	
	0,0	0,000	100	0,000	0,000	
	0,0	0,000	100	0,000	0,000	
Stålfiber (Dramix 65/69)	0,0	0,000			0,000	
Basalt Gen 3	19,0	11,020			11,020	

*Se fotnote på delark "Proporsjonering"   ** NB! Våte mengder, også for pozzolaner og fillere

Fersk betong					
Tid etter vanntilsetning					
Synkmål					
Utbredelsesmål					
Luft					
Densitet					

Prøvestykker (antall)					
Utstøpningstidspunkt					
Terninger					
150x300 sylindre					
100x200 sylindre					
100x200 sylindre					
Totalt tilsatt SP					

Delark "Blandeskjema"

Appendix E

Concrete Test-Cylinders.

SINTEF Byggforsk, betong- og natursteinlaboratoriet

Bjelke 1A – 1B 26/2.13

NS-EN 12390-3:2009 PRØVELEGEMERS TRYKKFASTHET

③ SINTEF

Oppdragsgiver: COIN FA 3.3

Reg.nr. vekt: B-181

Prosjektnr: 102000 4442.8

Oppdragsnummer:

Prøve nr.	Høyde etter planslip mm	Diam. mm	Trykk-flate mm²	Vekt i vann g	Vekt i luft g	Volum dm³	Rom-densitet kg/m³	Brudd-last kN el-kp	Brudd-form (se *)	Største nom. steinst. mm	Trykk-fasthet MPa	Høyde/diameter-forhold	Omregn.-faktor	Omregn. trykk-fasthet MPa
1 26/2	197	100	7854	1171	2715	1544	1.754	323	✓		41.1	1.97	1	41.1
2 "	198	"	"	1199	2752	1553	1.772	329	✓		41.9	1.98	1	41.9
3 "	198	"	"	1199	2754	1555	1.771	313	✓		39.9	"	1	39.9
4 26/2	198	"	"	1190	2735	1545	1.776	321	✓		40.9	"	1	40.9
5	198	"	"	1165	2720	1550	1.749	315	✓		40.1	"	1	40.1
6	198	"	"	1193	2747	1554	1.768	329	✓		41.9	"	1	41.9
7 26/2	199	100	7854	1174	2729	1555	1.76	2718			34.6	1.99	1	34.6
8 "	199	100	"	1169	2720	1558	1.74	2735			34.8	"	"	34.8

Prøvene ble lagt i vann: 27/2 v/anf. (Gille m. Bjørg 7-8)(Nr. 1-6 lagt samm m/Gjelby 5/3-13 EJ)

Trykkprøvd den ✓5/3 2/4 i Form Test B-62 ved innstilling 2000 kN / 5000 kN

* **Bruddform:** Ved **tilfredsstillende** bruddform (se s. 2) settes **kryss** i ruten for "Bruddform". Ved **utilfredsstillende** bruddform (se s. 2) settes **kode** i ruten for "Bruddform".
Kode for terning: 1 2 3 4 5 6 7 Kode for sylinder: A B C D E F G H I J K

Dato/sign: 2013-07-04

Dato/sign daglig lab.leder: 2013-07-02

Kommentarer: ✶

Rev. 2011-03-09 LH

I:\SKJEMAER\ORIGINALER dokx\NS-EN 12390-3 Trykkprøving av sylindrer og utboret betong.xltx

A-35

Bjelke 2A-2B 26/2.13

NS-EN 12390-3:2009 PRØVELEGEMERS TRYKKFASTHET

Ⓢ SINTE...

Oppdragsgiver: _OON FA 3.3_ Prosjektnr: _102000442-3_

Reg.nr. vekt: _B-181_ Oppdragsnummer: _____

39.1

Prøve nr.	Høyde etter planslip mm	Diam. mm	Trykk-flate mm²	Vekt i luft g	Vekt i vann g	Volum dm³	Rom-densitet kg/m3	Brudd-last kN el. kp	Brudd-form (se *)	Største nom. steinst. mm	Trykk-fasthet MPa	Høyde/diameter-forhold	Omregn.-faktor	Omregn.-trykk-fasthet MPa
11 26/2	198	100	7854	2558	1206			297			37.8	1.98	1	37.8
12 "	197	"	"	2784	1246			320			40.7	1.97	1	40.7
13 "	197	"	"	2361	1224			320			40.7	"	1	40.7
14 26/2	198	"	"	2366	1219			310			39.5	1.98	1	39.5
15 "	198	"	"	2770	1222			288			36.7	"	1	36.7
16 "				2790,3	1224,0									
								(Takk ut til ovnstørr densitet)						

Prøvene ble lagt i vann: _3/4 - 13_ Dato/sign: _3/4-13 E.J._

Trykkprøvd den _3/4 - 13_ i _los.hamp._ B-52 ved innstilling _5000 kN_ Dato/sign daglig lab.leder: _2013-04-03 K. Berntz_

* **Bruddform:** Ved **tilfredsstillende** bruddform (se s. 2) settes **kryss** i ruten for "Bruddform". Ved **utilfredsstillende** bruddform (se s. 2) settes **kode** i ruten for "Bruddform".
Kode for terning: 1 2 3 4 5 6 7 {Kode for sylinder: A B C D E F G H I J K

Kommentarer: _16 tatt ut til ovnstørr dens, nærmere middelvekt_

Bjelke 3A-3B 28/2-13

NS-EN 12390-3:2009 PRØVELEGEMERS TRYKKFASTHET

Ⓢ SINTEF

Oppdragsgiver: _OBIN FA 3.5_   Prosjektnr: _102000 9412-2_

Reg.nr. vekt: _B-181_   Oppdragsnummer:

Prøve nr.	Høyde etter planslip mm	Diam. mm	Trykk-flate mm²	Vekt i vann g	Vekt i luft g	Volum dm³	Rom-densitet kg/m3	Brudd-last kN el. kp	Brudd-form (se *)	Største nom. steinst. mm	Trykk-fasthet MPa	Høyde/diameter-forhold	Omregn.-faktor	Omregn. trykk-fasthet MPa
21 28/2	198	100	7854	1273	2822	1549	1.822	318			40.5	1.98	1	40.5
22 "	198	"	"	1276	2828	1552	1.822	347			40.4	"	1	40.4
23 "	196	"	"	1259	2796	1537	1.819	301			38.3	1.96	1	38.3
24 "	195	"	"	1241	2762	1521	1.816	320			40.7	1.95	1	40.7
25 "				1293.8	2856.7	1563	1.828							
26 "	198	100	7854	1277	2815	1538	1.830	315			40.1	1.98	1	40.1

40.c (rød note)

Prøvene ble lagret i vann: _lagret saune m/hardtgjerke 1/3-13_

Trykkprøvd den _4/4-13_ i Losenhausen _B-52_ ved innstilling _5000 kN_

Dato/sign: _4/4-13 E.F._

Dato/sign daglig lab.leder: _2013-04-05_ [signatur]

* **Bruddform:** Ved **tilfredsstillende** bruddform (se s. 2) settes **kryss** i ruten for "Bruddform". Ved **utilfredsstillende** bruddform (se s. 2) settes **kode** i ruten for "Bruddform".
Kode for terning: 1 2 3 4 5 6 7 {Kode for sylinder: A B C D E F G H I J K

Kommentarer: _syl nr 25 tatt ut til ovnstørr dub,_

SINTEF Byggforsk, betong- og natursteinlaboratoriet

Gjethe 4A - 4B 28/2 '13

NS-EN 12390-3:2009 PRØVELEGEMERS TRYKKFASTHET

© SINTEF

Oppdragsgiver: COIN FA 3.3   Prosjektnr:

Reg.nr. vekt: B-181   Oppdragsnummer: 102009442-8

Prøve nr.	Høyde etter planslip mm	Diam. mm	Trykk-flate mm²	Vekt i vann g	Vekt i luft g	Volum dm³	Rom-densitet kg/m3	Brudd-last kN el kp	Brudd-form (se *)	Største nom. steinst. mm	Trykk-fasthet MPa	Høyde/diameter-forhold	Omregn.-faktor	Omregn. trykk-fasthet MPa
31 28/2				1228,5	2794,3	1565	1785							
32 "	198	100	7854	1222	2771	1549	1789	318			40,5	1.98	1	40.5
33 "	198	"	"	1204	2756	1552	1776	319			40.6	"	1	40.6
34 "	199	"	"	1223	2779	1556	1786	310			39.5	1.99	1	39.5
35 "	198	"	"	1209	2760	1551	1780	324			41.3	1.98	1	41.3
36 "	198	"	"	1212	2766	1554	1780	320			40.7	"	1	40.7

40.5

Prøvene ble lagt i vann: Lagret sammen m/hovedgulv 1/3-13

Trykkprøvd den 5/4 – 13   i Losenhaven B-52   ved innstilling 5000 kN

Dato/sign: 5/4-13 C.Z

Dato/sign daglig lab.leder: 5/4 - 04-01

* **Bruddform:** Ved **tilfredsstillende** bruddform (se s. 2) settes **kryss** i ruten for "Bruddform". Ved **utilfredsstillende** bruddform (se s. 2) settes **kode** i ruten for "Bruddform".
Kode for terning: 1 2 3 4 5 6 7 Kode for sylinder: A B C D E F G H I J K

Kommentarer: Syl nr. 31 tett til ovnstørr dess.

Rev. 2011-03-09 LH   I:\SKJEMAER\ORIGINALER dotx\NS-EN 12390-3 Trykkprøving av sylinder og utboret betong.xltx

Appendix F

E-mail from Tore Myrland Jensen, Oven-dry Density.

Ovnstørr densitet ble bestemt for støp 2, 3 og 4.

Følgende resultater fremkommer:

- Bjelke 2 (sylinder nr. 16): Ovnstørr densitet: 1659 kg/m3 (Romdensitet var 1794 kg/m3, dvs. 135 kg fordampbart vann/m3)

- Bjelke 3 (sylinder nr. 25): Ovnstørr densitet: 1686 kg/m3 (Romdensitet var 1828 kg/m3, dvs. 142 kg fordampbart vann/m3)

- Bjelke 4 (sylinder nr. 31): Ovnstørr densitet: 1634 kg/m3 (Romdensitet var 1785 kg/m3, dvs. 151 kg fordampbart vann/m3)

Som input ved beregning av teoretiske tøyningsgrenser etter EC2 anbefaler jeg at ovnstørr densitet settes som **150 kg/m3** lavere enn middelverdien av romdensiteten. <u>Dette gjøres likt på alle fire betongene</u>.

Dersom andre antagelser eller beregninger av ovnstørr densitet er gjort, og endringer av dette medfører mye merarbeid (f.eks. i forbindelse med justering av rapportering, utarbeidede grafer, figurer etc.), så er det ingen krise om dere ikke endrer til 150 kg/m3. Dere får vurdere dette.....

Fint om dere informerer videre (har ikke e-postadressen til resten av stud.)

Tore

Appendix G

Bending Strength of Fibre Reinforced Test-Beams.

SINTEF Byggforsk, betong- og natursteinlaboratoriet

NS-EN 14651 MÅLING AV BØYESTREKKFASTHET - BETONG MED METALLISKE FIBERE ◎ SINTEF

Oppdragsgiver: COIN FA3.3 (Bjelkeforsøk) Mix 24-B

Prosjektnr: _____

Reg.nr. vekt: _____

Oppdragsnummer: 102006442-8

Støpedato: 26/2-13

Prøvestykke nr.	Vekt ved prøving	Lengde, L	Tverrsnittsbredde, b		Tverrsnittshøyde, h_{sp}		Areal	Bruddlast, F_L	Bruddlast, F_L	Limit of proportionality (LOP)
	g	mm	mm	mm	mm	mm	mm²	kN	MPa	
11 26/2			152	152	125	125		19,11 *		
12 "			152	152	126	126		25,61		
13 "			152	152	124	126		22,22		
14 "			152	152	126	126		19,57		
15			153	152	126	126		25,69		
16			153	153	126	125		24,95		

$$f_{ct,L}^{f} = \frac{3F_L l}{2bh_{sp}^2}$$

Prøvene ble lagt i vann: 27/2-13

Prøvingsdato/maskin: 3/4-13 i Instron 250kN   15kN/v 0,5mm/v

Største nominelle steinstørrelse i prøve: _____ mm

Beskrivelse av evtuell utilfredsstillende bruddform: _____

Kommentarer: _____

* ble kjørt på for mye last ved montering av prøven → litt riss i skjerv

Dato/sign: 3/4-13 _____

Dato/sign daglig lab.leder: _____

A-45

SINTEF Byggforsk, betong- og natursteinlaboratoriet

NS-EN 14651 MÅLING AV BØYESTREKKFASTHET - BETONG MED METALLISKE FIBERE ◎ SINTEF

Oppdragsgiver: COIN FA3.3 - Task 70 LWAC Mix 3A / 3B

Reg.nr. vekt:

Prosjektnr: 10200442 - 8

Oppdragsnummer:

Støpedato: 28/2 - 13

Prøvestykke nr.	Vekt ved prøving g	Lengde, L mm	Tverrsnittsbredde, b mm	mm	Tverrsnittshøyde, h_{sp} mm	mm	Areal mm²	Bruddlast, F_L kN	Bruddlast, F_L MPa
21 28/2			152	151	126	125		24,32	
22 "			152	152	124	126		24,06	
23 "			152	152	125	125		22,41	
24 "			152	152	126	126		25,75	
25 "			152	151	126	126		21,41	
26 "			154	154	126	126		32,77	

Limit of proportionality (LOP)

$$f_{ct,L}^{f} = \frac{3F_L l}{2bh_{sp}^2}$$

Prøvene ble lagt i vann: 1/3 - 13

Prøvingsdato/maskin: 4/3-12 i Instron 250 kN

15kN/V
0,5mm/V
0,21 mm/min

Dato/sign: 4/3 - 13 [signature]

Dato/sign daglig lab.leder:

Største nominelle steinstørrelse i prøve: _____ mm

Beskrivelse av evtuell utilfredsstillende bruddform:

Kommentarer:

SINTEF Byggforsk, betong- og natursteinlaboratoriet

NS-EN 14651 MÅLING AV BØYESTREKKFASTHET - BETONG MED MED METALLISKE FIBERE ⊙ SINTEF

Oppdragsgiver: _Con FA3.5 (Bjørke støp)_ Prosjektnr: _102004442-8_

Reg.nr. vekt: ___ Støpedato: ___ Oppdragsnummer: ___

Mix 4A-B

Prøvestykke nr.	Vekt ved prøving (g)	Lengde, L (mm)	Tverrsnittsbredde, b (mm)	(mm)	Tverrsnittshøyde, h_{sp} (mm)	(mm)	Areal (mm²)	Bruddlast, F_L (kN)	Bruddlast, F_L (MPa)
31 28/2			152 / 153	152 / 153	128 / 126	126 / 126		17,75	
32 "			152	152	125	126		20,34	
33 "			153	153	126	126		19,54	
34 "			152	152	125	125		18,01	
35 "			151	151	126	126		18,61	
36 "			153	153	126	126		21,68	

Limit of proportionality (LOP)

$$f_{ct,L}^{f} = \frac{3F_L l}{2bh_{sp}^2}$$

Prøvene ble lagt i vann: _1/3.13_

Prøvingsdato/maskin: _5/3-13_ _i Instron 250kN_ _15kN/v_ _0,5mm/V_ _0,21 mm/min_ Dato/sign: ___

Største nominelle steinstørrelse i prøve: _____ mm

Beskrivelse av evtuell utilfredsstillende bruddform: ___

Dato/sign daglig lab.leder: _5/3-13_

Kommentarer: ___

1 % Dramix 65/60_spec. 11-13

Summarized						
	B_1.1	**B_1.2**	**B_1.3**	**Mean value**	Unit	CoV
Average Width, b	152,0	152,0	152,0	**152,0**	mm	0,0%
Average high, h	125,0	126,0	125,0	**125,3**	mm	0,5%
Length, L	500	500	500	**500**	mm	0,0%
F_L	19,1	25,6	22,2	**22,3**	kN	14,6%
$f^f_{ct,L}$	6,0	8,0	7,0	**7,0**	N/mm^2	13,8%
$f_{R,1}$	5,8	7,5	6,3	**6,6**	N/mm^2	13,3%
$f_{R,2}$	5,8	7,3	6,9	**6,7**	N/mm^2	11,8%
$f_{R,3}$	5,3	7,0	6,9	**6,4**	N/mm^2	15,5%
$f_{R,4}$	4,8	6,7	6,8	**6,1**	N/mm^2	18,3%
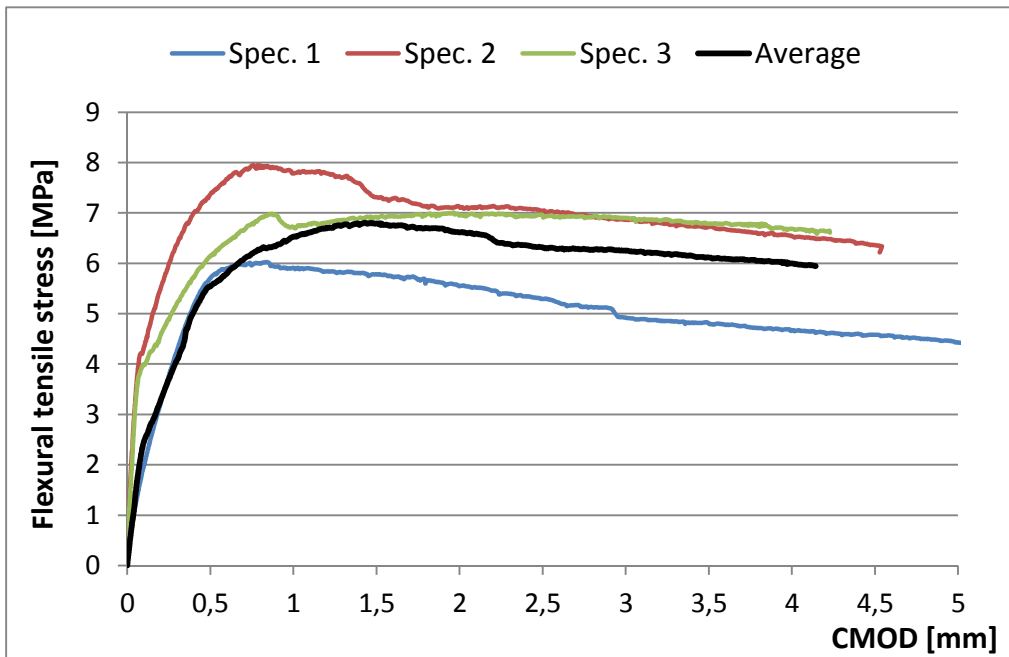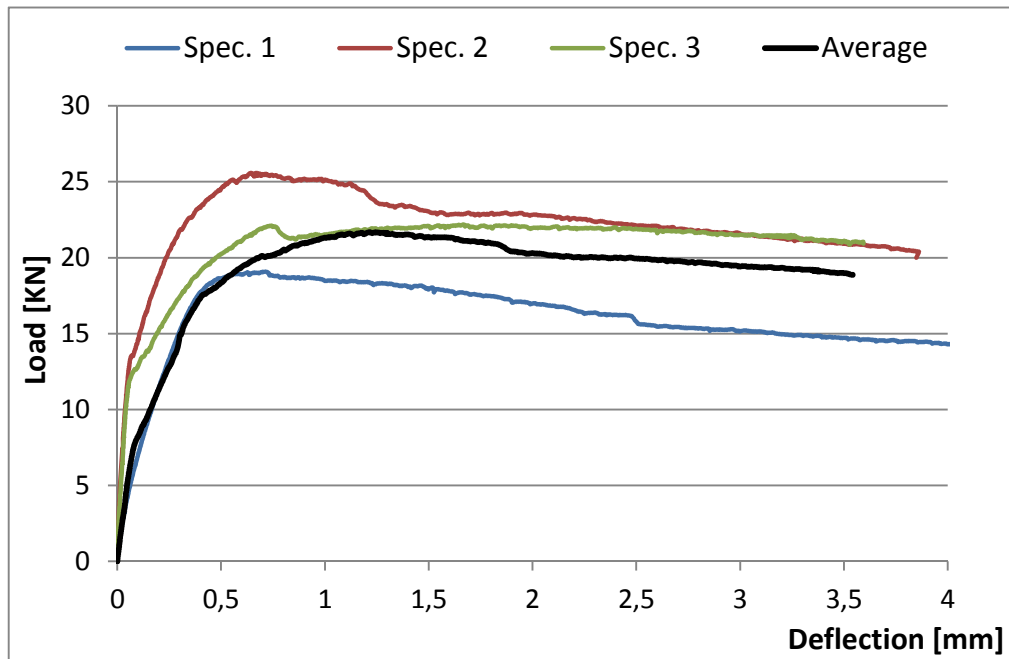
1 % Dramix 65/60_spec. 14-16

Summarized						
	B_1.1	**B_1.2**	**B_1.3**	**Mean value**	Unit	CoV
Average Width, b	152,0	152,5	153,0	**152,5**	mm	0,3%
Average high, h	126,0	126,0	125,5	**125,8**	mm	0,2%
Length, L	500	500	500	**500**	mm	0,0%
F_L	19,5	25,6	24,9	**23,3**	kN	14,2%
$f^f_{ct,L}$	6,1	7,9	7,8	**7,2**	N/mm^2	14,1%
$f_{R,1}$	6,0	7,5	7,3	**6,9**	N/mm^2	11,7%
$f_{R,2}$	5,9	7,8	6,8	**6,8**	N/mm^2	14,0%
$f_{R,3}$	5,8	7,7	6,4	**6,7**	N/mm^2	14,9%
$f_{R,4}$	5,5	7,7	5,9	**6,4**	N/mm^2	17,7%
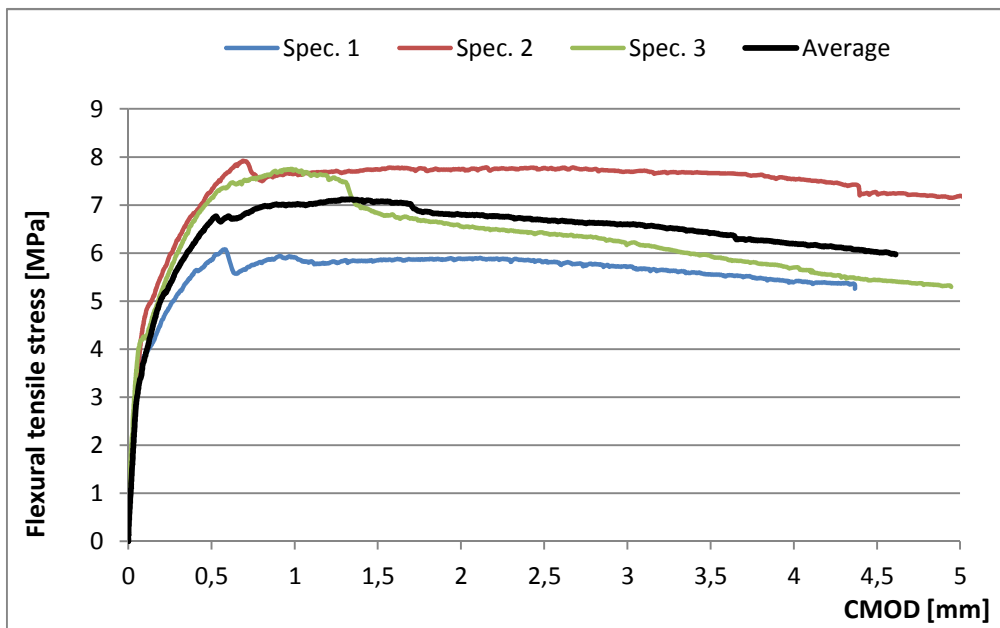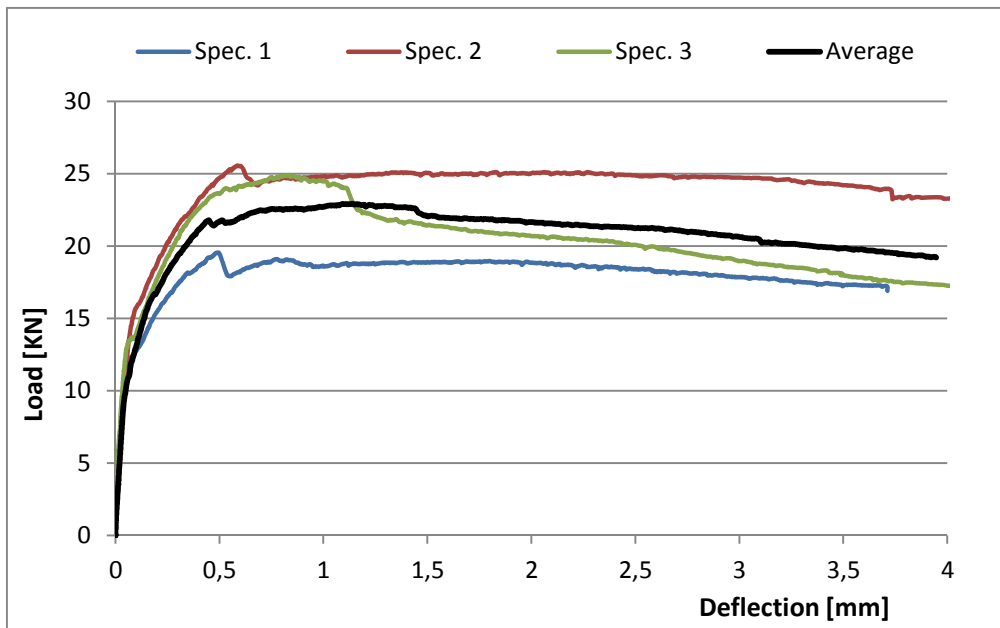
1 % Dramix 65/35_spec. 21-23

Summarized						
	B_1.1	**B_1.2**	**B_1.3**	**Mean value**	Unit	CoV
Average Width, b	151,5	152,0	152,0	**151,8**	mm	0,2%
Average high, h	125,5	126,0	125,0	**125,5**	mm	0,4%
Length, L	500	500	500	**500**	mm	0,0%
F_L	23,9	24,0	22,4	**23,4**	kN	4,0%
$f^f_{ct,L}$	7,5	7,5	7,1	**7,3**	N/mm^2	3,4%
$f_{R,1}$	7,4	7,4	6,9	**7,2**	N/mm^2	4,3%
$f_{R,2}$	7,0	6,8	6,3	**6,7**	N/mm^2	5,4%
$f_{R,3}$	5,9	6,1	5,9	**6,0**	N/mm^2	2,5%
$f_{R,4}$	5,1	5,6	5,2	**5,3**	N/mm^2	4,8%
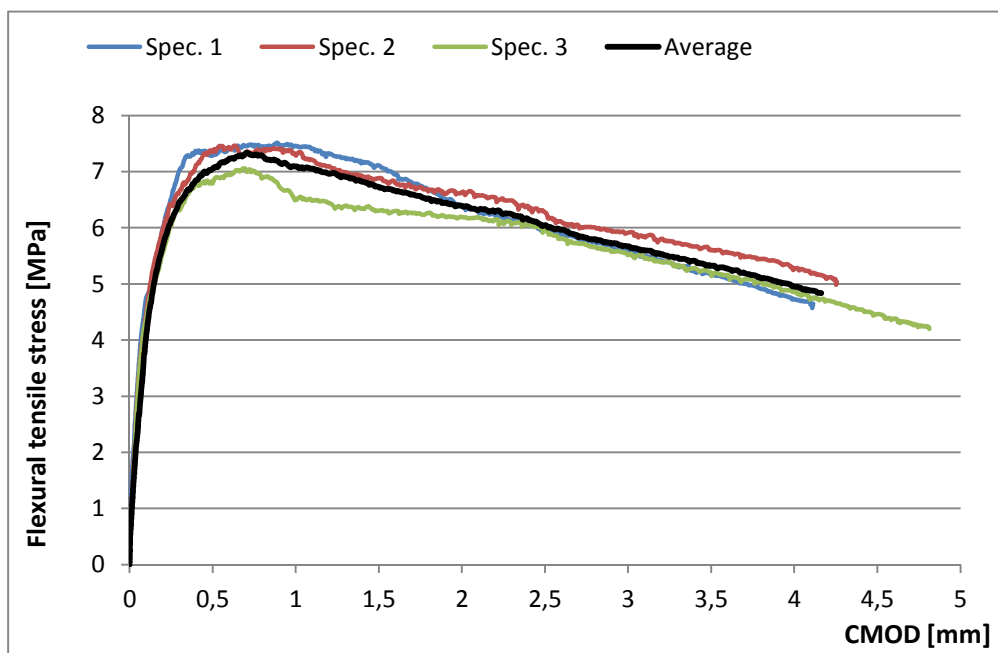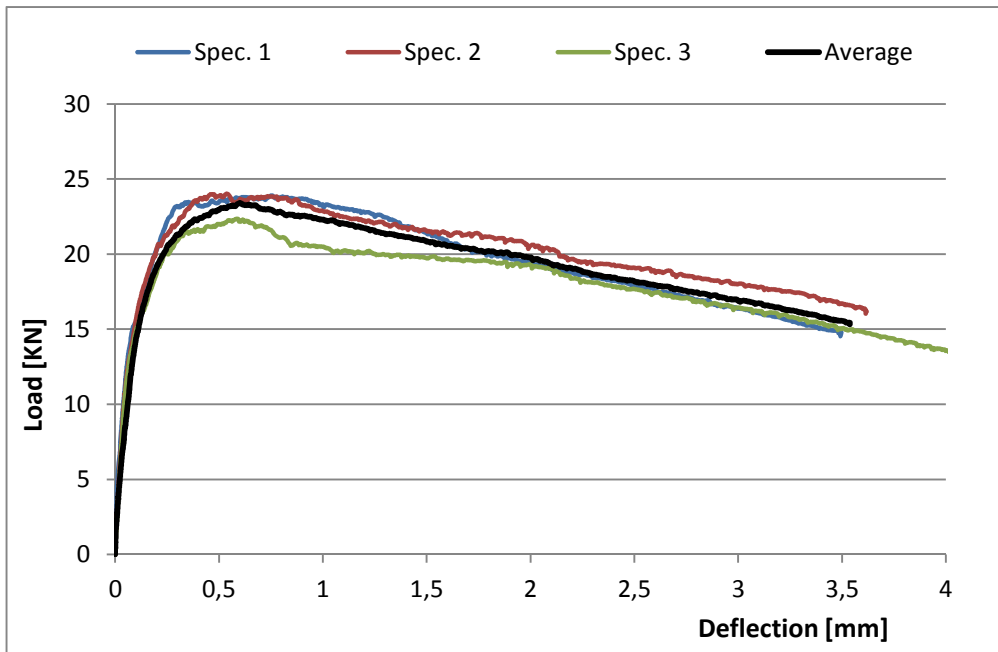
1 % Dramix 65/35_spec. 24-26

Summarized						
	B_1.1	**B_1.2**	**B_1.3**	**Mean value**	Unit	CoV
Average Width, b	152,0	151,5	154,0	**152,5**	mm	0,9%
Average high, h	126,0	126,0	126,0	**126,0**	mm	0,0%
Length, L	500	500	500	**500**	mm	0,0%
F_L	24,5	21,3	32,7	**26,2**	kN	22,3%
$f^f_{ct,L}$	7,6	6,7	10,0	**8,1**	N/mm^2	21,4%
$f_{R,1}$	7,5	6,6	9,6	**7,9**	N/mm^2	19,3%
$f_{R,2}$	6,9	5,8	9,9	**7,5**	N/mm^2	27,7%
$f_{R,3}$	6,2	4,9	9,3	**6,8**	N/mm^2	33,0%
$f_{R,4}$	5,3	4,2	8,6	**6,1**	N/mm^2	37,6%
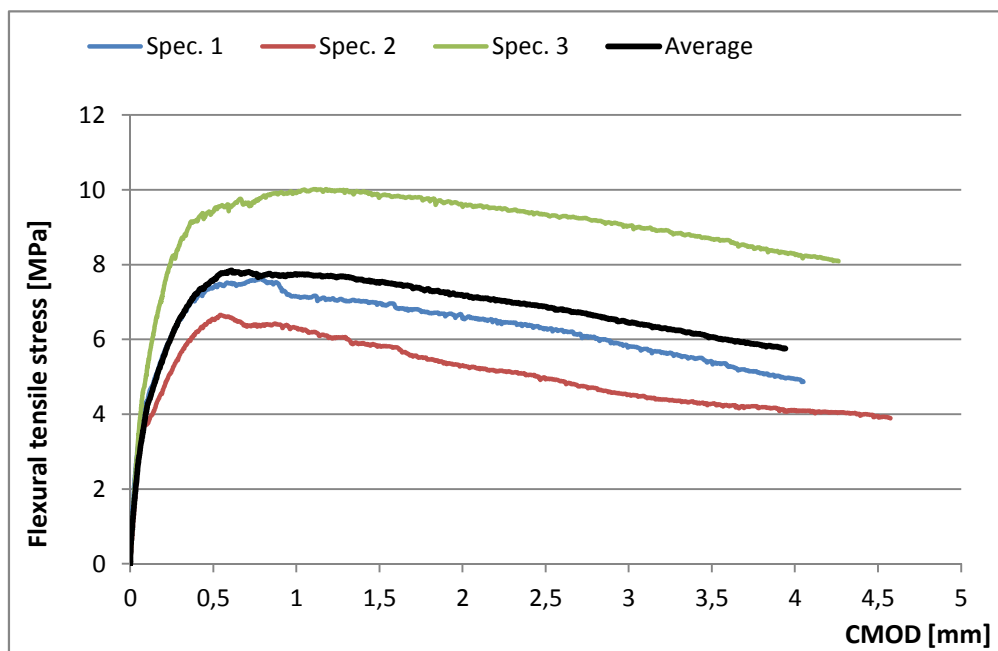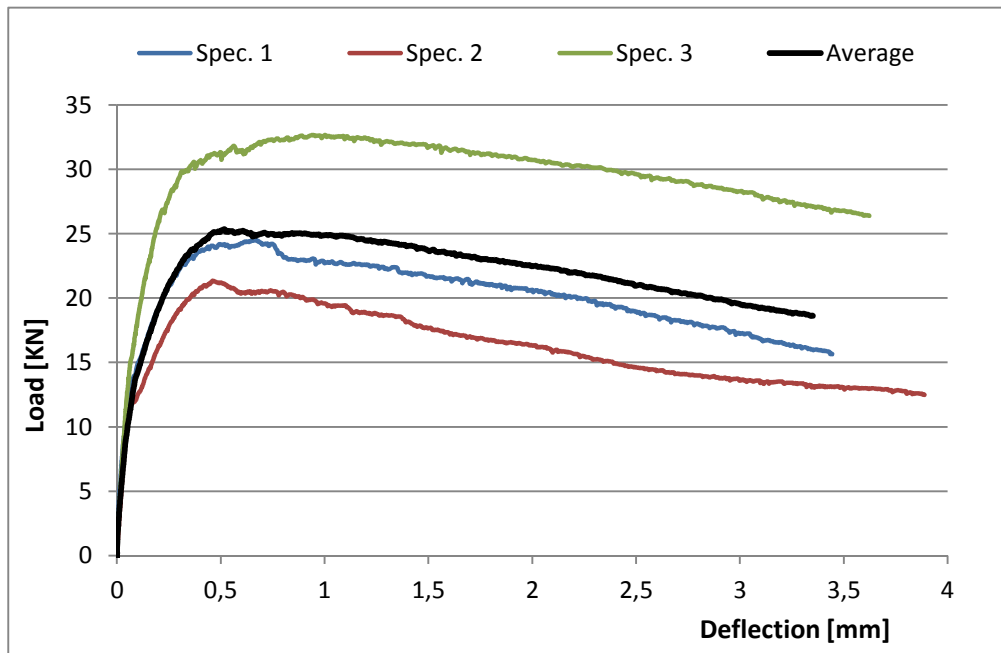
1 % Basalt MiniBar Generation 3_spec. 31-33

Summarized						
	B_1.1	**B_1.2**	**B_1.3**	**Mean value**	Unit	CoV
Average Width, b	152,0	152,0	153,0	**152,3**	mm	0,4%
Average high, h	125,5	125,5	125,5	**125,5**	mm	0,0%
Length, L	500	500	500	**500**	mm	0,0%
F_L	17,7	20,3	19,5	**19,1**	kN	6,9%
$f^f_{ct,L}$	5,5	6,3	6,1	**6,0**	N/mm^2	6,9%
$f_{R,1}$	5,5	6,2	6,0	**5,9**	N/mm^2	6,4%
$f_{R,2}$	2,5	3,6	3,5	**3,2**	N/mm^2	19,0%
$f_{R,3}$	1,5	2,2	2,1	**2,0**	N/mm^2	18,5%
$f_{R,4}$	1,0	1,5	1,6	**1,4**	N/mm^2	22,6%
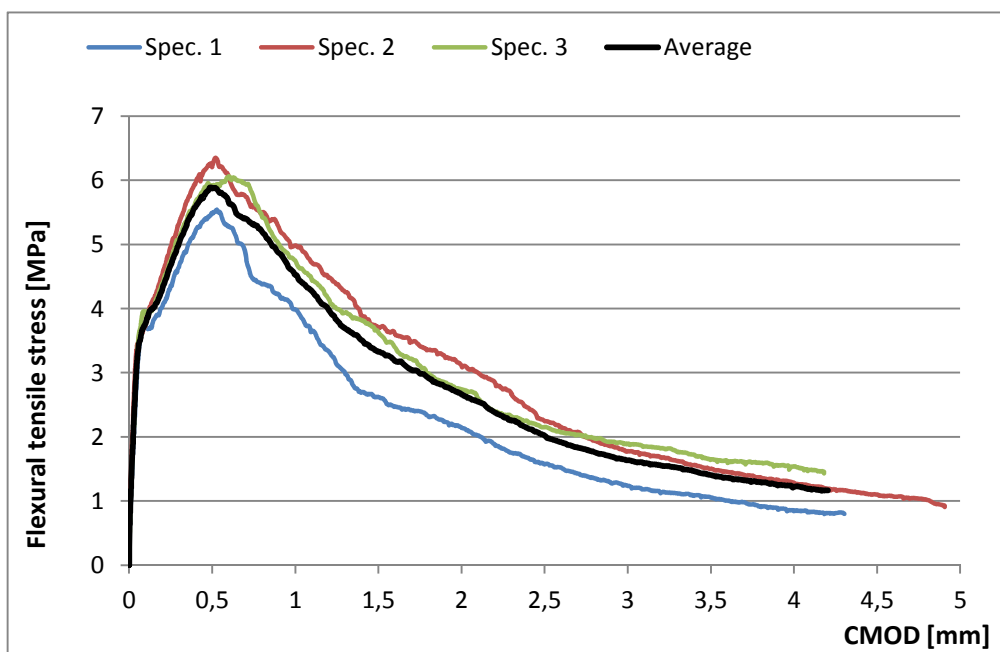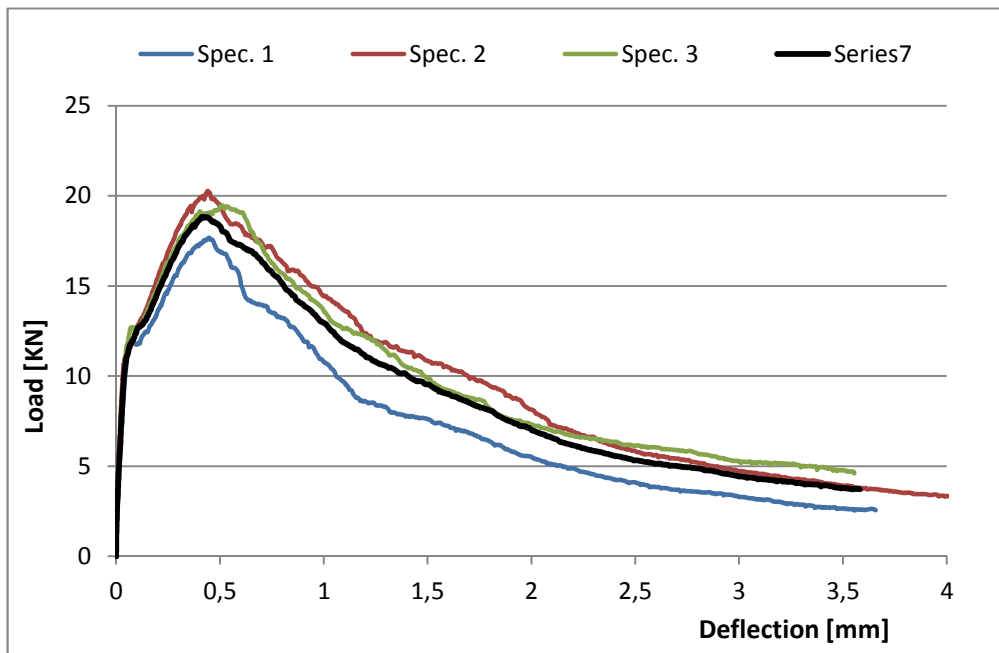
1 % Basalt MiniBar Generation 3_spec. 34-36

| Summarized						
	B_1.1	**B_1.2**	**B_1.3**	**Mean value**	Unit	CoV
Average Width, b	152,0	152,0	153,0	**152,3**	mm	0,4%
Average high, h	125,0	125,0	126,0	**125,3**	mm	0,5%
Length, L	500	500	500	**500**	mm	0,0%
F_L	17,9	18,5	21,6	**19,4**	kN	10,2%
$f^f_{ct,L}$	5,7	5,8	6,7	**6,1**	N/mm^2	8,8%
$f_{R,1}$	5,6	5,8	6,6	**6,0**	N/mm^2	8,4%
$f_{R,2}$	2,7	3,4	3,9	**3,3**	N/mm^2	18,4%
$f_{R,3}$	1,7	1,7	3,1	**2,2**	N/mm^2	36,5%
$f_{R,4}$	1,3	1,2	2,3	**1,6**	N/mm^2	39,3%
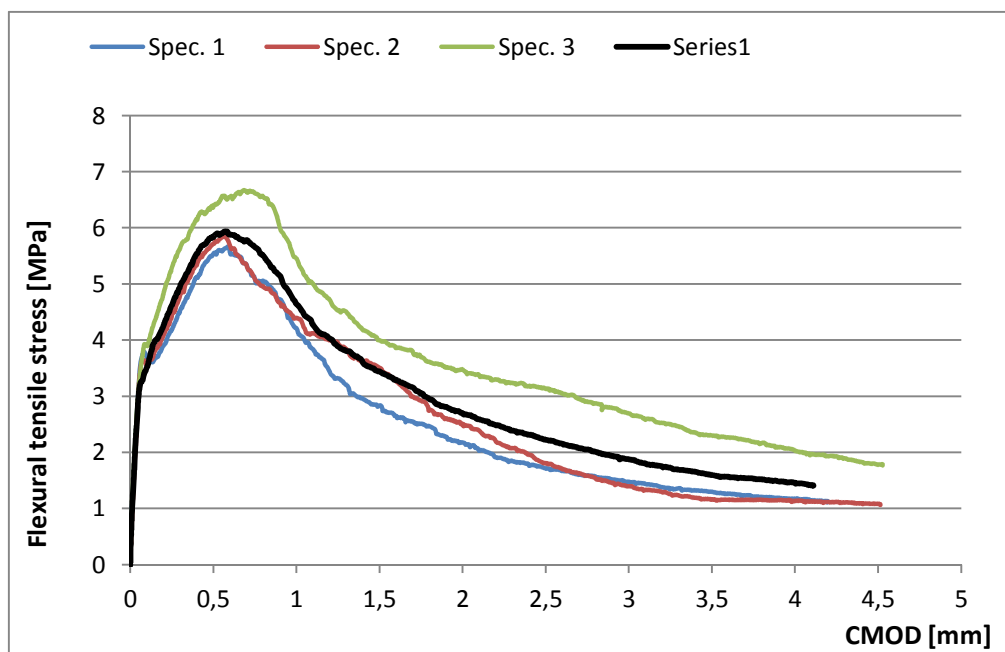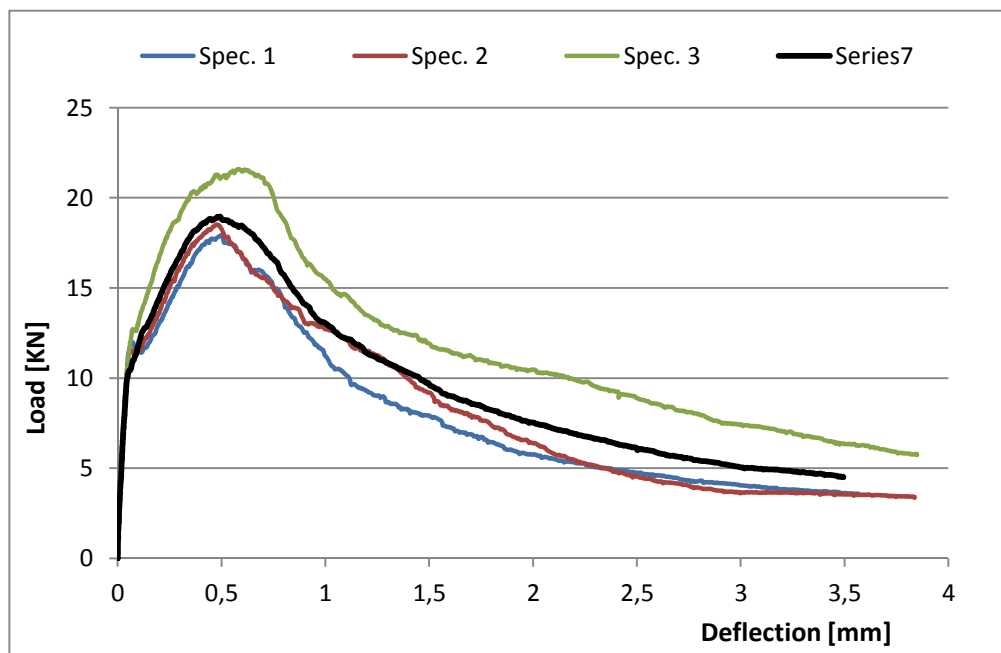
Appendix H

Fibre Counting

1 % Dramix 65/60_spec. 11-16

COUNTING FIBRES

Each slide was divided in 3 different parts to distinguish between the 25mm at the top (compression zone), 25 mm at the bottom (where the beams was notched) and 100mm in the middle zone was left

Mix 2A-2B, spec. 1.1-1.6

|	Number of Fibres							
	Beam 1	Beam 2	Beam 3	Beam 4	Beam 5	Beam 6	Mean	CoV
Upper	76	70	80	52	64	100	74	22,0 %
Middle	34	105	88	75	50	54	68	39,1 %
Bottom	72	60	80	102	121	105	90	25,6 %
Total	182	235	248	229	235	259	231	11,5 %
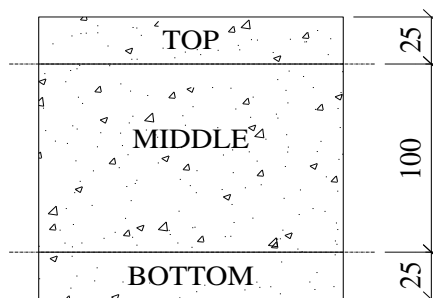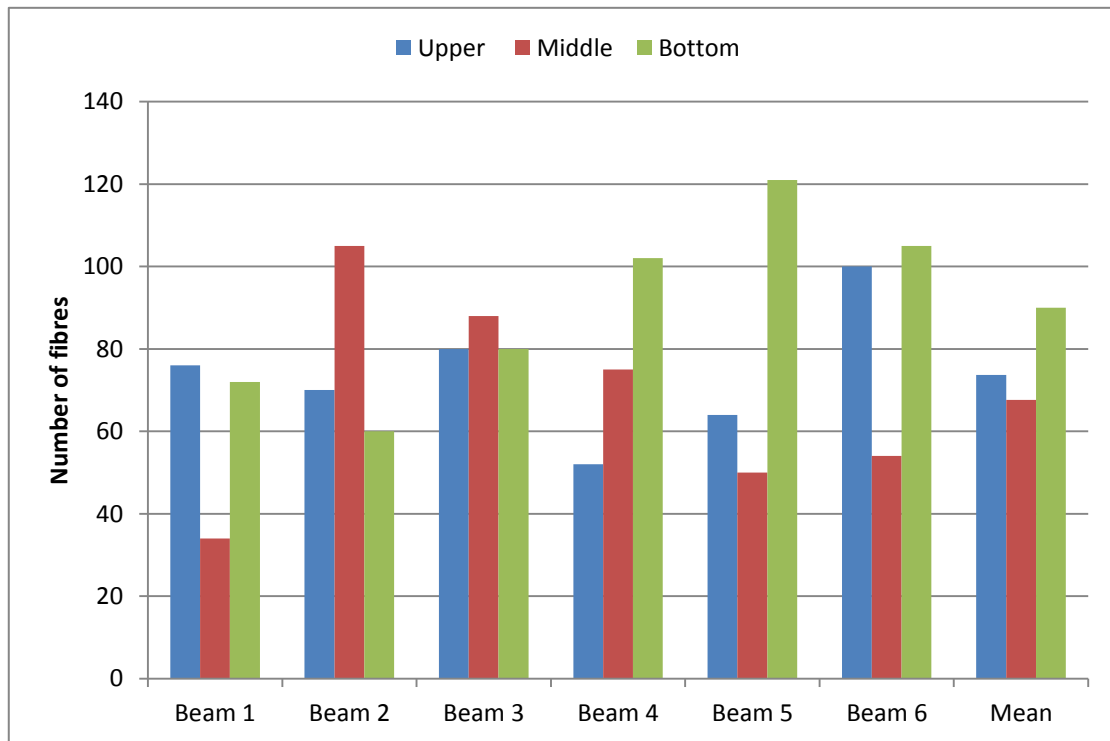
1 % Dramix 65/35_spec. 21-26

COUNTING FIBRES

Each slide was divided in 3 different parts to distinguish between the 25mm at the top (compression zone), 25 mm at the bottom (where the beams was notched) and 100mm in the middle zone was left

Mix 3A-3B, spec. 2.1-2.6

	Number of Fibres							
	Beam 1	Beam 2	Beam 3	Beam 4	Beam 5	Beam 6	Mean	CoV
Upper	100	150	126	193	194	197	160	25,7 %
Middle	55	184	160	182	183	217	164	34,4 %
Bottom	104	190	190	186	184	200	176	20,2 %
Total	259	524	476	561	561	614	499	25,3 %
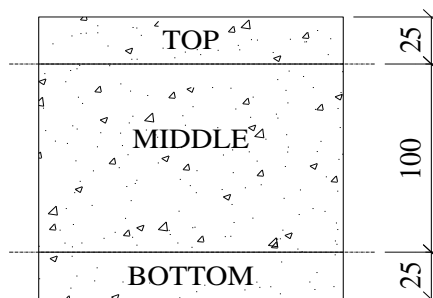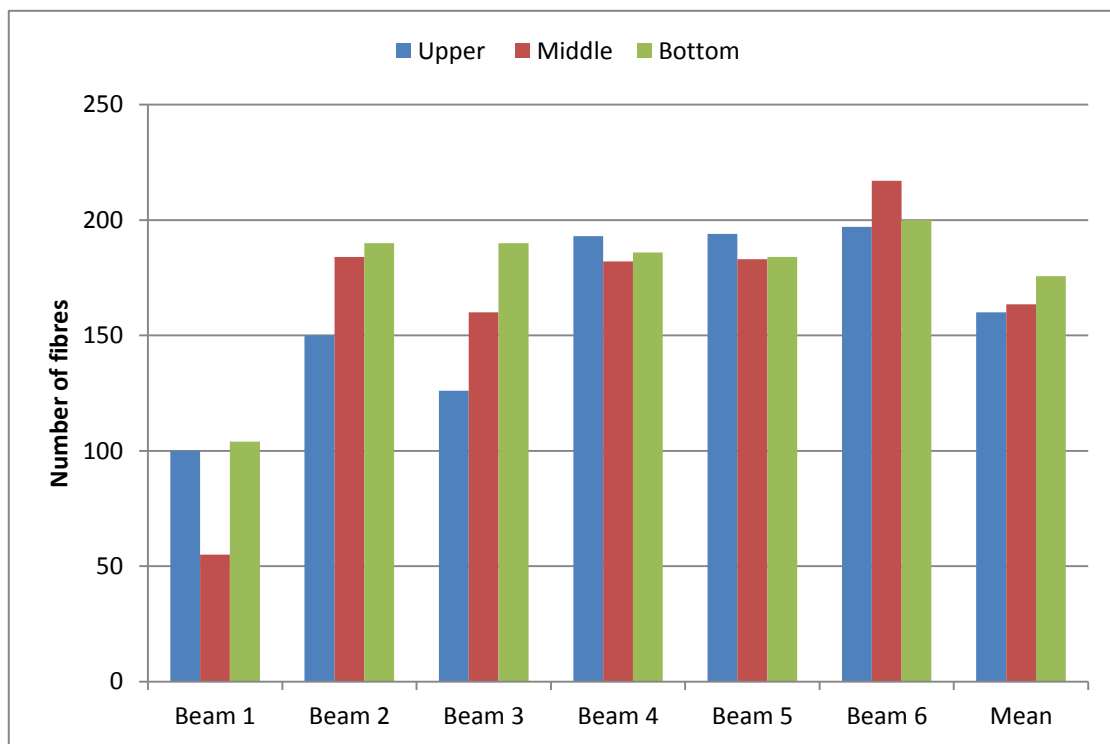
1 % Basalt MiniBar Generation 3_spec. 31-36

COUNTING FIBRES

Each slide was divided in 3 different parts to distinguish between the 25mm at the top (compression zone), 25 mm at the bottom (where the beams was notched) and 100mm in the middle zone was left

Mix 4A-4B, spec. 3.1-3.6

	Number of Fibres							
	Beam 1	Beam 2	Beam 3	Beam 4	Beam 5	Beam 6	Mean	CoV
Upper	74	49	45	41	50	69	55	24,7 %
Middle	86	56	51	50	65	84	65	24,7 %
Bottom	96	36	36	60	42	62	55	41,6 %
Total	256	141	132	151	157	215	175	28,0 %